Synthesis and Characterization of Novel Biodegradable Crosslinked Polyesters

PhD Thesis Submitted

By

Kanishka I. K. Herath

Supervisor: Associate Professor Tan Lay Poh

Nanyang Technological University

School of Materials Science and Engineering

2011

Synthesis and Characterization of Novel Biodegradable Crosslinked Polyesters

Kanishka I. K. Herath

School of Materials Science and Engineering

A Thesis Submitted to the Nanyang Technological University in Fulfillment of the Requirement for the Degree of Doctor of Philosophy

2011

Acknowledgements

This work was carried out under the supervision of Prof. Tan Lay Poh of the School of Materials Science and Engineering (MSE), Nanyang Technological University. I would like to express my sincere gratitude to her for giving me the opportunity to work on this project, and for her constant guidance and support.

I would also like to thank my co-supervisor, Dr. Christina Chai of the A*Star Institute of Chemical and Engineering Sciences (ICES) for her expertise and guidance on this project. I am grateful to ICES for their facilities support, and to all the staff there who have helped me.

This project would also not have succeeded without the collaborated help from Prof. Joachim Kohn and Prof. Das Bolikal of the New Jersey Centre for Biomaterials at Rutgers University, USA. I am very grateful for all the guidance I received on this work from Prof. Kohn, Dr. Bolikal and everyone at the centre.

I am truly grateful also to Dr Marc J. M. Abadie of NTU MSE, who very kindly shared his expertise, advised and guided me throughout this work.

I am also grateful to Dr Wen Feng, Angelina Octaviani Arykwan and Lee Min Hua, who helped out with parts of this work. My thanks to the entire faculty and staff at MSE who have helped me in one way, or another, throughout my studies.

I would like to thank my dear family for their patience and moral support throughout my studies. I am also grateful to my very supportive group of close friends.

This thesis is also dedicated to the memory of my dear feline friends, Squeaky and Gingy. I will always remember and miss them both.

CONTENTS

LIST OF SCHEMES

LIST OF FIGURES

LIST OF TABLES

Abstract

In this work, the synthesis of novel biodegradable crosslinked polyesters was explored via two different methods. The main objective was to obtain soft and elastomeric polymers suitable for future applications in soft tissue engineering. Currently, there are no elastomers on the market meeting the need for both low hysteresis and biodegradability.

The first synthetic route to achieving this objective was the photopolymerization of a multifunctional, non-toxic monomer to which biodegradable polymers were attached. Diallyl tartrate was the monomer of choice due to its pendant hydroxyl groups for subsequent polymer incorporation. As there has been no study on it before, the photopolymerizability of diallyl tartrate was first established using differential photocalorimetry and the obtained thermoset was characterized. It was found that the optimum amount of photoinitiator required was 3-4 wt% and samples of diallyl tartrate with thickness of about 2 mm polymerized within 2.5 h with 70 % degree of cure. Both the thermoset and its degradation products were shown to be non-toxic to cells over 24 h. Photopolymerized diallyl tartrate displayed a gradual rate of hydrolytic degradation, losing nearly 50 % of its mass in 3 months. Despite the potential of this material in other bio-applications, its high glass transition temperature of around 90 °C and its storage modulus of around 1 GPa deem it not suitable for applications in soft tissue engineering. There were difficulties in obtaining softer, more elastomeric polymers via this synthetic route.

The second route of synthesis involved a two-part system: an amine-terminated prepolymer and poly(ethylene glycol) diglycidyl ether (PEG-diglycidyl ether). In this work, two prepolymers were chosen: Poly(caprolactone) (PCL) of molecular weight 3000

g/mol and a random 50/50 copolymer, poly(caprolactone-co-d,l-lactide) of molecular weight 18000 g/mol. These prepolymers were successfully synthesized and characterized. The crosslinkers used for the subsequent crosslinking were PEG diglycidyl ether of two lengths: 500 g/mol and 1000 g/mol. Four different crosslinked polymers of gel contents of 40-50 % by mass were successfully synthesized and characterized.

It was found that the longer the PEG crosslinker used, the higher the amount of swelling exhibited and hence the faster the initial rate of hydrolytic degradation. It was also noted that the longer the prepolymer, the lower the crosslink density, hence the longer the maximum elongations attained by the crosslinked polymer. The Young's moduli of these polymers ranged from around 10-35 kPa. Two of the polymers were chosen for a cyclic tensile test and complete recovery with zero hysteresis was seen over 3 cycles up at a certain strain level. This is one of the most important advantages of chemically crosslinked polymers. Extracts of all the polymers were taken for cytotoxicity testing and it was shown that the polymers were non-toxic to cells over 24 h.

Hence this two-part epoxy-amine series of polymers have shown to be a highly tailorable system, with properties suitable for future applications in soft tissue engineering.

1 Introduction

1.1. Background

1.1.1. Bioresorbable Synthetic Polymers

The first significant mention of bioabsorbable or resorbable synthetic polymers was on their application as surgical suture material introduced in the 1960s, and the material used back then was poly(lactic acid) (PLA) [1]. The first commercial suture, Dexon (a glycolic acid/lactic acid copolymer), was formulated and marketed in 1970. Since then, biodegradable and resorbable polymers with hydrolyzable chemical bonds have been researched on extensively and there have been numerous advances in the development of such biomaterials for implant devices. A resorbable polymer is one that results in degradation products disposable by bodily processes. The products can either be resorbed through enzymatic or non-enzymatic hydrolysis, followed by metabolism or excretion [2]. The obvious reason for an implant device, which degrades over time, is that no second surgical intervention for retrieval is needed. Such polymers also reduce the risk of infection as they are disposed of after serving their function. There are other less obvious reasons for the use of resorbable polymers, for example, when they are used in orthopedic implants for bone fixation as they can increase the ultimate bone strength by slowly transferring load to the bone as it heals. An extremely rigid metallic implant, on the other hand, may pose "stress shielding" problems due to its high relative strength. Another example involves the use of such materials in drug delivery systems, where the degradation properties of the polymers can be suitably altered to attain the required release kinetics of the drug or active agent.

Some naturally occurring, resorbable biopolymers are chitin, cellulose, lignin and starch from trees. Chitin is commonly and abundantly found in crab, shellfish and mollusks. Several of such resorbable polymers also exist naturally in the body, such as collagen and albumin. Although these seem to provide ready-to-use materials for implants, several disadvantages have been encountered in the attempts to utilize them. These include their hydrophilicity, undesirable thermal and mechanical properties, and low processability [3]. There is no control over the molecular weight and other properties of the polymer if it were to be chemically modified. Furthermore, the introduction of familiar, naturally occurring polymers into the human body will give rise to immunogenic problems, hence rendering these materials as not biocompatible. Hence novel or modified polymers have been synthesized to answer the increasing demand for high performing, bioresorbable implant materials in the biomedical field. Such synthetic polymers pose fewer complications as they do not vary from source to source as natural polymers often do. The chemical and physical properties of a synthetic polymer can also be easily modified; and the degradation and mechanical characteristics can be altered by their chemical compositions. Functional groups may also be incorporated or their side chains modified to improve cell adhesion or growth. Additionally, synthetic polymers generally degrade by simple hydrolysis. This is desirable as then the degradation rate does not differ from host to host, except if there are inflammations and unusual implant degradation to affect the local pH.

Bioresorbable synthetic polymers such as poly(glycolic acid) (PGA), poly(lactic acid) (PLA) and their copolymers (PLGA), poly(p-dioxanone), and copolymers of trimethylene carbonate and glycolide have been used over the years in clinical applications [4-8]. The major applications include drug delivery systems, resorbable sutures and orthopedic fixation devices such as pins, rods and screws [9,10].

One of the most common biopolymers researched on is poly(ethylene glycol) (PEG). PEG is a water-soluble polymer that has been extensively used in biomaterial applications. It is extremely hydrophilic, which suppresses the adsorption of proteins, hence preventing a controllable cell response. This hydrophilicity can also be used to change the interactions between the material and tissue. In addition, the end-groups on PEG can be easily altered via various synthetic reactions. PEG however is not biodegradable and does not last in a biological environment on its own due to its water solubility. Hence it has often been copolymerized with other biodegradable polymers for applications that require some mechanical integrity in an aqueous environment.

Some commonly explored biopolymers containing hydrolysable bonds include anhydrides, carbonates, ortho-esters, amides and esters. Of these, polyesters are the most extensively used and studied. These are popular as they allow for hydrolytic degradation through their de-esterification. The monomers produced after degradation are removed by the body's natural pathways, the body already has highly regulated mechanisms for removing residuals of the polymers.

Poly(α-hydroxy esters) include PGA and PLA. PGA is very rigid due to its high crystallinity, however it is extremely sensitive to hydrolytic degradation. What makes PGA attractive as a biopolymer is the fact that its degradation product, glycolic acid, is a natural metabolite. Hence PGA has been successfully used in the fabrication of resorbable sutures (Dexon, American Cyanamide Co). PGA generally loses about half its mass in less than 2 months.

PLA exists in three isomeric forms: (d), (l) and the racemic (dl). Poly(l)LA and Poly(d)LA are both semi-crystalline with similar rates of degradation as PGA, while Poly(dl)LA is amorphous. All the isomeric forms degrade to form lactic acid, which exists naturally in the body. Lactic acid usually enters the tricarboxylic acid cycle and is

excreted as water and carbon dioxide. P(dl)LA generally degrades faster in aqueous media compared to its semi-crystalline counterparts, but it has been reported not to show significant mass loss until after 2 months. The end functional groups were also reported to make a difference; and if the polymer were acid-terminated instead of hydroxyl, more than 40% of mass loss was reported within 2 months [11]. The synthesis of the whole range of copolymers of PGA and PLA has been carried out and their properties have been explored. It has been shown that these intermediate copolymers are much more unstable with respect to hydrolytic degradation, as compared to their homopolymers [12]. Many studies on the biocompatibility of PLA and PGA have ascertained them to be sufficiently biocompatible, however there are some, [13-15] which show otherwise. Toxic solutions have been reported around PLA and PGA implants due to acidic degradation, however this is not a concern where the material volume is relatively small, as the smaller particles broken off can be phagocytosized by macrophages and multinucleated giant cells [16]. This is also not a concern when the material is implanted at a site where there is a flow or movement of fluid which would help prevent the build up of acid in one region.

Another widely studied polyester is polycaprolactone (PCL), which is a semi-crystalline polymer with a very low glass transition temperature and a low melting temperature as well. As PCL degrades at a much slower rate as compared to PLA, it is useful for longer-term applications. PCL has been reported to be non-toxic and tissue compatible [17].

Although these poly(α-hydroxy esters) may be synthesized using polycondensation of the hydroxyl acids, high molecular weights and their control and distribution are difficult to achieve via this route. More commonly, ring-opening polymerization of their cyclic monomers is carried out. Tin(II)-ethylhexanoate, or stannous octoate, is the most often used catalyst for the ring-opening polymerization of

cyclic esters as it is highly active and soluble in the monomer melts. The US Food and Drug Administration (FDA) has approved the use of this catalyst in small amounts for the preparation of polymers for implant applications [18]. The mechanism involved in the polymerization reaction has also been well studied [19,20]. It first involves the formation of a tin-alkoxide bond between the hydroxyl-containing initiator, in this case, butanediol, of the monomer and the tin catalyst. A monomer molecule then coordinates and inserts itself into this bond, and the polymerization propagates by the subsequent coordination and insertion of the next monomer. Due to the high reactivity of the catalyst, any small amounts of impurities containing hydroxyl groups in the reaction mixture can also take part in the reaction, hence preventing high molecular weight polymer chains from forming. Hence it is important to ensure that the monomer, catalyst and reaction environment is as free from moisture and as pure as possible.

1.1.2. Application of Biodegradable Polymers in Tissue Engineering

At present, there are three approaches to tissue engineering: using segregated cells or cell substitutes to replace cells; delivering tissue inducing substances to targeted locations including growth and differentiation factors; and the seeding and growing of cells on three-dimensional scaffolds [21]. Bioresorbable synthetic polymers have been explored as scaffold materials for the latter approach. These three dimensional scaffolds are built to accommodate mammalian cells, to guide cell growth and to regenerate three-dimensional tissue with proper structure and functions. The scaffolds are first fabricated in the desired sizes and shapes, the harvested cells from the patient are seeded onto the scaffolds, and the cell-scaffold construct is implanted at the wound site. Cells then migrate and proliferate to fill all regions of the construct. Besides external stimuli such as

growth factors, nutrients and other bioactive agents that modulate cell functions, the growth rate of the neo-tissue also depends a lot on the properties of the scaffolds, including their composition, structure, architecture and biocompatibility of the material used [22]. The major function of the scaffold is to provide a temporary support to body structures, allowing the stress transfer gradually to injured sites, and facilitating tissue regeneration on them. Hence the scaffold should have sufficient mechanical integrity to retain their shape and strength at the injury site until their function is done [23]. Usually, the properties of the scaffold should be as similar to the properties of the neo-tissue generated, in order to provide proper structural support in the healing stages. The load will gradually be transferred to the regenerated tissue as the scaffold degrades. The degradation rate of the scaffold should also ideally match the rate of neo-tissue formation so that the load is able to transfer over smoothly. In order to achieve this, several factors such as the polymer composition, conditions of loading and the environmental conditions have to be considered.

The material chosen for the scaffold must also be biocompatible, i.e. not induce any inflammatory response, extreme immunogenicity or cytotoxicity to cells, tissue or organs *in vivo*. Since the implants are to last for some time in the human body, the products resulting from the degradation process must also not invoke a harmful response. Hence bioresorbable polymers are preferred as their products are either eliminated with time and/or metabolized.

When the first phase of tissue engineering occurred in the 1990s, US Food and Drug Administration (FDA)-approved biomaterials of both natural and synthetic origin were used, coupled with conventional scaffold fabrication technologies. The main tissue of concern at the time was bone, as attempts were made to cure orthopedic injuries and diseases. The scaffold materials used included chitosan [24], collagen, fibrin, PLA, PGA

and PLGA. [25] Since then, there have been many studies on suitable biopolymers, both natural and synthetic, for hard tissue engineering [26].

These materials were evaluated to have sufficient mechanical strength to match the properties of bone and cartilage. Softer, more elastic tissue types, such as muscle, however, require a scaffold with high elasticity and a low modulus, properties that many of these polymers cannot achieve unmodified. Copolymers of PLA or poly(caprolactone) (PCL) with PGA [27]; with poly(trimethylene carbonate) (PTMC) [28-30]; with lysine [31]; and with PEG-monoamine [32], have been investigated for the engineering of soft tissue such as smooth muscle and cardiovascular tissue. However, in recent years, it has been shown that the application of cyclic mechanical strains during the smooth muscle tissue-engineering process results in increased elastin and collagen production and tissue organization, which in turn results in an overall increase in the mechanical properties of the final engineered tissue [33]. This means that not only does the material have to be soft and elastic, it has to have high fatigue strength as well and be able to undergo reversible strains. Crosslinking is the modification technique employed for polymers to acquire these combined properties.

1.1.3. Crosslinked Polymers for soft tissue engineering

Crosslinking is the introduction of physical or chemical bonds or links between the linear polymeric chains, resulting in a networked structure having relatively superior creep resistance and elastic properties.

Crosslinking is usually identified by the appearance of a *gel* point where there is a visible formation of an insoluble polymer fraction. This is due to the formation of the infinite network, which is formed when the polymer chains are crosslinked and a

macroscopic molecule is formed. The gel is insoluble in all solvents at high temperatures under conditions where polymer degradation does not occur, while the non-gel portion remains soluble [34]. The material then becomes a thermoset, which unlike a thermoplastic, degrades before going through the fluid state upon heating above a certain temperature. Hence due to this irreversible nature, the synthesis of a thermoset is usually carried out to produce the final material with the desired shape [35].

Besides the properties of the monomers or pre-polymers they are prepared from, the properties of these crosslinked polymers also depend on their crosslinking density, which is in turn dependant on the distance between crosslink points in the network. The shorter the chain length between crosslinks, the higher the crosslink density and this gives rise to higher glass transition temperatures and moduli [36]. Hence crosslinked polymers may be categorized as rigid thermosets having very high crosslink densities, or as elastomers having low crosslink densities.

Rigid crosslinked polymers have high moduli and low elongations. Due to the crosslinks between polymer chains, these materials also exhibit high creep resistance. Elastomers, on the other hand, are amorphous, crosslinked polymers with application temperatures above their glass transition temperatures. Therefore when an elastomer is in use, considerable chain segmental motion is possible. The ability of the long polymer chains to reconfigure and align themselves in the direction of a stress applied gives rise to the material's high elasticity. The crosslinks ensure that the chains are able to return to their original configuration when the stress is removed. Depending on the specific material, elastomers are able to extend up to 1000 % of their original lengths. Without the crosslinks, such deformations will result in irreversible extensions. However, elastomers generally have lower modulus values as compared to other flexible polymers.

The crosslinking of prepolymers to obtain elastomers can be done in several ways. The main objective is to keep the chain length between crosslinks as long as possible to allow for maximum extensions, hence targeting a low to moderate overall crosslink density. The crosslinks can either be chemical bonds or physical bonds.

Physical crosslinks are simply segments within the polymer chain, which are more rigid or "harder" as compared to other sections. These harder segments resist elongation, hence allowing the overall polymer to undergo reversible elongations. These are, however, temporary compared to chemical crosslinks and these polymers have inferior fatigue properties.

Chemical crosslinks can be introduced into linear polymers via the incorporation of reactive moieties and subsequent thermal or photoinitiation. Of these, photoinitiation is the most popular, due to the high rate of reaction that can be achieved at ambient conditions, depending on the light intensity used [37].

1.2. Motivation

Biodegradable elastomers find many applications in the biomedical field, especially in the fabrication of tissue engineering scaffolds or grafts for soft elastic tissue. This is because, the major component of most soft, elastic tissue: elastin, is also a crosslinked, elastomeric polymer. However at present, there are only two successful classes of synthetic elastomers available in the biomaterial market. One is that of polyurethanes. These are not biodegradable and if they do degrade in vivo, will produce toxic byproducts such as aromatic amines, which are reported to be carcinogenic. Another is the copolymer named "PLC", which is actually a copolymer of PLA and PCL in a 70:30 ratio. Both polyurethanes and PLCs have physical crosslinks, i.e. "hard" and

"soft" blocks, hence giving rise to mechanical properties that are more inferior, or more temporary as compared to materials having chemical crosslinks. For example, PLC exhibits great hysteresis loss when in use.

Hence there is a growing need for elastomers with controllable and biocompatible biodegradation behavior and tailorable properties. This project aims to address this need with the following objectives.

1.3. Objectives

This work generally aims to produce novel biodegradable elastomers with tailorable properties, based on chemical crosslinking methods. The projected future application for these polymers are as scaffold materials for soft and elastic tissue engineering, hence the targeted mechanical property range for these materials are to be matched to that of tissue such as skin, elastic cartilage, arteries and cardiac muscle. The tensile strength values reported for these natural materials range from 70 kPa to 7.6 MPa, and the ultimate elongation values range from 10 to 81%, some of which are 100% reversible [38]. Some reported Young's Modulus values for soft elastic tissue range from 5-6 kPa for lung tissue to 150 kPa for cardiac muscle [39].

Hence for the targeted application of soft tissue engineering, the main characteristics crucial for these polymers include biodegradability, biocompatibility, high reversible elongations and low Young's Moduli. Out of these, it is desirable for the biodegradation behaviour and mechanical properties to be tailorable within the range of properties of natural soft tissue, in order to deem these materials useful for a wide range of soft tissue types. In order to achieve these objectives in this work, elastomers were synthesized using two different chemical crosslinking routes: photocrosslinking and 2-

part epoxy amine crosslinking. UV-crosslinking was chosen for its ease of application and efficiency, while a 2-part system was chosen for its higher potential for tailorability.

1.4. Scope

In order to achieve the above objectives, soft, elastomeric polymers with tailorable properties had to be synthesized. UV-crosslinking was chosen as one of the synthesis routes, where a difunctional monomer would first act as a co-initiator in the ring opening polymerization of a known biodegradable and biocompatible polymer, such as PLA. The polymer would then be irradiated with UV to produce the crosslinks. The difunctional monomer used would therefore have to contain both hydroxyl groups for initiation of the polymerization, as well as photopolymerizable groups. Such a synthesis route to obtaining elastomers has not been previously explored; and since a wide range of biodegradable polymer types and targeted lengths could be explored, it is expected to be useful for obtaining tailorable properties as well. In order to attain low tensile strengths and high elongations, the degree of polymerization initiated by the difunctional monomer has to be high and the crosslinking amount low.

The second novel synthesis route investigated for obtaining soft, biodegradable elastomers would be a 2-part curing system based on epoxy-amine reactions. 2-part systems generally allow for greater tailorability as the amount and type of each part determines the final properties of the crosslinked polymer. Epoxy-amine curing had not previously been explored for the synthesis of biocompatible polymers due to the toxicity of commonly used epoxy and amine monomers. In this work, biocompatible amine-prepolymers would be synthesized based on PLA and PCL to overcome this issue. The epoxy component would be based on the biocompatible PEG polymer. In order to

achieve low tensile strengths and high elongations, the type and length of the 2 components used could be adjusted.

Besides chemical structure and physical characterization, the crosslinked polymers obtained via these novel synthetic routes would also be subjected to preliminary biodegradation and cytotoxicity tests in order to meet the objective of obtaining a biodegradable and biocompatible elastomer. No cell differentitation study will be carried out on these synthesized materials, as the main objective of this work is to obtain a polymer system with properties tailorable in the range required for soft tissue in general. Using the results from this work, it is hoped that ideal polymer candidates can be synthesized in future for the engineering of specific types of soft tissue by targeting and achieving the required mechanical and biodegradation properties.

2. Literature Review

2.1. Physically crosslinked polymers for soft tissue engineering

2.1.1. Polyurethanes

Polyurethanes have long been evaluated for various medical implants, especially biostable polyurethanes for long-term implants such as cardiac pace makers and vascular grafts, due to their excellent mechanical properties and excellent biocompatibility. A thermoplastic polyurethane essentially consists of hard segment (A) blocks and soft segment (B) blocks, arranged in a $(AB)_n$ order. The hard segment consists of a diisocyanate and a chain extender, which is a diamine or a diol. The soft segment consists of a polyol, such as a hydroxyl- or amine-terminated polyester, polyether, polycarbonate or even polyolefin. Both these segments form separate phases from a thermodynamic point of view. The hard segments act like "crosslinks", ensuring that the elongations provided by the soft segment are reversible. To achieve soft elastomeric properties for applications in soft tissue engineering, a higher concentration of soft segments, as compared to the concentration of hard segments, is simply used [40].

For polyurethanes to be utilized as tissue engineering scaffold materials however, they must be designed to have degradable chemical linkages, and there has been some interest in this area. A major problem has been the toxicity of their degradation products, especially those derived from the diisocyanate part. For example, polyurethanes based on diisocyanates such as 4,4-methylenediphenyldiisocyanate (MDI) and toluene diisocyanate (TDI) have been noted to have toxic degradation products [41,42]. In order to address this, other aliphatic diisocyanates such as lysine diisocyanate (LDI), hexamethylene diisocyanate (HDI) and 1,4-butanediisocyanate (BDI) have been used.

Poly(ester urethane) networks have been prepared from LDI and polyester triols based on lactide, caprolactone and their copolymers. Of these, the networks based on copolymers were found to be the most elastomeric, with elongations of up to 600% [43]. The same group then replaced the polyesters with glucose; hence the degradation products included lysine, glucose, ethanol and carbon dioxide [44]. The degradation products were reported to be harmless to cells below a certain concentration [45]. Guan et al used BDI instead of LDI because upon degradation, putrescine would be released, a polyamine that is important for cell growth and proliferation [46-48]. Polyurethanes exhibiting high elongations were also achieved by using star-shaped polyester precursors [49], and some of these resulted in no adverse tissue reactions when implanted in guinea pigs [50]. Other degradable polyurethane systems developed include those based on PCL, PEG, poly(hydroxy butyrate) and poly(hydroxy valerate) copolymers [51-53]; and those based on peptides [54]. Both these systems were reported to have promising initial *in vitro* cell growth results. Spaans et al used carbon dioxide to successfully incorporate pores into polyester urethanes, and these porous polymers were evaluated for the repair and replacement of knee-joint meniscus [55].

Polyurethanes present a very promising class of polymers for soft tissue engineering and there have been many reports on the biocompatibility of these degradable polyurethanes based on both *in vitro* and *in vivo* tests. However, it is still not known if there is any negative effect resulting from some of the degradation products over time in the body and how these degradation products are actually removed from the body.

2.1.2. Other physically-crosslinked systems

Besides urethanes, other di- or tri-block polymers can also display physically crosslinked characteristics. Li et al [56] synthesized such di- and tri-block polymers based on PLA and PEG. The PLA chains were the “hard” segments and the PEG was the hydrophilic and swollen component. Around 80 % mass loss was observed in these polymers within one month. PCL/PGA block copolymers have been reported to have elastic properties too, with elongations of up to 250 %. These have been explored for use in smooth muscle cell engineering and in vitro studies have shown growth and tissue formation on the scaffolds made out of these polymers [27].

Cohn et al [57] investigated tri-blocks based on PCL/PEG/PCL for soft tissue engineering. Hexamethylene diisocyanate chain extenders were used as the hard segments. The lengths of the different blocks affect the overall polymer properties, and the good biocompatibility of this system has also been shown [57].

Although these di- and tri-block polymers based on established degradable biopolymers rate high on biocompatibility as compared to polyurethanes, physically crosslinked systems still possess inferior mechanical stability as compared to chemically crosslinked systems. Hence when it comes to synthesizing scaffold material for the engineering of smooth muscle tissue, where fatigue strength is desirable as well, much research is going into the development of chemically crosslinked, biodegradable polymers.

2.2. Chemically crosslinked polymers for soft tissue engineering

2.2.1. Photocrosslinked polymers

2.2.1.1. Mechanism

The mechanism for photopolymerization is that of radical chain polymerization, consisting of initiation, propagation and termination steps (Scheme 1) [58]. The rate of initiation depends on the photoinitiator efficiency, photoinitiator concentration and light intensity. During propagation, radicals react to form long polymer chains. Chain transfer or radical termination occurs in the termination step to end chain growth.

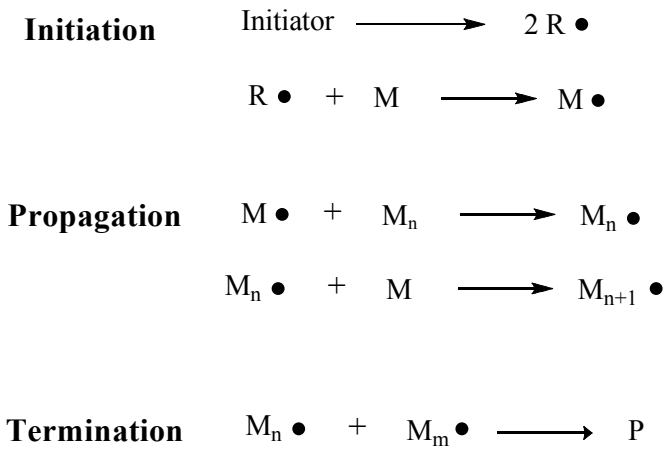

Scheme 1. Reaction mechanism in photopolymerization

From the start of the reaction, there is a region termed autoacceleration, where the polymerization rate increases with double bond conversion. This happens as the rate of termination decreases due to the restricted mobility of terminating macroradicals in the evolving 3-D network structure. After the polymerization rate reaches a maximum,

autodeceleration then occurs where the propagating chains become diffusion-controlled and the rate of termination increases [59,60]. Hence in highly crosslinked networks, a double bond conversion of 100% is almost never reached due to the restrictions on the mobility of the reacting species. In polymers aimed for use as biomaterials, low conversions can have significant effects. For example, it can result in less-than-desirable mechanical properties, making the polymer unsuitable for its end use. A low conversion would also mean a high concentration of unreacted monomers in the network, which can leach out over time and have toxic effects on the surrounding tissue.

2.2.1.2. Photocrosslinked Polymers based on bioresorbable prepolymers

The most common route to preparing elastomers via photocrosslinking is the crosslinking of functionalized prepolymers. Prepolymers are first synthesized with the desired molecular weights, then functionalized with unsaturated groups and subsequently irradiated, with a photoinitiator added, to obtain the crosslinks between chains. The unsaturated groups may be introduced to the ends of the polymer chains, or anywhere along the backbone. Due to the relatively high reactivity of acrylic and methacrylic double bonds to UV initiation, these have been extensively used in the functionalization step to introduce unsaturated groups. For the prepolymers, polymers such as PEG, PLA and PCL have been extensively used due to their known biodegradability and biocompatibility.

PEG can be reacted with acryoyl chloride or methacryoyl chloride in the presence of triethylamine to add photoreactive vinyl groups, which can subsequently be reacted to form crosslinks [61]. On its own, crosslinked PEG is a hydrogel with weak mechanical properties. This material has been explored for use in drug delivery applications [62] or

the delivery of growth factors [63,64], genes [65] or DNA [66]. In order to apply PEG to tissue engineering applications however, it has to be copolymerized with poly(α-hydroxy esters) such as PLA, PGA or PCL, in order to achieve better mechanical properties.

In 1993, Sawhney et al [67] copolymerized PEG with PLA and PGA, before functionalizing the copolymers with acrylate groups using acryoyl chloride. These were then irradiated with UV light to form networked polymers. The crosslinked polymers had up to about 66 % gel content. The degradation rates were tailorable, depending on the length and components of the main chain. It was found that the shorter the main chain, the slower the degradation rate, due to the denser crosslinks formed. The more PEG units in the main chain, the faster the degradation rate, due to the greater absorption of water into the polymer. Metters et el [68-70] studied the degradation behavior of these PEG-PLA networks in-depth using a statistical kinetic model which accurately predicts the cleavage of the crosslinks. Due to the presence of the PEG units in the backbones of these polymers, which give them hydrogel characteristics, they have been targeted for use as matrices in drug delivery systems. There has been some work however on utilizing these networks for tissue engineering applications, mostly for the regeneration of musculoskeletal tissue, e.g. cartilage [71].

In 2000, Kim et al [72] extended the work by Sawhney et al to include the more hydrophobic polypropylene glycol (PPG) and poly(tetramethylene glycol) (PTMG) to copolymerize with PLA, besides just PEG. These were then similarly end-functionalized with acrylate groups for photocrosslinking. Degradation times varied from 20min to 7 days. Storey et al [73] used PLA and PCL triols, instead of diols, for achieving a higher crosslink density and therefore better mechanical properties. This method also eliminated the need for solvents as the triols are less viscous. Strengths of up to 50 MPa and strains of up to 12 % were achieved. A similar method of using multi-arm, photocrosslinkable

prepolymers was used by Takao et al [74] in 1994 but no mechanical properties were reported. In 2004, Amsden et al [75] reported a completely amorphous, crosslinked star-copolymer of acrylated PLA and PCL, with their glass transition temperatures below physiological temperatures such that they are elastomeric in vivo.

Acrylate groups can also be introduced by other means instead of using acid chlorides to functionalize OH-terminated polyesters. Coullerez et al [76] carried out transesterification using a high molecular weight PLA and a low molar mass diacrylate, however this resulted in fairly rigid networked polymers. Pendant groups such as hydroxyl [77] or carboxyl [78] have also been incorporated along the main PLLA or PCL chains for subsequent acrylation or methacrylation. The degree of methacrylation can be controlled for tailorable crosslink densities.

Besides the usual PEG or polyester prepolymers, photocrosslinkable polyfumarate-based materials have also been developed [79-82]. Specifically, poly(propylene fumarate)s are the copolymers studied, and these are linear polymers with repeating units of both ester groups and unsaturated groups along its main chain. The degradation of these materials leads to the production of fumaric acid, which is also a substance naturally found in the tricarboxylic acid cycle. Due to the short curing times needed, these polymers have been used in injectable formulations where *in situ* curing could be carried out. However, these crosslinked polymers were mainly aimed for hard tissue engineering [83-85], as high crosslink densities, hence high compressive strengths, were inevitably obtained due to the numerous crosslinking sites along the main polymer backbone.

Poly(vinyl alcohol) (PVA) has also been functionalized with acrylates and methacrylates for subsequent photocrosslinking [86-90]. These crosslinked polymers are hydrogels due to their high water content hence they have been used in applications such

as contact lenses. Studies carried out on the degradation of these hydrogels indicate that they degrade via hydrolysis of the ester linkages but only until there is no longer an infinite network present, only branched soluble chains. This is when reverse gelation takes over. In tissue engineering, these polymers, as well as their copolymers, have been explored as scaffolds for hard tissue such as cartilage [91].

Yet another group of polymers that has been functionalized with acrylates and then photocrosslinked is that of poly(-amino ester)s. Anderson et al [92] produced and characterized a whole series of such polymers using different amines and diacrylates, resulting in varying hydrophobicity, degradation times and mechanical properties. The effect of the macromer molecular weight on the network properties and cellular attachment has also been studied [93].

2.2.1.3. Photopolymerization of multifunctional monomers

A more convenient method to obtain photocrosslinked polymers is by polymerizing multifunctional monomers.

Anseth et al [94-96] prepared a series of multifunctional monomers having both photopolymerizable (acrylate) and biodegradable (anhydride) moieties in their structures. The dimethacrylated anhydride monomers were synthesized from sebacic acid and subsequently photopolymerized, to obtain crosslinked biodegradable polymers. This method required only a simple, 2-step synthesis procedure; in just 2 min, maximum conversions of up to 96 % were achieved when irradiated with UV light, and with a photoinitiator added. Due to the high concentration of double bonds available per unit volume, relatively high crosslink densities were obtained, hence most of the final polymers were rigid. Tensile moduli of up to 2 GPa were observed and degradation times

ranged from 1 week to nearly 1 year depending on the monomer length, with moduli retentions of over 90 % at 40 % mass loss. The biocompatibility responses from in vivo tests of the networks and in situ curing were acceptable for their use as osteo-compatible materials [97,98]. The attractiveness of this method is the ability to use a wide range of monomer types in order to achieve varying properties. However only rigid thermosets were obtained, due to the resulting relatively short chain lengths between crosslinks. No other photocrosslinked, biodegradable systems based on similar multifunctional monomers have been reported to date.

2.2.1.4. Issues with current photocrosslinked systems

The use of acrylated or methacrylated precursors has raised some safety issues. Bruining et al [99] reported on the intrinsic cytotoxicity of their system, which uses dimethylamino ethyl methacrylate networks, crosslinked with dimethacrylate crosslinkers. A dose-dependant cytotoxic reponse by the degradation products of such crosslinked systems has also been reported [100]. Generally, a very high degree of curing and high crosslink density is required of these polymers for minimal adverse effects on tissue. This is in contrast to what is needed for elastomers. Besides acrylates and methacrylates, there have also been studies using other photo-reactive moieties for elastomer preparation. For example, there have been reports on maleic [101] or the more reactive itaconic unsaturated bonds [102]. Nagata and Sato [103] also synthesized PCL diols chain extended with a diacyl chloride of 4,4'-(adipoyldioxy) dicinnamic acid for subsequent photocrosslinking without the need for a photoinitiator. However there has been no biocompatibility study on these materials.

Furthermore, all of the photocrosslinked systems mentioned above result in polymers with or without limited functional groups along the main chain. Such functional groups aid the covalent conjugation of biomolecules such as peptides that enhance cell adhesion; and/or growth factors that induce a specific and desired cellular response. The ability to attach these biologically active molecules is a property crucial for a material used as a scaffold in tissue engineering [32].

2.2.1.5. Photopolymerization of diallyl dicarboxylates

In general, the allyl functionality has not received much interest, compared to groups like acrylate and vinyl, due to its lower susceptibility to polymerize. This is largely due to hydrogen abstraction from the carbon adjacent to the double bond during chain propagation. This "degradative chain transfer" results in resonance-stabilized allyl radicasl that are less active or have less tendency to initiate new polymer chains, leading to reaction termination. A review by Matsumoto [104] summarizes his group's extensive work on the reaction kinetics of such multiallyl compounds. Their key findings include the enhanced polymerizability of diallyl tartrate, a compound derived from tartaric acid, a renewable resource found abundantly in several plant species. This is in comparison to other diallyl esters of aliphatic dicarboxylic acids such as diallyl succinate and diallyl oxalate due to its pendant hydroxyl groups, which were reported to entropically increase the ability of the allylic radical to re-initiate the polymer chain [105]. However, there has been no further study of diallyl tartrate polymerization, despite the potential of this material in biomaterial applications, because the rate and extent of monomer conversion *via* thermal initiation is still too low for practical applications. Ohata et al [106] reported only 10 % monomer conversion after 4 h at a polymerization temperature of 60 °C, using

2,2-azobisisobutyronitrile (AIBN) as the thermal initiator at a concentration of 0.04 mol/l (approx. 1 wt%).

The first part of the work reported here aims to increase the rate and extent of diallyl tartrate polymerization using photoinitiation instead of thermal initiation as it is well-known that photoinitiation generally results in greater rates of reaction, even at ambient conditions, depending on the light intensity used. The resulting polymer, after some further modification, is aimed for use as a scaffold material in soft tissue engineering. Diallyl tartrate not only has both ester bonds and polymerizable allyl functionalities in its chemical structure, it also has pendant hydroxyl groups, useful for any future biomolecule attachment.

2.2.2. Thermally crosslinked polymers

A method that allows for more tailorability is a 2-part thermal curing system, consisting of either a prepolymer and a crosslinker; or two reactive oligomers. The reaction between the prepolymer and crosslinker can be that of addition or condensation, but the main criterion is to have more than 1 functional group per reacting compound, in order for the reaction to result in a crosslinked network.

Polycondensation between glycerol and sebacic acid has been explored using a molar ratio of 1:1, obtaining the polymer: poly(glycerol sebacate) (PGS). This has a low crosslink density and a molecular weight between crosslinks of 18 000 g/mol [107,108]. Free hydroxyl groups on the polymer chains made the polymer surface very hydrophilic and contributed to mechanical properties by hydrogen bonding. When PGS degrades, glycerol and sebacic acid are formed again; and these are non-toxic degradation products. In fact, glycerol and copolymers containing sebacic acid have been approved for their

medical applications by the U.S. Food and Drug Association (FDA) [109]. PGS had a Young's Modulus of around 0.3 MPa, and elongations of at least 270 %. These mechanical properties are similar to those of some types of soft tissue. PGS was also shown to be biocompatible, even more so than PLGA, with significantly less fibrosis and inflammation seen at the implant site [110]. It was also shown to degrade by a surface erosion mechanism, resulting in a linear and gradual decrease in mass and mechanical properties over time [107].

This work was extended by Bruggeman et al to using polyols, such as xylitol and maltitol, instead of glycerol to react with sebacic acid [111]. These crosslinked polymers had Young's Modulus values ranging from 0.4 MPa to nearly 400 MPa; and elongations from 11 % to around 200 %. The varying properties were obtained by changing the polyol used or by changing the stoichiometric ratio of the acid and polyol added.

Yang et al similarly used condensation reactions to form networked polymers, but based on citric acid. It was found that citric acid was able to react with many hydroxyl-containing monomers under mild conditions [112]. Although a series of aliphatic diols were explored, the polymers formed with 1,8-octanediol (POC) and 1,10-decandiol (PDC), were focused on. These polymers had Young's modulus values ranging from approximately 2 MPa to 14 MPa; and up to 500 % maximum elongation to break [112,113]. POCs have already been evaluated for applications as scaffold materials in tissue engineering [114]. Composites of these polymers with hydroxyapatite (HA) [115], chitosan and PLA [116] have been explored for orthopedic tissue engineering.

Nagata et al mixed succinic acid, 1,12-dodecanedicarboxylic acid, 1,18-octadecanedicarboxylic acid or terephthalic acids into similar polycondensation reactions between sebacic acid and glycerol to obtain copolyester networks with higher crosslink density [117]. The same group also synthesized elastomeric polyesters from the

polycondensation between multifunctional aromatic carboxylic acids and PCL diols; and elongations of up to 500 % were observed [117,118].

Lee et al also synthesized crosslinked polymers based on condensation reactions between malic acid and 1,12-dodecandiol [119]. These were aimed specifically for soft tissue engineering applications. The polymer properties were varied using different curing ratios of acid to alcohol monomers. Modulus values obtained ranged from 1 MPa to about 4 MPa and elongations of up to about 700 % were obtained.

Besides polyesters, crosslinked polymers based on amide linkages have also been synthesized via condensation reactions [120]. These poly(ester amide) elastomers were polymerized using an amino alcohol, a polyol and a diacid. Modulus values averaged around 2 MPa, and elongations of up to 90 % were achieved. Amine groups found on the polymer surface could be used for biomolecular attachment. Favorable *in vitro* and *in vivo* cellular responses were reported.

2.2.2.1. Issues with current thermally crosslinked polymers

One important issue when it comes to polycondensation reactions is that the yield of the reaction is generally low; it is very difficult for the reaction to reach high conversions. A very strict stoichiometric ratio is required to ensure maximum conversions.

Furthermore, all the above mentioned thermally crosslinked systems have modulus values which are still too high for applications in soft tissue engineering, except for PGSs. PGS has, in fact, been explored for use in the engineering of myocardial tissue [121]. However the only way to obtain tunable properties for this system is by altering the curing temperature.

2.2.2.2. Epoxy-amine systems

The epoxy resin system is the most common 2-part curing reaction employed in many commercial applications. The basic chemistry of epoxy resins involves addition reactions between a diepoxide and a polyfunctional amine, leading to a crosslinked system, which is generally insoluble and chemical-resistant. The general reaction between an epoxy group and an amine group is shown in Scheme 2. After the primary amine reacts, the secondary amine reaction becomes catalyzed by the increasing number of hydroxyl groups in the system [122].

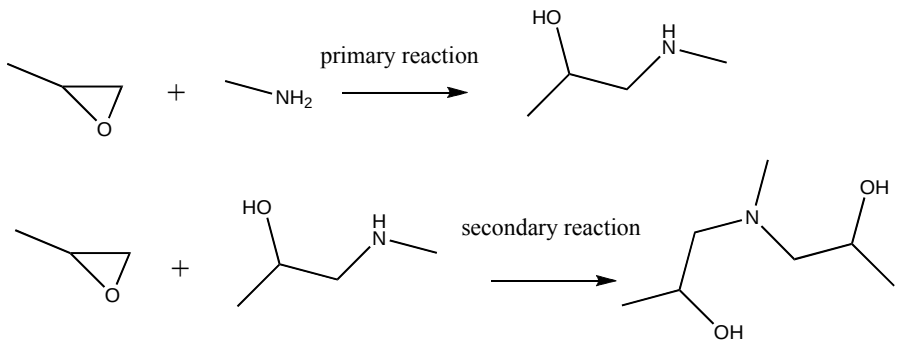

Scheme 2. Mechanism for epoxy-amine reactions

For most commercial use, the diepoxide is derived from epichlorohydrin and bisphenol A. The reaction conditions can be controlled to produce either a simple diglycidyl derivative of bisphenol A or oligomeric compounds terminating in epoxide groups. The polyfunctional amine reactant can be a simple small molecule or an oligomeric compound with primary amine terminal groups. The rate of curing depends on the reactivity of the nucleophilic amine groups and the temperature. The many hydroxyl groups contained in the resulting crosslinked polymer provide hydrogen bonding, useful for adhesion to polar surfaces such as glass or wood.

There has been little reported work so far on using such chemistry in the synthesis of biopolymers, possibly due to the reported toxicity of epoxy resins. However, this toxicity occurs during the use of the separate component monomers, which may be packed as powders or liquids; and give off irritable vapors or cause skin irritation. Examples of two highly toxic monomers used commonly are n-butyl glycidyl ether and diethylenetriamine; Epichlorohydrin is also the usual suspected carcinogen and curing agents such as simple aliphatic amines are suspected irritants. Hence, if higher molecular weight components or components based on non-toxic molecules are used instead, the risk of toxicity can be greatly reduced.

The synthesis of elastomeric bioresorbable polymers based on epoxy-amine curing has been reported by Yaganeh et al [123,124] to date. However these were actually polyurethanes, which contained chemical crosslinks as well. Epoxy-terminated polyurethanes based on PEG and PCL were prepared and reacted with 1,6-hexamethylene diamine. Gel contents of over 90 % were reported after 5 hours of reaction time at 60 °C. The reported elastic modulus values ranged from 1.6 MPa to 11.3 MPa and elongations of up to 400 % were seen. The degradation rate increased with higher amount of PEG polymer used in the initial mixture; and the crosslinked material with only PEG showed 45 % degradation by mass in less than 200 days.

The fourth chapter of this thesis explores the use of such epoxy-amine chemistry in the development of a 2-part curing system, in order to obtain a series of soft, elastomeric biodegradable and biocompatible polymers. The amine compound is based on the biopolymer, PCL, and the epoxy compound is based on the biopolymer, PEG. The final polymer is expected to have free residual amine functional groups on its surface for any future covalent attachment of peptides or growth factors. This system is expected to

have potential for tailorability of the final degradation and mechanical properties of crosslinked polymers obtained.

3 Materials and Methods

3.1. Materials

3.1.1. Photocrosslinked System

The reagents required for diallyl tartrate synthesis:

L(+)-Tartaric acid (99 %) and allyl bromide (98+ %) were purchased from Lancaster Synthesis, England. Triethylamine for synthesis was obtained from MERCK, Germany. The solvents used were N,N-dimethylformamide (DMF, 99.9 %) of biotech grade from Sigma-Aldrich and ethyl acetate of analysis grade from J.T.Baker. Sodium hydrogen carbonate ($NaHCO_3$), sodium chloride (NaCl) and anhydrous magnesium sulphate ($MgSO_4$) were from Kanto Chemical, Japan.

The reagents required for allyl poly(d,l-lactide) synthesis:

D,l-lactide (3,6-dimethyl-1,4-dioxan-2,5-dion) and tin octoate ($Sn(Oct)_2$), were obtained from Sigma-Aldrich, Germany. Toluene of analysis grade, and fuming hydrochloric acid (HCL, 37 %, GR for analysis) were obtained from MERCK, Germany. Hexane for actual analysis was from J.T. Baker.

The reagents required for UV-curing and characterization:

The photoinitiator 2,2-dimethoxy-2-phenylacetophenone (DMPA, 99%) was obtained from Aldrich, Germany and dichloromethane (DCM) of HPLC grade was supplied from Tedia Company, USA.

3.1.2. Epoxy-amine system

ε-Caprolactone, d,l-lactide, stannous octoate and the initiator, 1,4-butanediol (99+ %), were purchased from Sigma-Aldrich. Trifluoroacetic acid (99 %) and diisopropylcarbidiimide (DIPC) were also purchased from Sigma-Aldrich. Di-boc lysine dicyclohexylammonium salt was purchased from iDNA Biotechnology Pte Ltd, Singapore. The materials for the synthesis of the catalyst for acid-alcohol coupling, DPTS: p-toluene sulfonic acid and dimethylaminopyridine (DMAP), were also from Aldrich. The solvents: Chloroform, dichloromethane, diethyl ether, ethyl acetate and methanol of reagent grade were purchased from J.T. Baker. All solvents were distilled before use.

3.2. Synthesis Methods

3.2.1. Photocrosslinked system

Synthesis of diallyl tartrate:

The synthesis of diallyl tartrate was carried out as reported [125]. In a typical procedure, tartaric acid (30 g, 0.2 mol) was dissolved in 150 mL of DMF. While cooling the reaction vessel to 0 ºC using an ice bath, triethylamine (111.2 mL, 0.8 mol) was added under nitrogen flow. The ice bath was removed and the reaction mixture was allowed to warm to room temperature. A solution of allyl bromide (69.15 mL, 0.8 mol) in 100 mL of DMF was added to the reaction vessel in portions over 3 h. The reaction mixture was then stirred for 24 h at room temperature under nitrogen. DMF was removed under vacuum and 400 mL of ethyl acetate was added. The mixture was poured into a separation flask and washed twice with 100 mL of water, twice with 100 mL of ice-cold saturated aqueous sodium hydrogen carbonate solution and then twice with 50 mL of ice-cold

saturated aqueous sodium chloride solution. The aqueous layers were collected and stored for future extraction using 400 mL of ethyl acetate, if the final yield obtained is low. The organic layers were combined and dried using anhydrous magnesium sulphate. Filtration was then carried out and ethyl acetate removed under vacuum to obtain a yellow liquid.

UV-polymerization of diallyl tartrate:

A modulated differential scanning calorimeter (DSC 2920, TA Instruments), fitted with a UV-lamp and a differential photocalorimeter, was used for the polymerization. For the preparation of samples for DPC, a stock solution of DMPA in dichloromethane with known concentration was prepared and the required amount was added to diallyl tartrate from this solution. Samples from this solution were placed in standard aluminum pans and then dried until an equilibrium mass of 5.5 ±0.4 mg was achieved. The pans were placed on the heat cell and covered with a quartz window. The reference used was a 1 mg sample of fully cured epoxy resin. Under 50 cc/min of nitrogen purging, the samples were polymerized for a fixed time period of 10 min using UV irradiation of 40 mW/cm^2, as measured by a photometer (Model IL 1400A from International Light, Massachusetts). The DPC experiments were carried out using computer-controlled methods. The samples were first allowed to equilibrate at the selected temperature and then held isothermally without UV exposure for 1 min. The UV lamp was then switched on and the sample irradiated isothermally for 10 min before the lamp was switched off. The heat flow with respect to exposure time for each sample was obtained and the curves analyzed using TA Universal Analysis Specialty Library software, from which parameters such as polymerization enthalpy, time to reach peak maximum, percentage reacted at peak maximum and induction time (time for 1% conversion) could be obtained.

For the preparation of samples for dynamic mechanical analysis (DMA), rectangular Teflon molds of dimensions 35 mm × 12 mm and × 2 mm were used and a fixed DMPA amount of 4 wt% was added to all samples. UV-irradiation of the samples was carried out at an intensity of 40 mW/cm^2 on a platform at a distance of 0.2 m from the UV source. Photopolymerization was done in air at room temperature until the samples visibly hardened in the molds. For the preparation of samples for both the biodegradation and cytotoxicity study, circular Teflon molds of diameter 20mm and 2mm thickness were used. The photopolymerization procedure was the same as for the preparation of the samples for DMA.

Incorporation of Poly(d,l-lactide) oligomers:

Ring-opening polymerization of lactide was first carried out using stannous octoate as the catalyst according to a typical procedure [126]. 0.02 mol% of stannous octoate (with respect to the amount of lactide monomer) in toluene was added to a predetermined amount of diallyl tartrate under nitrogen and stirred for 15 min. D,l-lactide was then added and the total toluene amount made up to 10 ml/g concentration with respect to lactide. The reaction mixture was heated to 130 ºC and the toluene was allowed to reflux for 24 h under nitrogen flow. The reaction was stopped and toluene was removed under vacuum.

Ring-opening polymerization was also carried out using triethylaluminum catalyst as similarly reported [127]. To a vacuum-dried, predetermined amount of diallyl tartrate, 2.2 times molar amount of the catalyst in toluene solution was added at 0 ºC under nitrogen and the mixture allowed to stir for 2.5 h at room temperature. Lactide was then added and the total toluene amount made up to 10 ml/g with respect to lactide. The reaction mixture was heated to 70 ºC and allowed to stir under nitrogen for 24 h. Molar

equivalents (with respect to diallyl tartrate) of hydrochloric acid (0.1 M) were then added to stop the reaction. The salt formed was then removed by filtration and toluene removed under vacuum. Chloroform was added to the reaction product and the polymer was precipitated into cold hexane.

3.2.2. Epoxy-amine system

3.2.2.1. Synthesis of amine-functionalized prepolymers

Ring-opening polymerization:

The ring-opening polymerization reaction was carried out without solvent. The two prepolymers prepared were PCL homopolymer of targeted molecular weight 2 000 g/mol, and the random copolymer of PCL and P(dl)LA in a 50/50 ratio of target molecular weight 10 000 g/mol. For each polymer, the required ratio of 1,4-butanediol to monomer, according to the targeted molecular weight, was used (See Appendix II). In a typical procedure to obtain a PCL homopolymer of target molecular weight 2000 g/mol, 1.35 g of butanediol (0.015 mol) was added to 30 g of caprolactone monomer (0.26 mol) and 1.5 g of stannous octoate in a reaction vessel and the mixture flushed with nitrogen for 10 min. The mixture was then heated to 150 °C under nitrogen and stirred vigorously for 3 h. It was then allowed to cool to around 50 °C, before 150 mL of THF was added. The polymer was precipitated from this solution into 300 mL of hexane. A white solid is obtained after filtration and subsequent drying of the residue. Typical yields obtained are ~70 % for the PCL homopolymer of target 2000 g/mol and ~89 % for the PCL-PLA copolymer of target 10 000 g/mol.

End-group functionalization:

The catalyst, DPTS, was first synthesized. 39.9 g (0.21 mol) of 4- tolunesulfonic acid (PTSA) was added to 200 mL of toluene and heated to reflux with a Dean-Stark trap and a water cooled reflux condenser attached. The reaction was stopped when 3.78 mL of water was collected in the Dean-Stark trap. The resulting solution was then cooled to room temperature. A solution of 23.2 g (0.18 mol) dimethylaminopyridine (DMAP) in 400 mL of toluene was prepared separately in a 1-L Erlenmeyer flask. The PTSA solution was added to the contents of the Erlenmeyer flask under stirring. The mixture was stirred for one hour and the precipitated product was collected via filtration. The residue was dried under a stream of nitrogen and recrystallized from 400 mL of dichloroethane to obtain 46.3 g of the product, DPTS. Yield: ~80 %

The dicyclohexyammonium (DCHA) salt was then removed from di-boc lysine before the coupling reaction was carried out. 1 part of the DCHA salt (The amount measured was twice that needed for the coupling reaction later on.) was suspended in 10 volume parts of cold ethyl acetate (-20 ºC). Cold (5 ºC) phosphoric acid (10 % in aqueous solution) was added under stirring until the salt completely dissolved and two clear phases appeared. The pH of the lower, aqueous phase should read 2-3. The aqueous phase was removed and the organic phase was washed once with 2 volume parts of cold phosphoric acid. The aqueous phase was removed again and the organic phase washed three times with 2 volume parts of cold water. The pH of the aqueous phase should read 0-4. The organic phase was then dried over anhydrous sodium sulfate, filtered and the filtrate transferred to a reaction vessel before drying in vacuo to obtain a viscous, clear oil.

The weight of the free lysine obtained in the reaction vessel was measured and 1/3 the molar amount of the OH-terminated polymer was added to it. Dichloromethane was added such that 1 g of polymer is dissolved in 10 ml of solvent. Under nitrogen atmosphere and stirring, an equal molar amount (compared with the amount of OH-terminated polymer used) of catalyst, DPTS, was added. When all the reagents have been completely dissolved, an equal molar amount (compared with the amount of lysine used) of coupling agent, DIPC, was added. The reaction was left at room temperature under nitrogen atmosphere for 24 h. The polymer obtained was precipitated into 20 volume parts of cold methanol and left at 5-8 ºC overnight before filtering. The residue after filtration was then dried at 40 ºC in vacuo. Typical yield obtained for lower molecular weight PCL homopolymer = ~53 %. Typical yield obtained for higher molecular weight PCL-PLA copolymer = ~76 %.

Deprotection of amine groups:

The protected amine-functionalized polymer was dissolved in dichloromethane such that 1 g of polymer is dissolved in 10 ml of solvent. For every 1 g of polymer used, 3 ml of trifluoroacetic acid was added under nitrogen atmosphere at 0 ºC (ice bath). The reaction was left stirring at 0 ºC for 4 h. The acid and solvent were then mostly removed in vacuo at room temperature before the polymer was precipitated three times into cold diethyl ether. The residue after filtration was then dried at 40 ºC in vacuo to obtain the amine-terminated pre-polymer. Typical yield obtained for lower molecular weight PCL homopolymer = ~74 %. Typical yield obtained for higher molecular weight PCL-PLA copolymer = ~85 %.

3.2.2.2. Curing of pre-polymers with crosslinkers

The amine-terminated polymer was mixed with 2 times the molar amount of polyethylene glycol diglycidyl ether directly in a mold. The mold was heated to about 90 °C to allow the contents to melt completely. After vigorous stirring with a spatula for about 10 min, the molds were placed in an oven and the temperature was increased to the cure temperature needed (140 ºC for the PCL prepolymer and 160 ºC for the PCL-co-PLA prepolymer). The reaction mixtures were kept in the oven until gelation (no visible flow at cure temperature) was observed.

3.3. Characterization methods

3.3.1. Chemical properties

Nuclear Magnetic Resonance, NMR, spectra of samples were recorded on a 400 Ultrashield spectrometer (Bruker Instruments) in deuterated chloroform with TMS as the internal reference. Chemical shifts were reported in parts per million (ppm).

Fourier Transform Infra-Red, FTIR, spectra were obtained either from thin film samples or thin pellets on an Excalibur Series spectrometer (Bio-Rad Laboratories). Thin film samples were prepared by casting a chloroform solution of the sample onto a potassium bromide crystal disk and drying in a vacuum oven at room temperature to remove the solvent. Thin pellet samples were prepared for insoluble materials by mixing the powdered form of the specimen with potassium bromide powder. 80 MPa of pressure was applied to this mixture in a circular die to obtain the thin pellet. Bio-Rad Win IR Pro Version 3.1 software was used for data acquisition and presentation.

Molecular weights (M_n and M_w) and molecular weight distributions or polydispersities (PD) were determined relative to polystyrene standards by size exclusion chromatography, SEC. Tetrahydrofuran was used as the eluent, delivered at 0.3 ml/min under 400 MPa. A Waters Series 2414 refractive index detector and Waters 515 HPLC pump was used. The sample concentrations used were 20-25 mg/ml in tetrahydrofuran.

Contact angle measurements were performed using a Dynamic Contact Angle and Surface Tension Analyzer FTÅ 200 (First Ten Ångstroms instruments).

3.3.2. Network Characterization

Samples of the bulk polymer were extracted for 24 h with 150 mL of refluxing methylene chloride using a Soxhlet extractor. The insoluble solid obtained was dried under vacuum until there was no further decrease in mass. The percent gel content, which is the insoluble portion of the polymer, gives the yield of the crosslinked polymer. This can be evaluated by the following equation:

$$\%Gel\ content = \frac{W_i - W_f}{W_i} \times 100\% \qquad \text{---------- (7)}$$

where W_i is the initial dry mass of the bulk polymer sample before the extraction and W_f is the final dried mass of the polymer after extraction.

The degree of swelling by mass and time taken to reach swelling equilibrium were attained by immersing pre-weighed samples in 20 mL of PBS and measuring the wet weight, W_w, after regular time intervals. The time taken to reach swelling equilibrium

is the time taken for W_w to reach a constant value, W_s, after the initial increase due to water absorption. The degree of swelling is calculated by the equation:

$$\%Swelling = \frac{W_s - W_i}{W_i} \times 100\% \quad \text{---------- (8)}$$

3.3.3. Mechanical and Thermal properties

A Thermal Gravimetric Analyzer (TGA, TA Instruments) was used to measure the material's thermal stability. A temperature ramp was carried out from room temperature to 600°C at 10 °C/min in air for the photocrosslinked polymer.

A Modulated Differential Scanning Calorimeter (MDSC, TA Instruments) was used to measure the material's thermal behavior. A temperature ramp was performed from -60 °C to 250 °C at 2 °C/min or 5 °C/min, using a modulation amplitude of 0.3 °C and 0.8 °C respectively every 60 seconds in order to determine the polymer's glass transition temperature, T_g. For measurement of the melting temperature and/or melting enthalpy, a ramp was performed in the standard mode from room temperature to 200 °C at 5 °C/min. For epoxy-amine curing studies, a temperature ramp was performed from room temperature to 250°C at 2 °C/min, using a modulation amplitude of 0.3 °C every 60 seconds.

A Dynamic Mechanical Analyzer 2980 (DMA, TA Instruments) with a single cantilever clamp was used to measure the mechanical properties and glass transition temperature of photocrosslinked material. The amplitude and static force used were 10

μm and 1.0 N respectively at a frequency of 1 Hz. The samples were heated from room temperature to 160 °C at 10 °C/min. Triplicate samples were tested.

The mechanical properties of the final epoxy-amine crosslinked polymers were obtained from stress-strain curves using a microtester 5800, TA Instruments with a load cell of 50 N. The measurements were carried out on samples of 0.5 mm thickness, stamped out with an ASTM D 638 die. The loading rate used was 1 mm/min for obtaining typical stress-strain curves until the break point. Cyclic tests were carried out at 10 mm/min for both the loading and unloading step. The load values experienced by the grips were measured for each step as the sample is extended and distended.

3.3.4. Calculations

FTIR:

For FTIR measurements, an approximate degree of conversion was measured using this equation

$$Degree\ of\ Conversion\,(\%) = 100 - \frac{[Abs(C{=}C)_{1646} / Abs(C{=}O)_{1742}]_{polymerized}}{[Abs(C{=}C)_{1646} / Abs(C{=}O)_{1742}]_{monomer}} \times 100\% \qquad \text{----(1)}$$

where *Abs* is the height of the absorbance peak corresponding to the functional group stated in brackets, occurring at the specific wavenumber stated. For photopolymerized diallyl tartrate, the peak corresponding to the allyl functionality appears at 1646 cm^{-1} and in order to measure any change in this peak before and after polymerization, an internal reference peak corresponding to the ester functionality at 1742 cm^{-1} was used, as this functional group is not expected to be affected by the reaction. This method is in

accordance with that used in similarly reported FTIR measurements for degree of conversion studies [128].

Monomer conversion was also calculated according to the equation [129]

$$\%Conversion = \frac{\Delta H_{experimental}}{\Delta H_{theoretical}} \times 100\% = \frac{\Delta H_{experimental}}{(f\Delta H_f)/M} \times 100\% \quad \text{----(2)}$$

where $\Delta H_{experimental}$(J/g) is the experimental enthalpy of polymerization obtained with the help of the software mentioned earlier from the area under the recorded DPC thermogram curves; and f is the number of double bonds in the monomer, ΔH_f (J/g) is the reaction enthalpy of the type of double bond and M (g/mol) is the molar mass of the monomer. For diallyl tartrate: f = 2, M = 230 g/mol, $\Delta H_f \approx$ 85 kJ/mol [130], and hence the theoretical enthalpy of polymerization calculated, $\Delta H_{theoretical}$ = 739.1 J/g.

DPC:

The rate of reaction from DPC measurements was based on the following rate law [131]

$$d\alpha_{(t,T)}/dt = k_{(T)} f(\alpha)$$

where α is the fraction of the converted monomer, $k_{(T)}$ is the temperature-dependent rate coefficient and f(α) is a function describing the hypothetical model of the reaction mechanism. Assuming an autocatalytic kinetic model, the most common differential equation [132] for this is

$$R_{(T)} = d\alpha_{(t,T)} / dt = k_{(T)}\alpha^{m}(1-\alpha)^{n}[-\ln(1-\alpha)]^{p}$$

where $R_{(T)}$ is the temperature-dependant rate of reaction; and m, n and p are the partial orders of reaction for the initiation, propagation and termination steps respectively.

In such an autocatalyzed curing reaction, the assumption is made that at least one of the reaction products is also involved in the propagating reaction. It is thus characterized by an accelerating isothermal conversion rate that usually reaches its maximum after the initial conversion stage. The rate coefficient, k_T, was measured experimentally in the time interval between the opening of the UV-lamp and the attainment of a maximum on the photocalorimetry curve. Hence, as this period is considered the beginning of the reaction, the order of reaction for termination, p, is considered to be zero; and the equation above will then reduce to [133]

$$R_{(T)} = d\alpha_{(t,T)} / dt = k_{(T)}\alpha^{m}(1-\alpha)^{n} \quad \text{---(3)}$$

To simplify the analysis, it was assumed that the total order of reaction was two (m+n = 2). The individual orders of initiation and propagation, m and n, were each input as variable for this study. This ensures a better fit of the experimental data in calculating the activation energy, E_a, using the Arrhenius equation

$$k_{(T)} = A\exp(-E_a / RT) \quad \text{---(4)}$$

where A is the collision factor, T is the temperature and R is the Universal Gas Constant. The fit of the experimental data in calculating this activation energy value is crucial as it affects the accuracy of the calculated value of the rate coefficient, $k_{(T)}$ [134].

Biodegradation:

In the biodegradation study, the percent weight loss, W (%), was calculated at each time point of the study according to the equation

$$W = \frac{W_i - W_d}{W_i} \times 100\% \quad \text{---(5)}$$

where W_i is the initial weight of the samples before immersion and W_d is the final weight after immersion and vacuum-drying.

3.3.5. Biodegradation

Pre-weighed samples of identical shape and size were first washed with phosphate buffer solution (PBS) of 0.1 M and pH 7.2 from GIBCO (Invitrogen), USA, before being immersed in 20 ml of it for various periods of time at 37 °C. Triplicate samples were used for each time period. The PBS was replaced weekly. At the end of each time period, the samples were patted dry and the wet weights, W_w, were recorded. The samples were then further dried in a vacuum oven until constant mass before the dry weights, W_d, were measured. The mass loss was recorded using Equation (5).

3.3.6. Cell Culture

A mouse fibroblast cell line, L-929 (ATCC, CCL1, USA), was used in this study. *In vitro* mammalian cell culture studies have been used historically to evaluate

cytotoxicity of biomaterials and medical devices, and L-929 cells are recommended by the ISO 10993-5 standard. The cell line was cultured in T-75 culture flasks using Minimal Essential Media (MEM, Gibco Life) supplemented with 10 % (v/v) fetal bovine serum (FBS, Invitrogen), 1 % (v/v) 10mM non-essential amino acid solution (Sigma), 1 % (v/v) 200mM L-Glutamine (Invitrogen) and 1 % (v/v) antibiotic solution containing penicillin and streptomycin (Invitrogen).

3.3.7. Cytotoxicity of crosslinked polymers

Photocrosslinked system:

Samples were prepared as described in Chapter 3.2.1 and sterilized using UV-irradiation for 48 h. They were then fitted into the wells of a 12-well plate and washed successively 3 times with 70 % ethanol, and 2 times with PBS. Cells were directly cultured onto the samples in the wells (5×10^3 cells/well) and culture media added. The negative control for cell toxicity used was cells seeded onto empty wells and the positive control was latex rubber. The samples were then incubated at 37 °C, 95% relative humidity, and 5 % CO_2 for 24h. The relative cytotoxicity of the leachable products was assessed with CellTiter 96® Aqueous One Solution Cell Proliferation Assay (MTS tetrazolium compound, Promega, USA). Following the 24 h incubation, 20 µL of the MTS solution was added to each well. The plates were wrapped in tin foil and incubated at 37 °C, 95 % relative humidity, and 5 % CO_2 for 3 h. The solution in each well was mixed with a pipette, and then transferred to a 96-well plate before the absorbance values were measured at 490 nm with an absorbance microplate reader (Infinite M200, Tecan Instruments, Austria, GmbH).

Epoxy-amine system:

Triplicate culture wells, which contained a confluent cell mono-layer were selected. The culture medium was replaced with 300 µL of each sample extract. The crosslinked polymer samples used were initially washed with PBS, and then immersed in culture medium at a concentration of 0.1 g/mL over 24 h. The culture medium extracts were sterilized via filtration using sterile syringe filters of pore size 0.45 µm. Similarly, triplicate culture wells were prepared for each negative and positive control replacing the growth medium in each culture by 300 µL of extract from the controls. The negative control used for cytotoxicity was high-density polyethylene (HDPE) membrane and the positive control for cytotoxicity was ZDEC polyurethane membrane. The blanks used were wells with culture medium but no cells. The wells were incubated at 37 ±1 °C in 5 ±1 % $C0_2$ for 24 ±2 h. The cultures were microscopically examined (at least 100X) after 24 ±2 h of incubation. The scoring for the observations was carried out using the United States Pharmacopoeia (USP 30-NF 25) scoring guidelines (Table 1).

Grade	Observed Conditions of Culture	Toxicity
0	Discrete intracytoplasmic granules; no cell lysis.	None
1	Not more than 20% of the cells are round, cells loosely attached, no intracytoplasmic granules; occasional presence of lysed cells.	Slight
2	Not more than 50% of the cells are round, no intracytoplasmic granules; no extensive cell lysis and empty spaces between cells.	Mild
3	Not more than 70% of the cells layers contain rounded or lysed cells.	Moderate
4	Nearly complete destruction of the cell layer.	Severe

Table 1 The USP 30-NF 25 Scoring guidelines for cell morphology

AlamarBlue® was also used to examine the cells' metabolism function. 300 µl of 10 % alamarBlue® solutions in DMEM culture medium (without FBS) were added to

each well of a 24-well culture plate after washing it 2 times with PBS. The plate was incubated at 37 ^{o}C for 2.5 h, and the absorbances of the well contents were measured at wavelengths of 570 nm and 600 nm.

The percentage reduction of alamarBlue® in each well was then calculated according to the equation below:

$$Percentage\ reduction\ of\ AlamarBlue = \frac{(O2 \times A1) - (O1 \times A2)}{(R1 \times N2) - (R2 \times N1)} \times 100 \quad \text{----- (9)}$$

where *O1* is the molar extinction coefficient of oxidized alamarBlue® solution at one wavelength (80586 for 570 nm), *O2* is the molar extinction coefficient of oxidized alamarBlue® solution at the second wavelength (117216 for 600 nm), *R1* is the molar extinction coefficient of reduced alamarBlue® solution at the first wavelength (155677 for 570 nm), *R2* is the molar extinction coefficient of reduced alamarBlue® solution at the second wavelength (14652 for 600 nm), *A1* is the absorbance of the sample well at the first wavelength, *A2* is the absorbance of the sample well at the second wavelength, *N1* is the absorbance of the blank wells at the first wavelength and *N2* is the absorbance of the blank wells at the second wavelength.

3.3.8. Cytotoxicity of degradation products of photocrosslinked system

Cells were first harvested at 80-90 % confluency and seeded into 96 well tissue culture plates for a seeding density of 5×10^3 cells/well. The plates were then incubated

for 24 h before testing to achieve 70-80 % confluency within the well. Degradation media was obtained from a crosslinked photopolymerized diallyl tartrate sample immersed in PBS until 50 % of its mass remained (12 weeks); and sterilization was carried out using filtration via sterile syringe filters of pore size 0.45 μm. The filtered media was then further sterilized using UV-irradiation for 48 h before being mixed with culture media in varying concentrations. The dilution factor is defined as the ratio, by volume, of culture media to the degradation media in the mixture. These mixtures were added to the cultured fibroblast cells in the 96 well plates (100 μL/well), replacing the previous culture media. For comparison purposes, the same test was concurrently carried out on the degradation medium obtained from the biodegradation of a sample of poly(lactic-co-glycolic acid) (PLGA 53/47) until 50 % of its mass remained as well (2 weeks). Sterile PBS similarly mixed with culture medium of the same concentrations, was added to the cultured cells to serve as the negative control for cytotoxicity, and wells with 70 % ethanol mixed with culture medium of the same concentrations were utilized as the positive control. The cells were then incubated at 37 °C, 95 % relative humidity, and 5 % CO_2 for 24 h. After the incubation, an MTS assay was used to assess the cytotoxicity of the samples, following the same procedure as in the previous section. Cell viability was calculated according to the equation:

$$\%Cell\ Viability = \frac{Average\ value\ for\ sample}{Average\ value\ for\ negative\ control} \times 100 \qquad \text{---- (6)}$$

4 Results and Discussion

4.1. Photocrosslinked system

4.1.1. UV-polymerizability of diallyl tartrate

Scheme 3 shows the process involved in the synthesis of photopolymerized diallyl tartrate. Diallyl tartrate was first synthesized according to an established procedure and was vacuum dried to minimize the presence of DMF. Figure 1 shows the ^{1}HNMR analysis obtained of the compound. Yield: 70 %. ^{1}H NMR (400 MHz, $CDCl_3$, ppm): 3.52 (broad s, 2H, 2 O*H*), 4.58 (d, 2H, 2 C*H*), 4.72 (d, 4H, 2 -CH_2-CH=), 5.25 (d, 2H, CH_2=CH-), 5.35 (d, 2H, CH_2=CH-), 5.85–5.95 (m, 2H, 2 CH_2=C*H*-) ppm; ^{13}C NMR (100 MHz, $CDCl_3$, ppm): 66.69 (-CH-*C*H_2-), 72.20 (*C*H), 119.08 (*C*H_2=CH-), 131.23 (CH_2=*C*H-), 171.21 (*C*=O) ppm. Residual solvent peaks appear in the ^{1}H NMR spectra as two singlet peaks at 2.15 ppm and 2.25 ppm.

Figures 2a and 2b show the FTIR spectra obtained of the samples before and after 5 min of UV irradiation with 3 wt% photoinitiator added. The obvious reduction in the peak corresponding to the allyl peak at 1646 cm^{-1} confirms that diallyl tartrate is photopolymerizing via its allyl groups. Further evidence is the reduction of similar magnitude observed in the peaks in the 1350 cm^{-1} to 1450 cm^{-1} and 925 cm^{-1} to 975 cm^{-1} regions, which are attributed to the in-plane bending of the unsaturated C-H bond, and the out-of-plane bending or wagging vibrations of the hydrogen atoms attached to the unsaturated carbons respectively [135].

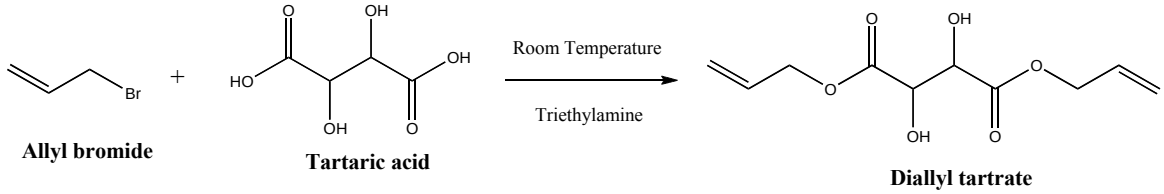

Scheme 3. Synthesis of diallyl tartrate

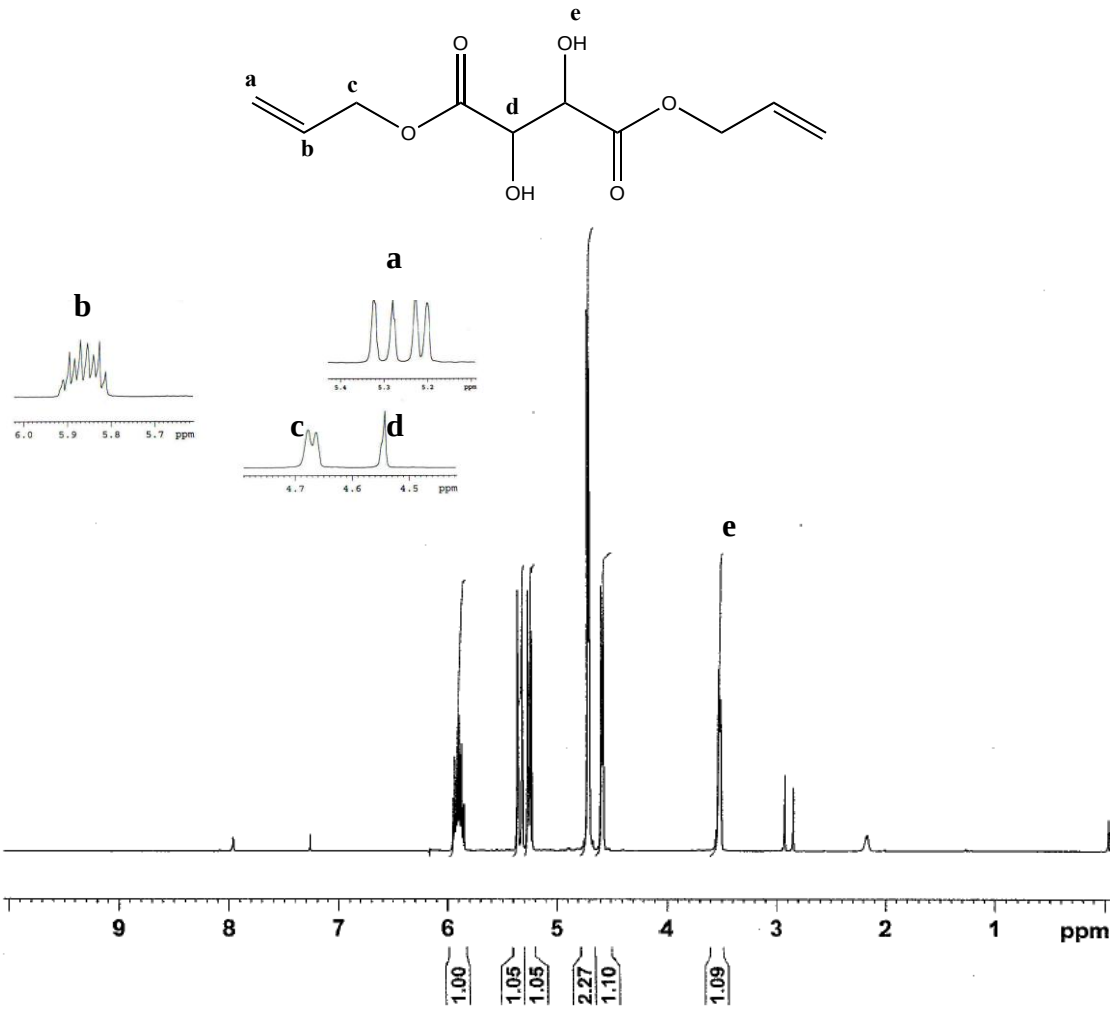

Figure 1. ^{1}HNMR analysis of diallyl tartrate

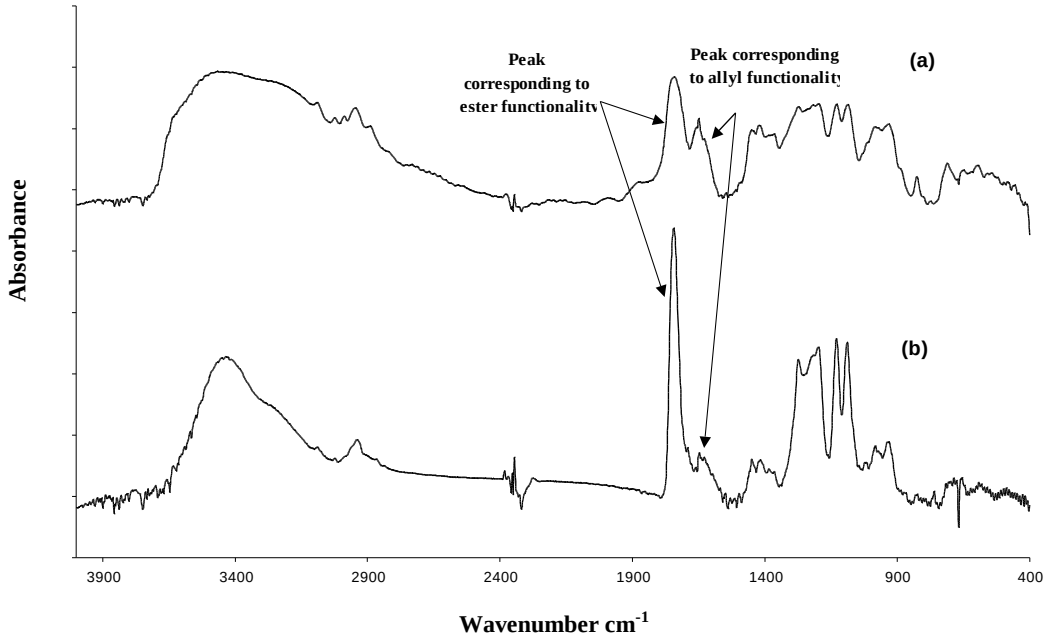

Figure 2. FTIR analysis of (a) diallyl tartrate monomer and (b) photopolymerized diallyl tartrate

Figure 3 shows the general exotherm curve obtained from the photopolymerization of a typical diallyl tartrate sample with 3 wt% DMPA added. The initial part of this curve is typical of an autocatalytic reaction, where the rate of reaction would reach a maximum and then start to decrease as crosslinking and subsequent vitrification reduce the propagation rate. The broadness of the peak however, as compared to those reported in literature on monomers such as glycidyl acrylate [136], is indicative of the difference between the termination characteristics of allyl polymerization and that of other unsaturated monomer polymerizations.

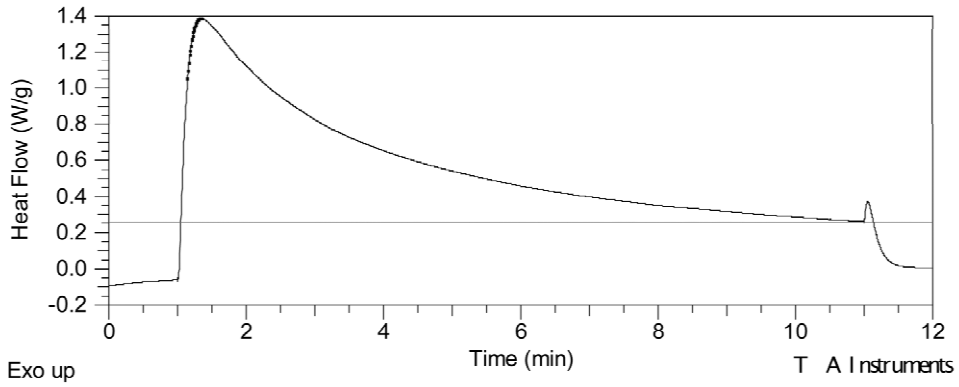

Figure 3. Typical DPC curve from photopolymerization of diallyl tartrate

The rate and extent at which the monomer is converted in a photopolymerization reaction generally depends on the number of photons absorbed in the sample, the efficiency with which energy for radical formation is used, and the reactivity of the radicals with the monomer molecules or the growing chain [137]. These factors are strongly affected not only by the type of photoinitiator used but also its concentration in the reaction formulation. DMPA is a Type I free-radical initiator that undergoes unimolecular fragmentation [138]. It was chosen as the photoinitiator for diallyl tartrate due to its relatively high reactivity [139] and also because it has been extensively used in forming hydrogels in several biomaterial synthesis work [140]. Figure 4 shows the exotherms obtained at room temperature with different concentrations of DMPA added. It shows an increasing maxima and a peak broadening effect as the concentration of DMPA increases.

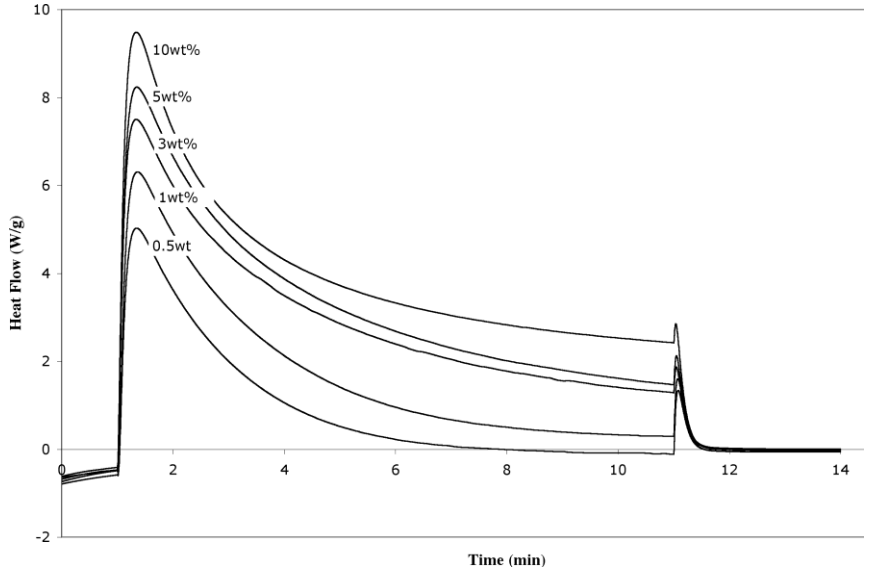

Figure 4. DPC curves from the photopolymerization of DPC using various amounts of DMPA

The derived degree of conversion curve using the enthalpy values measured from the curves in Figure 4 and Equation (1) is shown in Figure 5. It indicates an increase in conversion obtained during the fixed time period with increasing DMPA concentration. The degree of conversion obtained then reaches a maximum and starts to decrease thereafter. This is in accordance with the effect seen in the photopolymerization of other systems [141,142] and has been attributed to excess initiator molecules at higher concentrations absorbing most of the light intensity in the surface layer, preventing it from penetrating the entire depth of the sample. The optimum amount of photoinitiator is one that minimizes this absorption, as well as gives a high degree of monomer conversion. For the case of diallyl tartrate, this amount was inferred from the curve in Figure 5 to be in the range of 3-4 wt%. It is important to note that as compared to the work on the thermal polymerization of diallyl tartrate which reports 10 % monomer conversion at 60 °C after 4 h [106], approximately double the conversion was obtained with photopolymerization at room temperature in just 10 min. This is indicative of the

higher efficiency of photoinitiation as compared to thermal initiation in allyl polymerization.

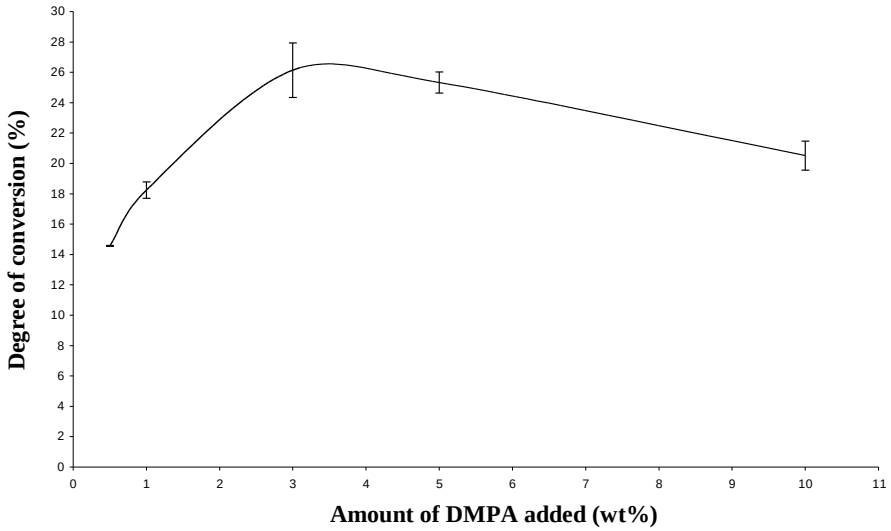

Figure 5. Effect of DMPA amount on the degree of conversion of diallyl tartrate, calculated using Equation (2)

Using a fixed DMPA concentration of 3 wt%, samples were then irradiated at five different isothermal temperatures: 25 °C, 40 °C, 50 °C, 60 °C and 70 °C and the values obtained from the differential photocalorimetry curves are given in Table 2. The values were calculated using Equation (3). This equation assuming an autocatalytic reaction was used as the values are calculated only from the initial part of the curve. It can be observed that as the temperature is increased from room temperature to 40 °C, there is an increase in the order of the propagation reaction, *m*, and a decrease in the order of the initiation reaction, *n*. No significant change is observed in both values as the temperature is increased further.

The natural logarithm (ln) of the rate coefficient values obtained, k_T, were then plotted versus the inverse of the temperature of reaction (Figure 6). The activation energy, E_a, of diallyl tartrate was determined from the slope of this curve, according to Equation (3). The calculation yielded an activation energy value of 14 ±1.2 kJ/mol and although this value is more than double that of known UV-reactive compounds such as 1,6-hexanediol diacrylate (6.18 kJ/mol) [143], it is comparable to the reported value of a cycloaliphatic diepoxide system, Uvacure 1500, (14.8 kJ/mol) [144]. It is also surprisingly much lower than the values reported for some vinyl ethers such as triethylene glycol divinyl ether (43 kJ/mol) [145], indicating a higher reactivity to photoinitiation.

Temperature of Experiment (°C)	Experimental Enthalpy (J/g)	Peak Maximum (s)	Induction Time (s)	Amount reacted at Peak (%)	Order of Reaction, *m*	Order of Reaction, *n*
25.34	194.195	33	7.305	8	0.20	1.80
40.34	267.17	43.5	7.39	11.0	0.27	1.73
49.65	313.425	40.5	6.86	10.7	0.26	1.74
58.87	343.56	41	6.44	11.2	0.27	1.73
68.11	368.26	44.5	7.03	11.7	0.27	1.73

Table 2. Reaction parameters obtained from the photopolymerization of diallyl tartrate at various temperatures

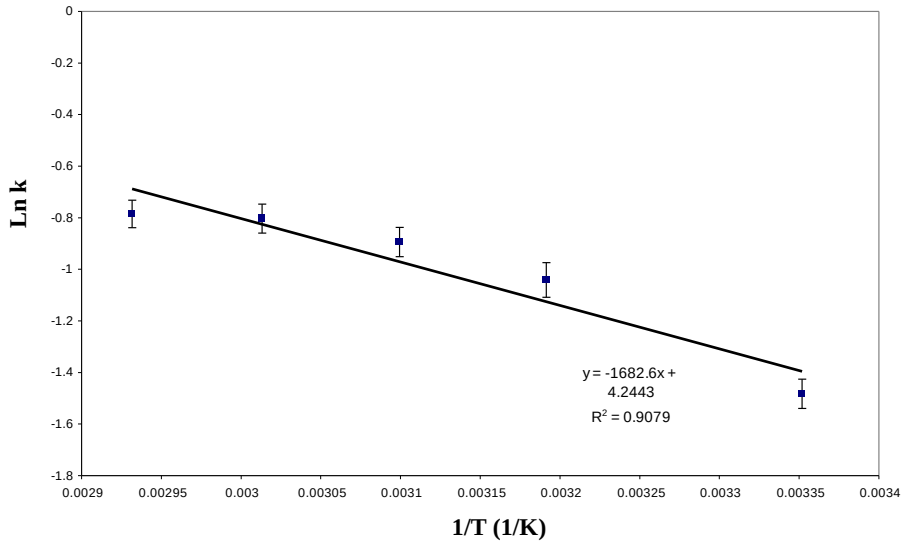

Figure 6. Graph of ln k versus inverse temperature

4.1.2. Degree of cure of larger samples

It was established that for sample thicknesses of about 2 mm in a Teflon mold, the time taken to visibly harden was 2.5 h. From the FTIR spectra obtained of such a sample before and after curing (Figures 7a and 7b), and the application of Equation (1), an approximate 72 % degree of cure was obtained. An attempt was made to further increase the degree of cure by using post-curing treatment on the samples for 2 h in an 80 °C oven. However, a similar calculation using FTIR spectra (Figures 7a and 7c) did not show significant improvement in the degree of cure.

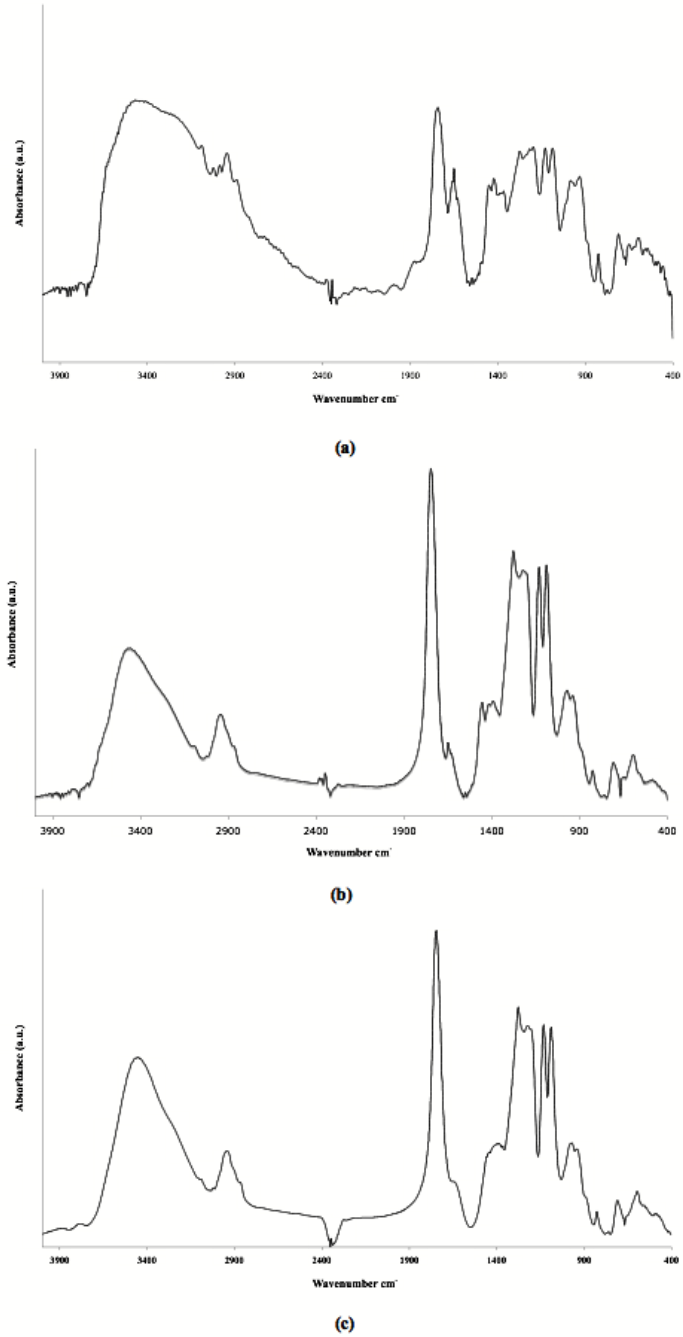

Figure 7. FTIR spectra of diallyl tartrate (a) monomer, (b) after 2.5 h of photopolymerization and (c) after 2 h of post-curing

TGA was then used to confirm this degree of cure. From Figure 8, there are three decomposition temperature regions: 100 °C to 250 °C, 300 °C to 400 °C and ≥400 °C. The temperature range over which the diallyl tartrate monomer decomposes, as shown in

the figure, is 100 °C to 200 °C, similar to the temperature range of the first decomposition step of the bulk polymer. The corresponding weight loss of the polymer during this first decomposition step is 30 %, hence indicating the approximate amount of residual monomer (by weight) in the cured polymer. This agrees well with the degree of cure value of 72 % obtained from FTIR spectra. Hence it can be concluded that the polymer obtained from the photopolymerization procedure described above has a gel content of at least about 70 %, which indicates a relatively high crosslink density.

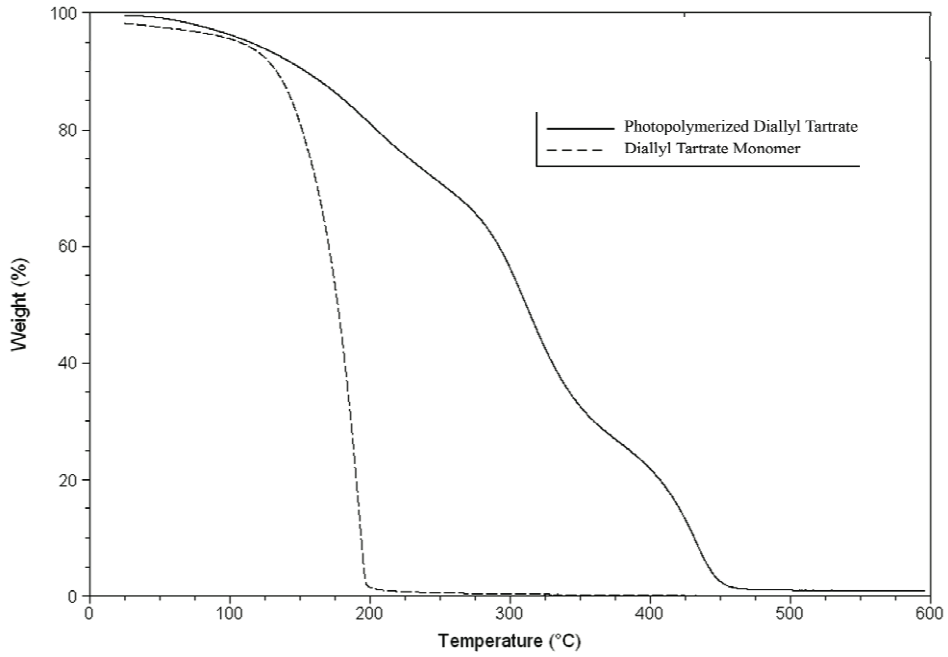

Figure 8. TGA curves of the diallyl tartrate monomer and polymer

The remaining two stages of decomposition shown in Figure 8 have been compared to what has been previously reported on highly crosslinked polymers [146]; and can hence be attributed to the decomposition and char formation of the crosslinked polymer structure (300 °C to 400 °C), and subsequent oxidation of the char residues (≥400 °C).

4.1.3. T_g measurement of photopolymerized diallyl tartrate

MDSC was then carried out and from Figure 9, no melting peak was observed in the reversible heat flow signal, confirming that the material is fully amorphous. However, the glass transition temperature (T_g) was difficult to determine from this curve. Such a flat and diffused T_g is common in MDSC curves of highly crosslinked polymers [147] and dynamic mechanical analysis (DMA) was subsequently used to detect it instead.

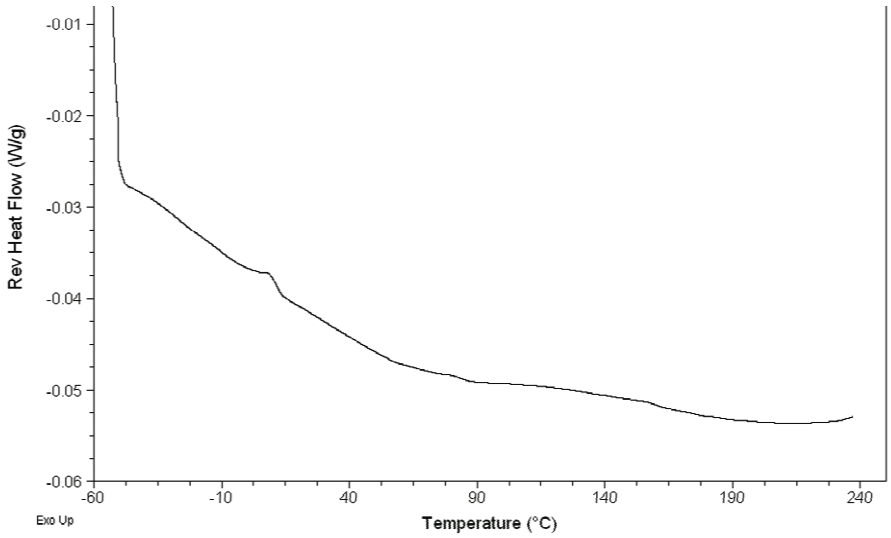

Figure 9. MDSC result of photopolymerized diallyl tartrate

Crosslinked polymers produced from multifunctional monomers usually contain microgels, which are highly crosslinked regions, as well as pools of unreacted monomer [148]. Such a heterogeneous environment would result in a widely distributed relaxation time, or overall mobility, of the polymer segments. Figure 10 shows the DMA result on the photopolymerized diallyl tartrate after a temperature ramp from room temperature to 160°C. The broad loss tangent peak shown in Figure 10 indicates the wide distribution of

relaxation times due to heterogeneity in the polymer [149]. Although an exact glass transition temperature is still difficult to ascertain from this DMA curve due to the large temperature range over which the storage modulus decreases, the convention of using the peak of the loss tangent curve would give a value of 90 °C.

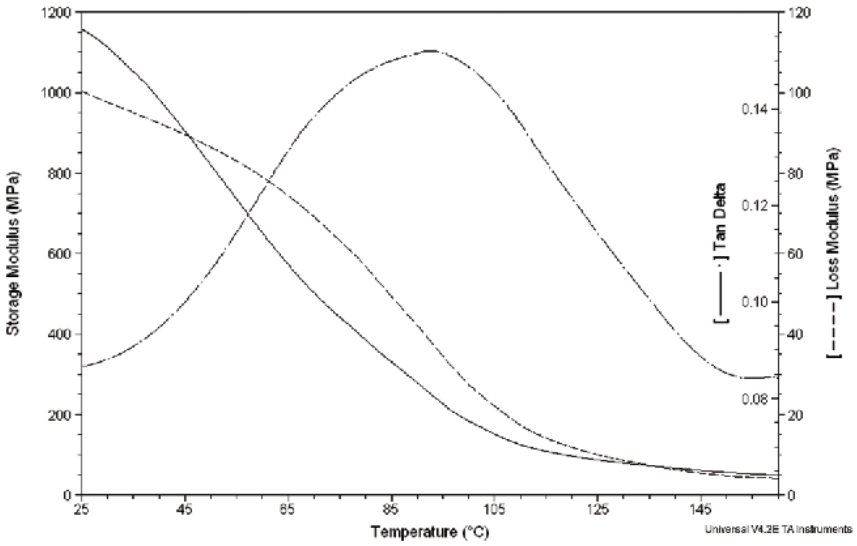

Figure 10. DMA result of photopolymerized diallyl tartrate

4.1.4. Biodegradation of photopolymerized diallyl tartrate

The desirable degradation behavior for an implant material is one that demonstrates controlled, non-toxic and time-dependent degradation while maintaining its mechanical integrity for a suitable time period depending on its application. Scheme 4 shows the proposed degradation products for photopolymerized diallyl tartrate. Similar to other widely-used biopolymers based on acids such as PLGA or polycaprolactone (PCL), one of the degradation byproducts is expected to be the respective acid monomer. In this case, it is tartaric acid. The other byproduct is expected to be the corresponding alcohol resulting from the hydrolysis of the ester bonds in the polymer. To confirm these

degradation products, FTIR spectra were obtained of the samples before, and after 4 and 12 weeks of degradation (Figure 11a, 11b, and 11c respectively). Instead of a peak at around 1700cm^{-1} due to the acid functional groups, the gradual appearance of a peak at 1618 cm^{-1} with degradation time can be seen. This peak can be attributed to that of a metal ester functionality, in this case, sodium tartrate due to ion exchange having taken place in the phosphate buffer solution, between the hydrogen ion of the tartaric acid end groups and sodium phosphate. The FTIR peak for the sodium tartrate group has been reported to appear at 1620cm^{-1} [150].

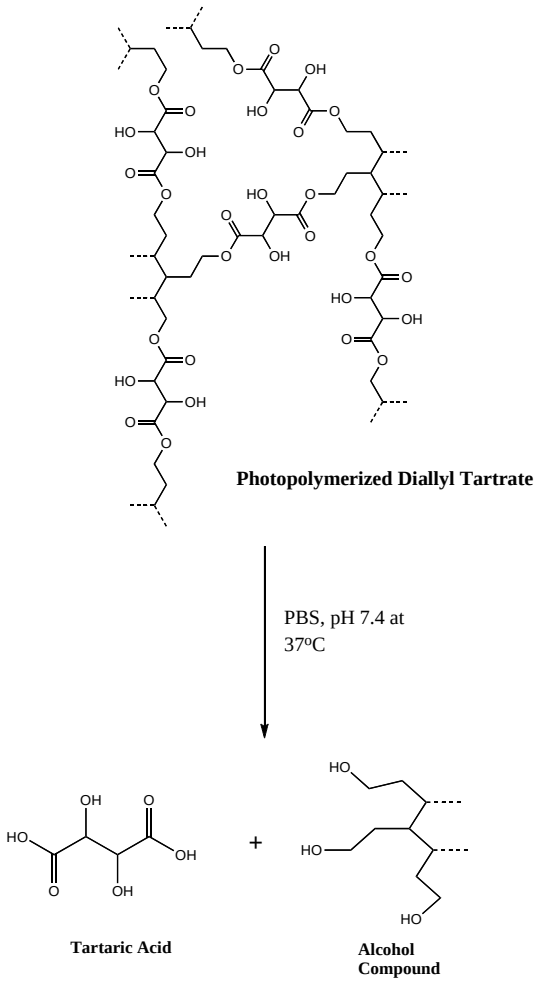

Scheme 4. Hydrolytic degradation of photopolymerized diallyl tartrate

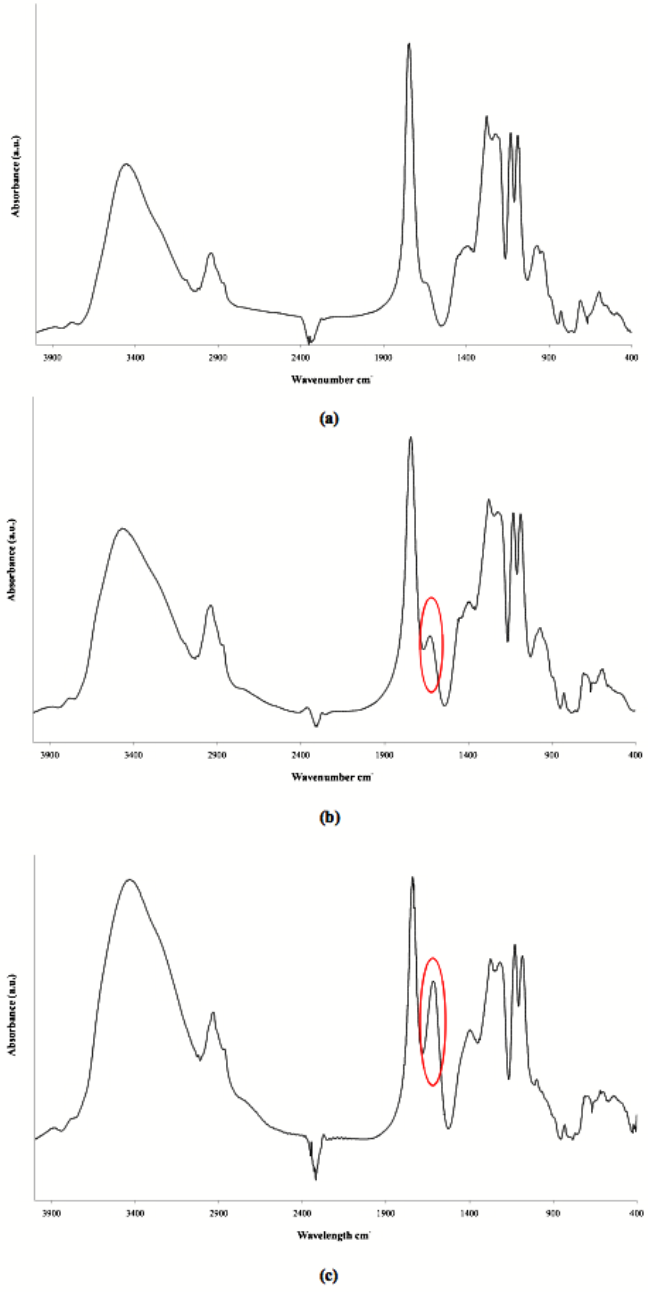

Figure 11. FTIR analysis of photopolymerized diallyl tartrate (a) before degradation, (b) after 4 weeks and (c) after 12 weeks of degradation

The variation of the average percent weight loss measured and calculated according to Equation (5), over a period of 83 days, is shown in Figure 12. Mass loss was observed from Day 1, with the samples reaching about 50% of their initial mass within 3 months.

Polymer degradation is highly dependent on the water diffusion rate into the system. In a polyester-based biodegradable polymer, when the rate of water diffusion into the polymer is faster than the rate of hydrolysis of the ester bonds, bulk erosion will occur. This is generally the case for more hydrophilic polymers such as the linear α-polyester-based polymers [151]. In the reversed situation where the rate of hydrolysis is faster than the rate of diffusion of water into the polymer, a surface eroding phenomena, a layer-by-layer "peeling" of the polymer, would be observed. In this case, there will be gradual mass loss with time accompanied by almost linear loss in mechanical integrity with time instead of a sudden breakdown in bulk eroding polymers.

In the case of a crosslinked polymer, the rate of water diffusion into the polymer is highly dependant on both the crosslink density as well as the hydrophilicity of the network. Based on the degradation profile of the photopolymerized diallyl tartrate, where there was a gradual increase in mass loss observed over time; and the samples retaining their overall shape, even after 3 months, it is deemed that the polymer underwent surface erosion. Although the polymer has a very hydrophilic surface with an average water-in-air contact angle of 45°, the highly crosslinked regions in polymer structures significantly reduce the amount of water diffusing into the polymer [67].

The reduction in pH observed is due to the increased acidity of the aqueous medium, which indicates the release of acidic degradation products from within the polymer structure into the surrounding medium. A higher accumulation of acid groups in the medium would lead to a higher drop in pH. During the degradation of a crosslinked polymer, the initial increase in acidity can be attributed to the leeching out of solubles, e.g. residual monomers, from within the network. Subsequent reduction in pH may be due to the gradual formation of soluble acidic degradation products after the cleavage of

the hydrolytically labile ester bonds in the polymer. However, more studies have to be carried out in future if these mechanisms are to be confirmed.

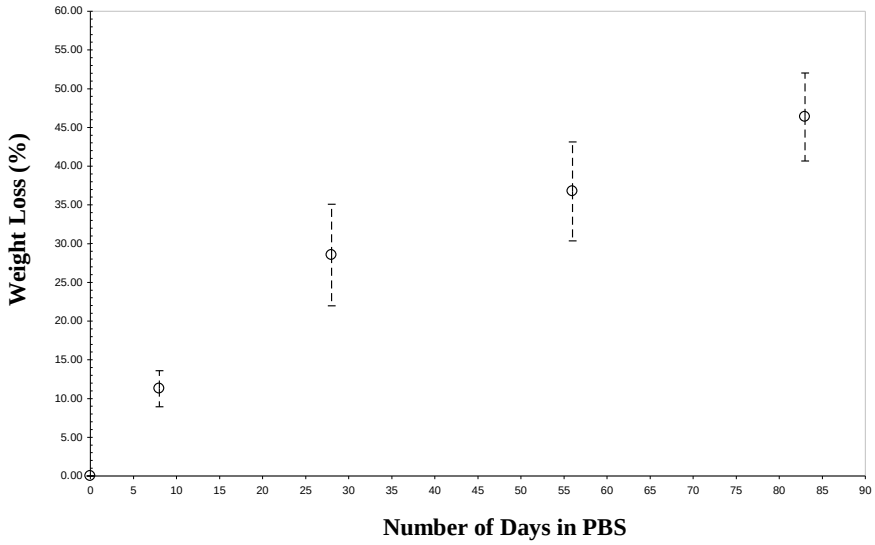

Figure 12. Mass loss profile of photopolymerized diallyl tartrate

4.1.5. Cytotoxicity of photopolymerized diallyl tartrate

The MTS absorbance for cells in direct contact with the crosslinked samples over a 24 h period is shown in Figure 13. The absorbance values measured from the photopolymerized diallyl tartrate samples are comparable to that from the negative controls (p>0.05) for cytotoxicity, hence confirming that this material has no short-term toxicity effects.

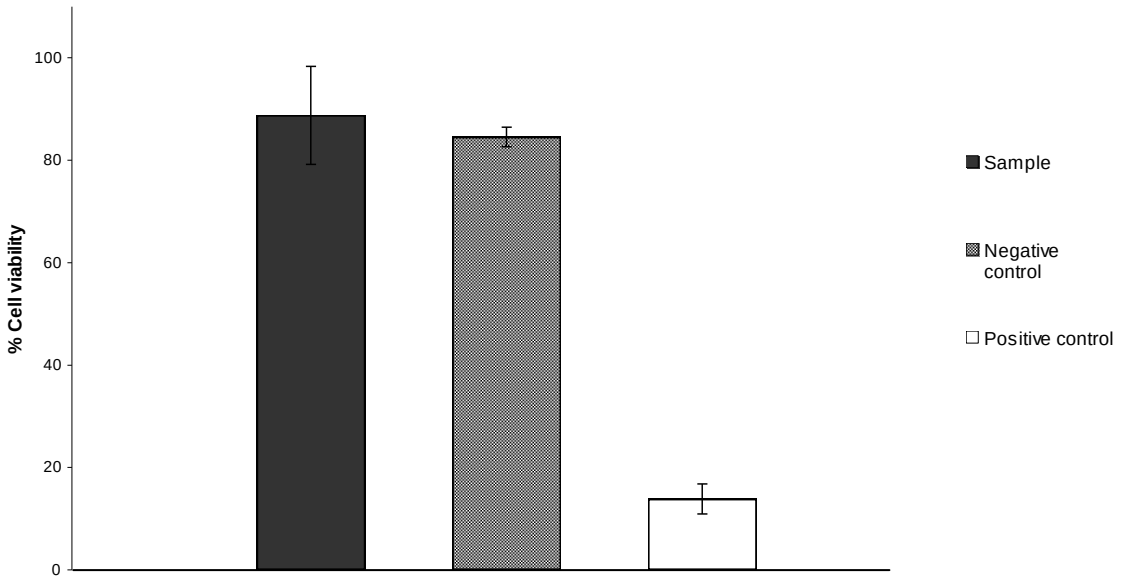

Figure 13. MTS result of photopolymerized diallyl tartrate

The relative average cell viability values were calculated according to Equation (6) over a 24 h period when exposed to the degradation products of the biodegraded crosslinked diallyl tartrate is shown in Figure 14. Two other samples were used for comparison, besides the positive and negative controls: pure PBS and medium obtained from the biodegradation of a widely used biopolymer: PLGA 53/47. Both photopolymerized diallyl tartrate and PLGA samples were degraded in PBS until 50 % of their initial mass remained, which, due to their differing degradation rates, took different

periods of time: 3 months for photopolymerized diallyl tartrate and 2 weeks for PLGA. The concentration of degradation products in the degradation medium at the end of both these time periods is 7.5 mg/ml for PLGA and 11.8 mg/ml for photopolymerized DAT. The concentration was measured using the difference between the initial and final dry masses of the samples and dividing this loss in mass by the volume of PBS used for the degradation. The pH values of the degradation media obtained were measured to be 2.33 and 2.42 of the polymerized diallyl tartrate and PLGA respectively. The pH of the media used was not adjusted to a neutral pH, as it was desirable to test the total dose effect of the media on cell toxicity.

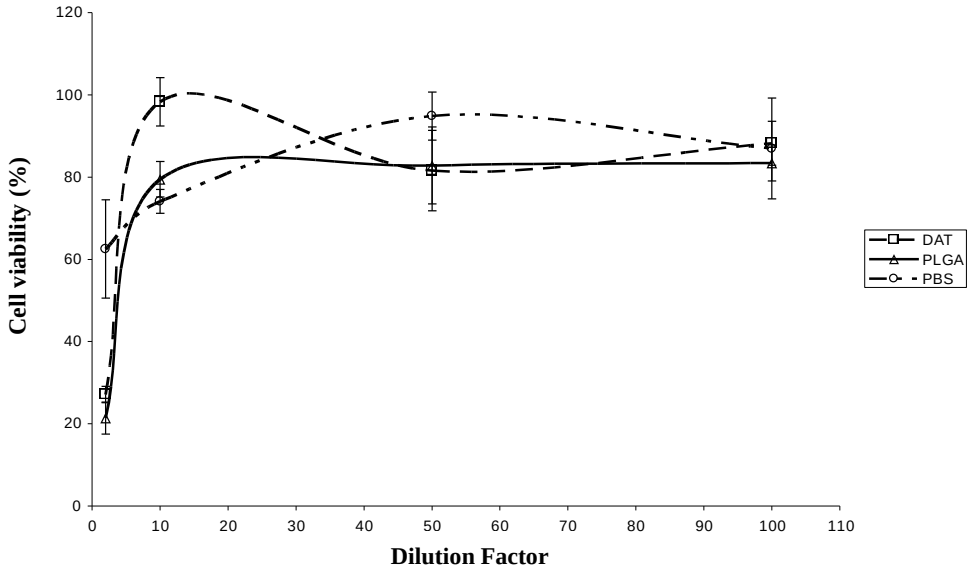

Figure 14. Effect of the degradation products of photopolymerized diallyl tartrate on cell viability

The aqueous-soluble degradation products of both PLGA and photopolymerized DAT displayed a dose-dependant effect on the cytotoxicity of L929 cells. The cell viabilities for both samples were comparable for all dilution factors ($p>0.05$) except for the dilution factor of 10×, where the cell viability for photopolymerized DAT was higher

than that for PLGA ($p<0.05$). It is recommended that for future such studies, the initial media concentrations be adjusted to similar values before the cytotoxicity test is conducted for a more accurate comparison. In this case, the test material, DAT, had a higher initial concentration, hence the comparable result to PLGA in Figure 14 means that if the concentrations were adjusted to be similar, the result would show even higher cell viability values for DAT as compared to PLGA. The conclusion that DAT has comparable cytotoxicity to PLGA, would therefore still be valid.

It can be inferred that a gradual release of degradation products from a sample of photopolymerized DAT, instead of accumulation, would avoid adverse biocompatibility issues. For this material, the cell viability reduces to <80 % over a period of 12 weeks only when the dilution factor is less than or equal to about 5. When calculated back from the initial concentration of 11.8 mg/mL, this refers to a maximum concentration of 2.36 mg/mL. In standard in vitro biodegradation tests modeled after in vivo conditions, the PBS is replaced every week to mimic flow conditions. Using the mass loss data in Figure 12, it can be calculated that the highest concentration of degradation products from a sample of photopolymerized DAT at any one time in PBS that is replaced weekly over a maximum test period of 12 weeks is about 1.65 mg/mL, which is well below the maximum concentration that shows cytotoxic effects. Hence it can be inferred that the degradation products of photopolymerized DAT should not be cytotoxic over at least 24 h of exposure.

4.1.6 Incorporation of Poly(d,l-lactide) oligomers

It has been established that diallyl tartrate is a highly photopolymerizable monomer. The resulting polymer is biodegradable and biocompatible. From Figure 10, it

can be observed that the storage modulus of as-polymerized diallyl tartrate at room temperature is about 1.1 GPa. The rigidity of this thermoset is expected due to the short chain length, or low molecular weight, between crosslinks. However, this property is not desirable for the objective of using this material in soft tissue engineering, hence the next step is to attempt to reduce the rigidity of this polymer by incorporating PLA into the monomer before photopolymerization is carried out. One of the reasons why diallyl tartrate was chosen as the monomer in this synthesis is the availability of hydroxyl groups in its structure for such modification.

To incorporate the PLA oligomers, diallyl tartrate was used as the initiator in the ring-opening polymerization of d,l-lactide (Scheme 5).

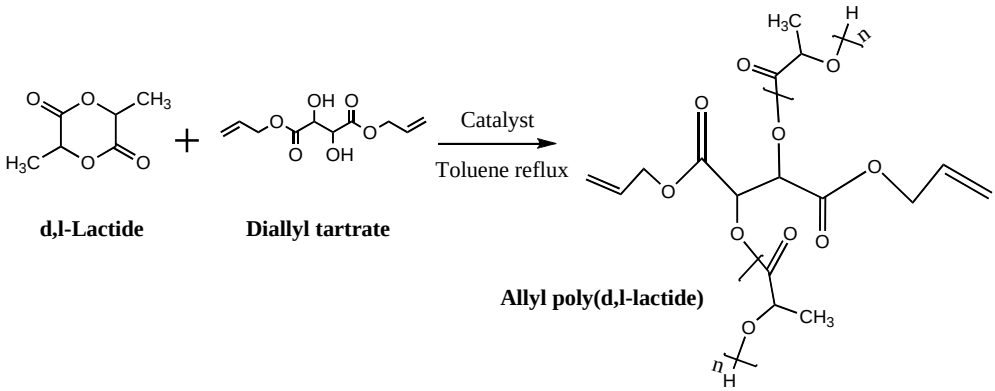

Scheme 5. Ring-opening polymerization of PLA using diallyl tartrate as an initiator

Stannous octoate was initially used as the catalyst as it is commonly used for ring-opening polymerization reactions [152]. However, some lactide monomer was observed on the wall of the reaction vessel, indicating that the reaction was not complete. To confirm this, a SEC measurement was carried out and it showed a number-average molecular weight of only 780 g/mol, which is lower than the targeted molecular weight of 2000 g/mol. The SEC measurements, which are taken relative to polystyrene standards, usually show a molecular weight much higher than the actual value in the case of PLAs.

Hence, it was suspected that for the relatively unreactive, secondary hydroxyl groups on diallyl tartrate to initiate polymerization, the mechanism of coordination-insertion utilized by stannous octoate was not effective.

A different catalyst, triethylaluminum, which initiates polymerization in the presence of hydroxyl groups by forming an alkoxide initiator, was then tried as an alternative. This time, there was no lactide monomer observed on the walls of the reaction flask, hence the polymer was precipitated and then a ^{1}HNMR measurement was carried out. However the peaks corresponding to the allyl group protons CH_2 (doublet of doublets) have merged with the peak for CH of PLA, hence they cannot be observed clearly. FTIR measurements were then carried out to compare the peaks of both diallyl tartrate and the resulting polymer (Figure 15). The peak corresponding to the alkenyl C=C stretch occurs at 1651 cm^{-1} in diallyl tartrate (Fig. 15a). However, FTIR spectra (Fig. 15b) obtained on the polymer showed no such peak.

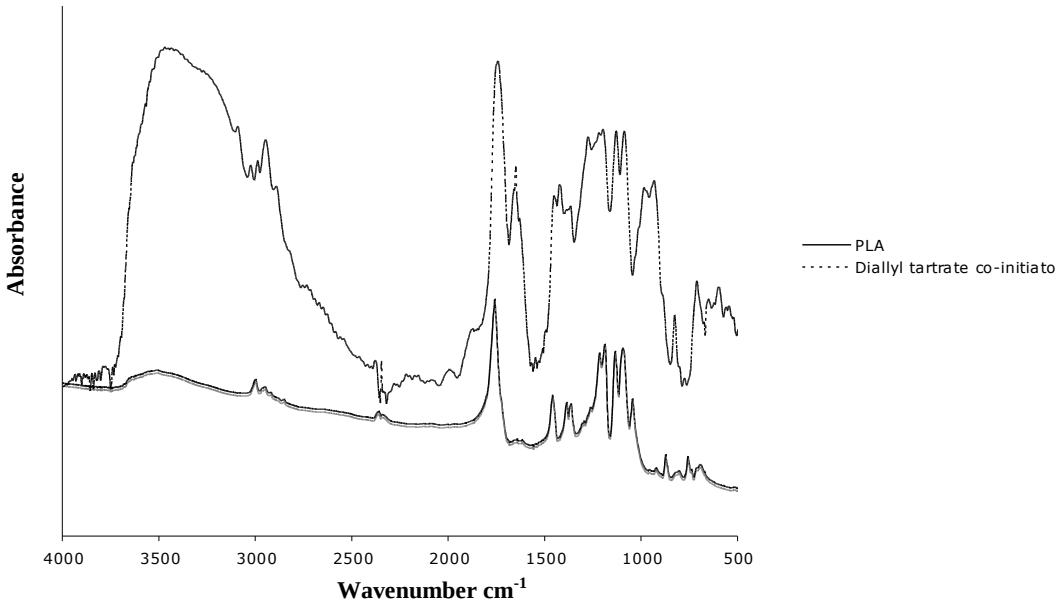

Figure 15. FTIR spectra of synthesized PLA

The use of triethylaluminum requires the very stringent criterion of a moisture-free environment and this result could have been due to the presence of water molecules in the reaction, which would have initiated the polymerization instead of diallyl tartrate. There were subsequent difficulties in continuing these polymerization reactions using the triethylaluminum catalyst due to strict delivery, usage and storage restrictions. Hence no further attempts were made at incorporating oligomers to diallyl tartrate.

4.2. Epoxy-amine system

4.2.1. Synthesis of amine-terminated pre-polymers

The OH-terminated polymers were first synthesized via ring-opening polymerization using stannous octoate as the catalyst and butanediol as the initiator. The targeted molecular weights were achieved using varying ratios of initiator to monomer molar amounts. These polymers were then functionalized with protected-lysine end-groups and the protecting groups were subsequently removed to obtain amine-terminated biodegradable polymers. The method of attaching amino acids to the ends of OH-terminated polymers has been previously reported by Lu et al [153] as a convenient means of obtaining amine-terminated polymers. The reported procedure involved using dicyclohexylcarbodiimide, DCC, as the coupling agent to attach (CBZ)-protected amino acids to the polymers, and subsequent deprotection via catalytic hydrogenolysis. Following the same procedure, however, gave rise to some inconveniences. First, the use of dicyclohexylcarbodiimide, DCC, as the coupling agent between lysine and the OH-terminated PCL produced a urea by-product, dicyclohexylurea (DCU), during the reaction, which was difficult to remove. DCU has low solubility in methanol, hence

before precipitating to obtain the polymer, the entire mixture has to be filtered several times to remove the urea by-product. Second, although CBZ-lysine was successfully coupled to PCL (See Appendix I), the method of catalytic hydrogenation reported for the deprotection step, also presented a purification problem. In order to fully remove the palladium on activated carbon catalyst, filtration over Celite was necessary and this resulted in extremely low yields due to the polymers' adsorption on Celite. Since these polymers were targeted for bio-applications, it was desirable to seek out cleaner and more efficient synthesis procedures, which would result in greater polymer yields as well.

The coupling agent was changed to DIPC, which resulted in a by-product with high solubility in methanol. This made it relatively simple to remove during precipitation of the polymer. The deprotection method was changed to acid-cleavage of the BOC group using trifluoroacetic acid instead. The purification method simply involves precipitation three times into methanol. The final polymers obtained had a pH of around 6 in solution. Scheme 6 shows the overall synthesis steps involved, using the PCL homopolymer as an example.

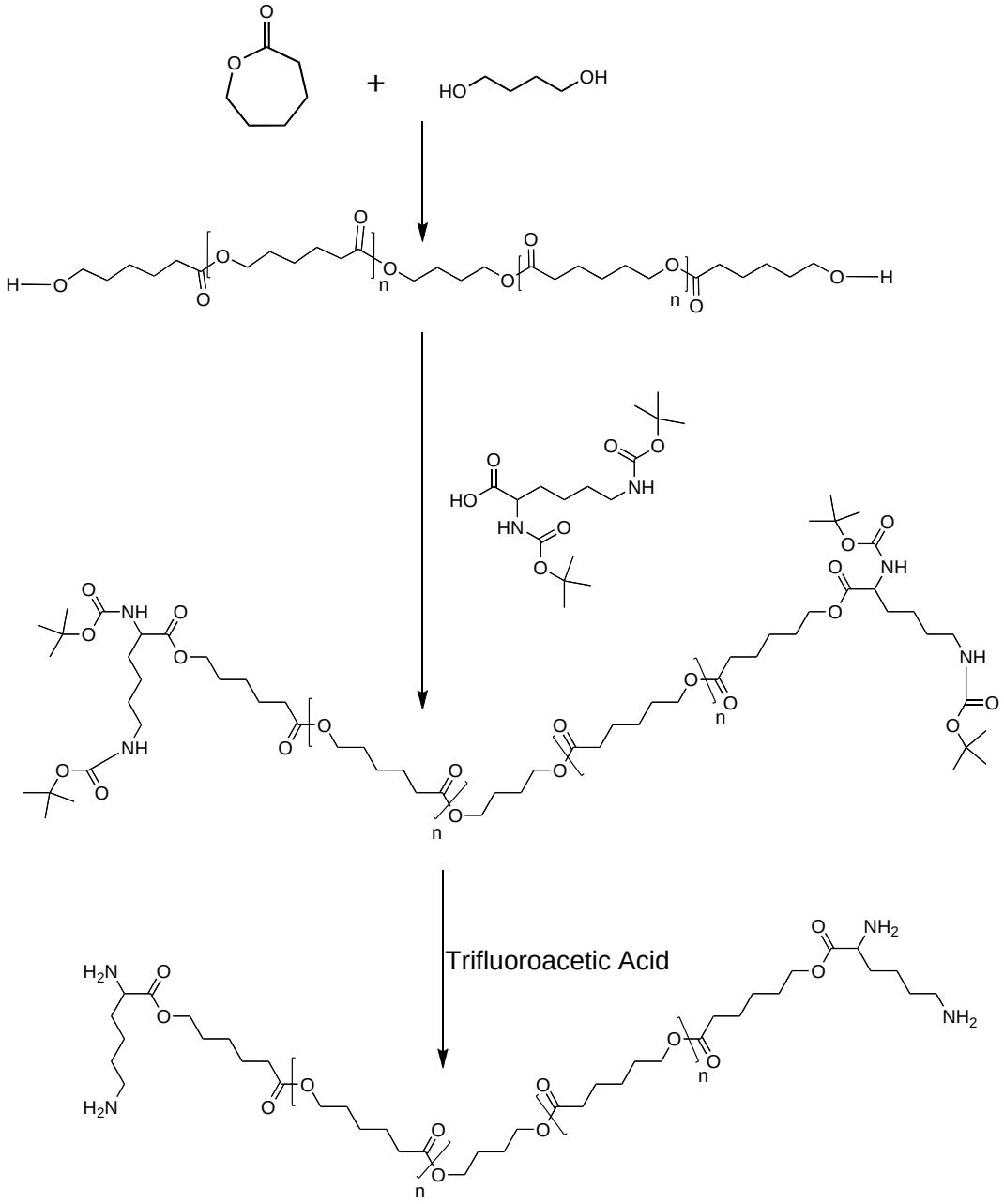

Scheme 6. Overall synthesis route to obtaining amine-terminated PCL

Two different prepolymers following this procedure were synthesized for a comparison of properties later on. The first is a homopolymer of PCL with a targeted molecular weight of 2000 g/mol and the second is a random copolymer of PCL and P(dl)LA with a targeted molecular weight of 10000 g/mol. The yields obtained after each

step of this synthesis were lower for the polymer with the lower molecular weight as it precipitates less easily in hexane and methanol, compared to the polymer with the higher molecular weight.

Figure 16 shows the ^{1}HNMR spectra obtained of the first PCL prepolymer and analyzed at each step of this synthesis procedure. Comparison of the BOC – CH_3 group integral with the butanediol – CH_2 group integral would give an indication of whether the BOC-lysine has been fully incorporated at both ends of the polymer (Figure 16b). Successful functionalization is shown by a ratio of 9:1, indicating the 9 protons on the one of the BOC groups of lysine and the 2 protons on one of the CH_2 groups of the initiator. Subsequent observation of the disappearance of the peak corresponding to the BOC group from the spectra after the deprotection step confirms the availability of free NH_2 groups at the polymer ends (Figure 16c).

Figure 17 shows this monitoring of the BOC group with each synthesis step more clearly.

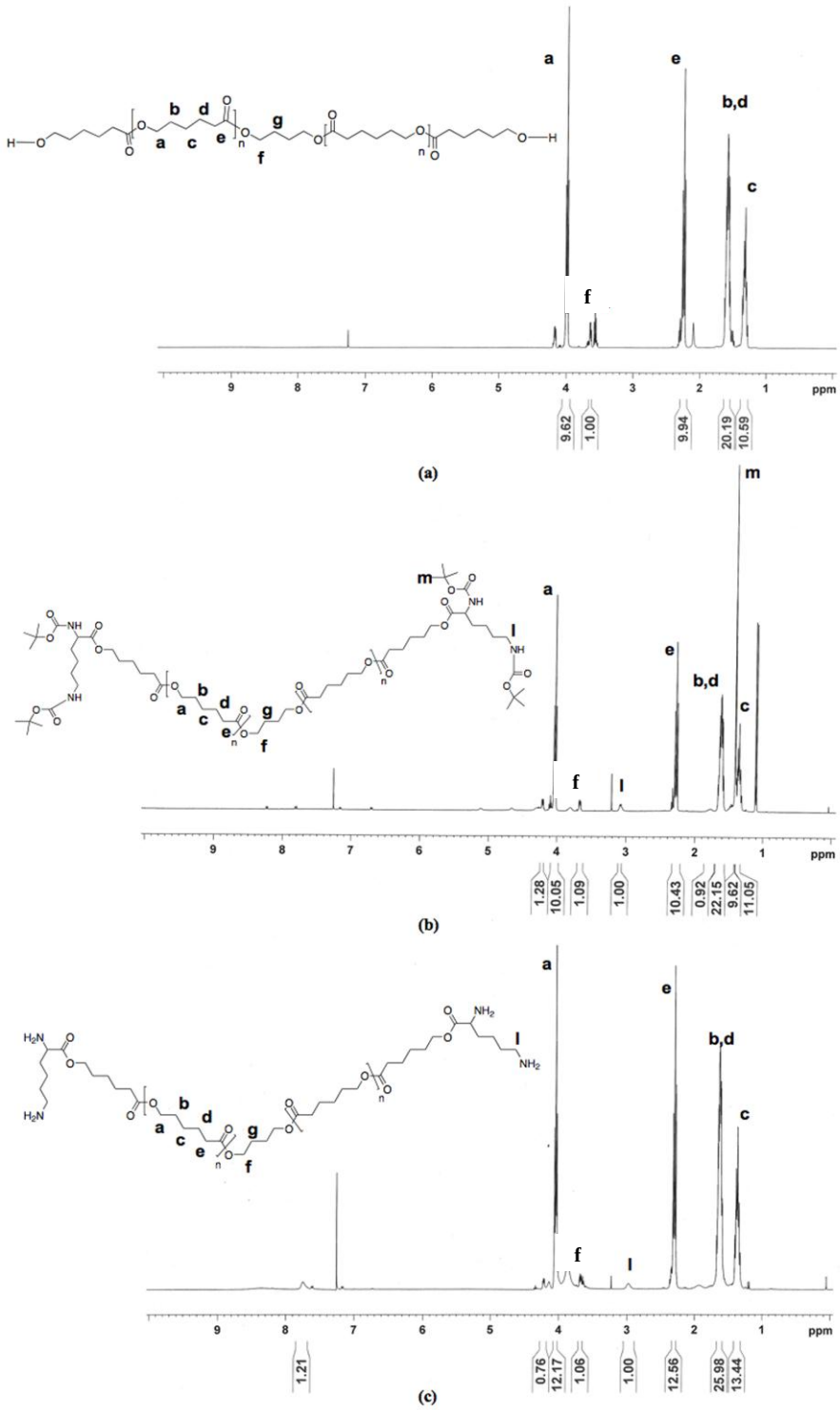

Figure 16. [1]HNMR analysis of (a) OH-terminated PCL, (b) BOC-NH-PCL and (c) NH_2-PCL

.

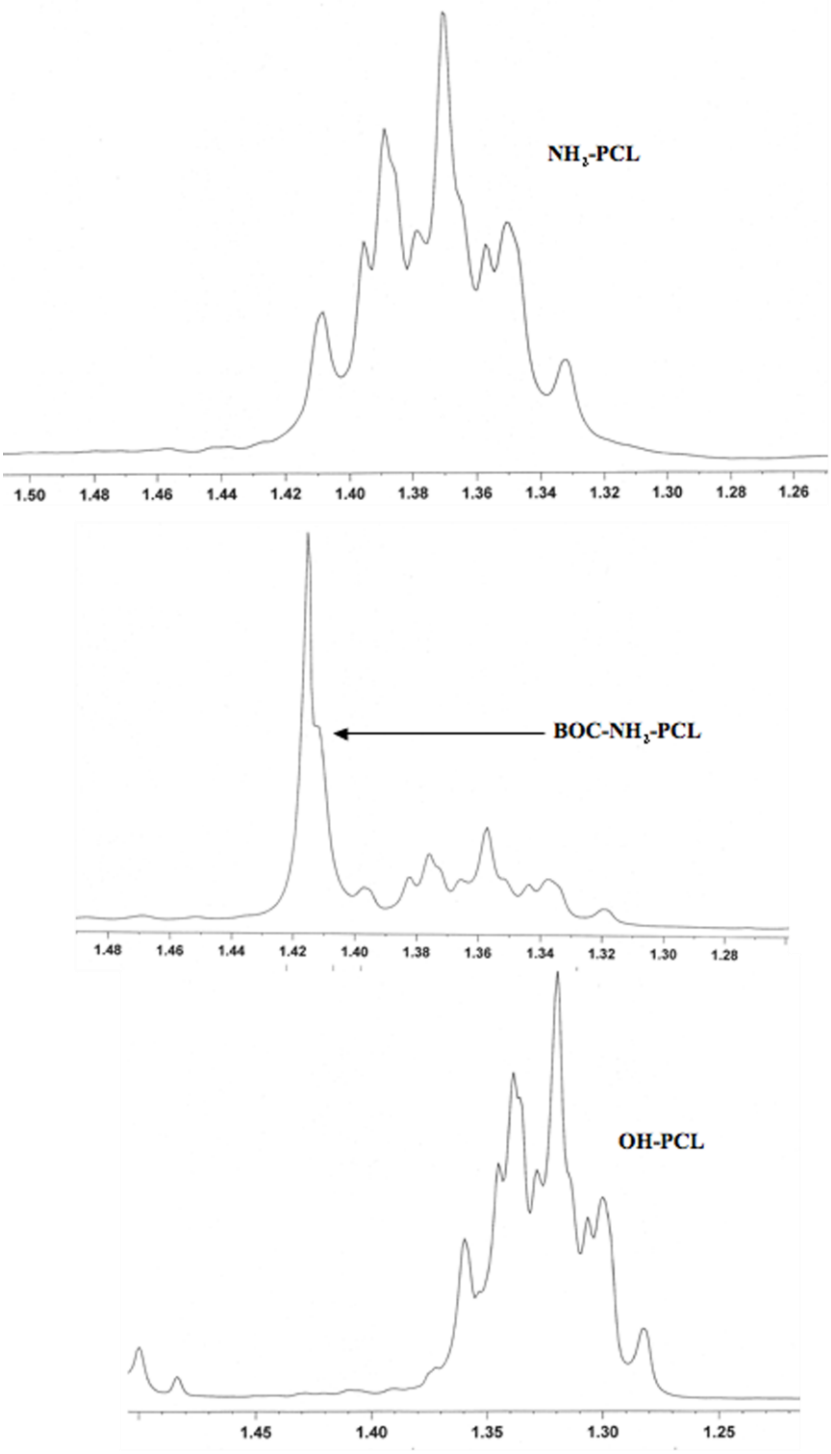

Figure 17. Monitoring the appearance and disappearance of the BOC group using ^{1}HNMR

The same analysis was carried out on the PCLcoPLA prepolymer (Figure 18).

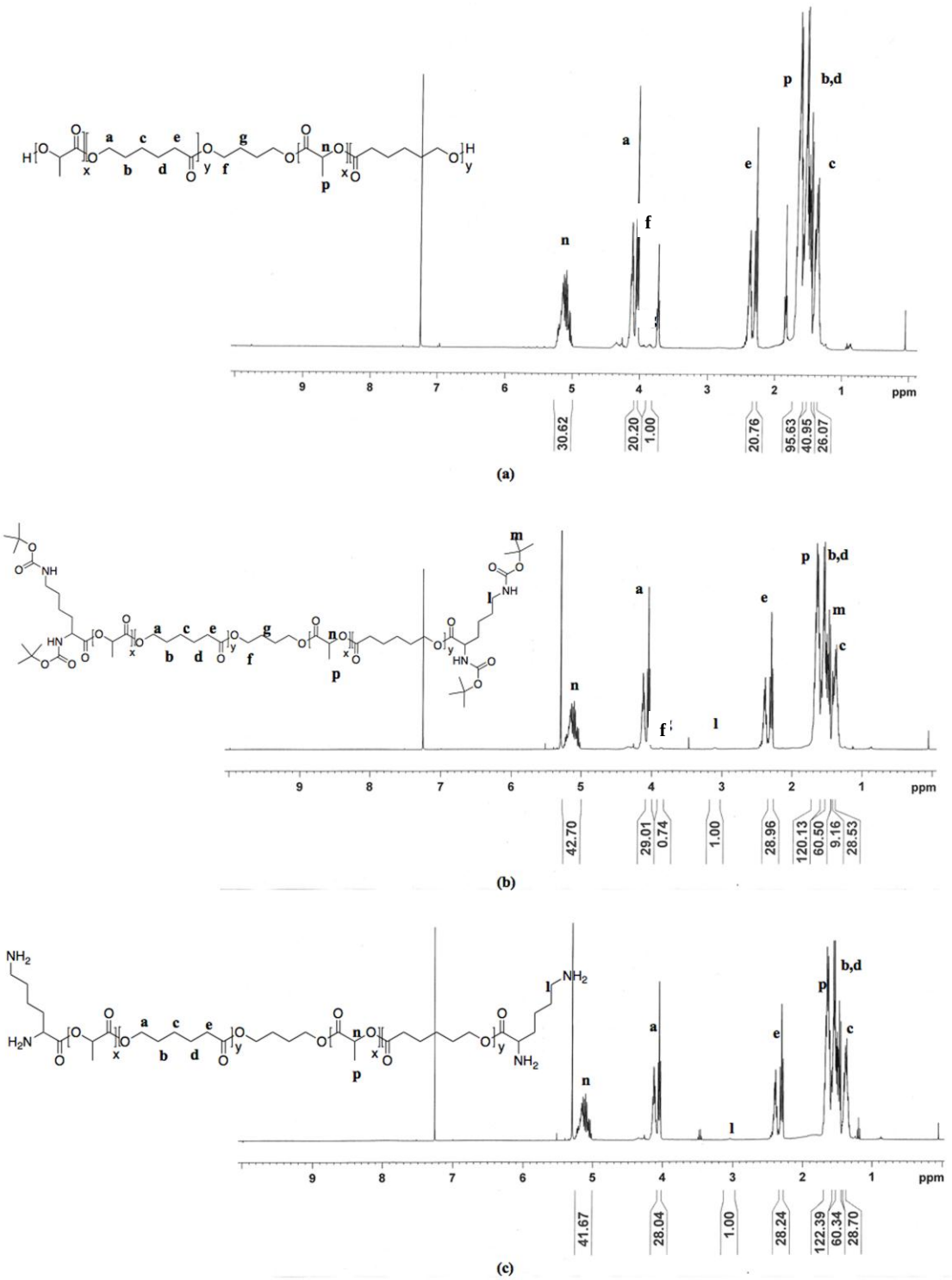

Figure 18. ^{1}HNMR analysis of (a) OH-terminated PCLcoPLA, (b) BOC-NH-PCLcoPLA and (c) NH_2-PCLcoPLA

Molecular weight measurements were carried out on the polymers at each step of the synthesis procedure using both ^{1}HNMR and SEC; and the values are shown in Table 2. The values for M_n of the OH-polymers from HNMR were obtained from the ratio of the CH_2 peak integral of the initiator, butanediol, at around δ= 3.8 ppm to that of either a CH_2 peak integral of PCL, or the CH peak integral of PLA (See Appendix I for calculation procedure). The values for M_n of the BOC-NH-polymers and NH_2-polymers from HNMR were obtained from the ratio of the CH_2 peak integral of lysine at around δ= 3.1 ppm to that of either a CH_2 peak integral of PCL, or the CH peak integral of PLA. It can be observed that the Mn values for the BOC-polymers are much higher than their deprotected counterparts. This is due to the greater hydrodynamic volume of the polymers, resulting from the BOC group when the polymers are in solution [154]. The NH_2-polymers obtained were then characterized using MDSC. The values for the glass transition temperature, T_g, and the melting temperature, T_m, obtained for each polymer are also presented in Table 3.

Prepolymers		**Molecular Weight Measurements g/mol**				**Thermal Measurements**	
		^{1}HNMR	**GPC**			**MDSC**	
		M_n	**M_n**	**M_w**	**PD**	**T_g /°C**	**T_m /°C**
PCL3K	- OH	2300	3232	5353	1.6	< -60	60.2
	- BOC-NH	3026	8340	9779	1.2	-1.4	58
	- NH_2	3282	5211	6996	1.3	-2.4	57.7
PCLcoPLA 18K	- OH	13260	18850	29720	1.6	0.8	-
	- BOC-NH	18293	33477	55953	1.4	6.0	-
	- NH_2	18093	19291	27914	1.6	3.4	-

Table 3. Properties of the prepolymers

4.2.2. Crosslinking

The NH_2-polymers were subsequently crosslinked using PEG-diglycidyl ether of 2 different molecular weights. This crosslinker was chosen based on the work by Nishi et al [155], who evaluated the relative cytotoxicity of common diepoxy compounds used in biomaterial modification. It was reported that PEG-diglycidyl ether of 500 g/mol and above had a very low primary irritation index to L929 cells; and a high concentration of about 150 μg/mL was required to reduce cell viability to 50 %, compared to the mere 20 μg/mL needed for glycerol polyglycidyl ether for example.

The notation used for the elastomers obtained henceforth will be as follows: Px-PEGy, where P represents the name of the prepolymer used; and x and y represent the molecular weight (M_n) values of the prepolymer and PEG crosslinker respectively. Scheme 7 shows this crosslinking process and the final polymers expected. Thus 4 different crosslinked polymers were obtained: PCL3K-PEG500, PCL3K-PEG1K, PCLcoPLA18K-PEG500 and PCLcoPLA18K-PEG1K.

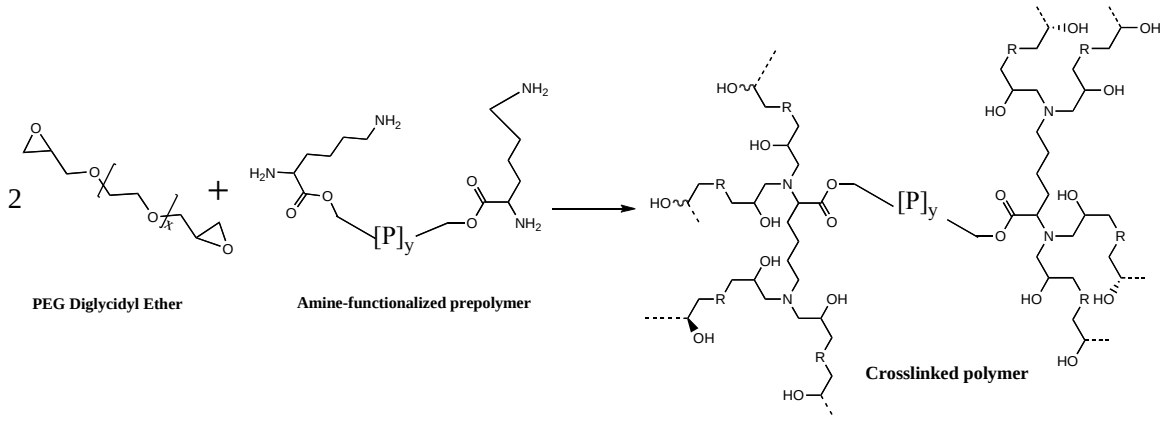

Scheme 7. Crosslinking of amine-terminated prepolymer with epoxy-crosslinker

MDSC was used initially to determine the temperature above which curing is likely to take place. For example, for the curing of PCL3K with PEG1K, an exothermic peak in the non-reversible heat flow occurred with its maximum at 120 °C (Figure 19). Hence this was taken as the minimum temperature required for curing.

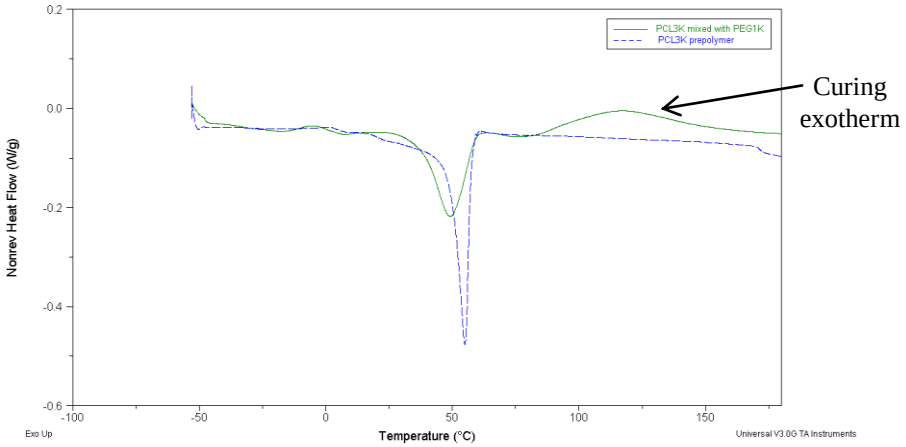

Figure 19. Measurement of cure exotherm using MDSC

The time taken for gelation was taken as the time taken for a visible visco-elastic rubbery solid to form at this curing temperature. This depended on a few factors, such as the thermal conductivity of the curing mold, the amount of stirring and the stoichiometric ratio of the epoxy to amine groups in the reaction mixture. In order to produce samples for some studies such as biodegradation and mechanical testing, teflon molds were used in order to prevent sticking of the polymer to the glass surface. Due to the poor heat conductivity of Teflon, and also the thicker samples required, gelation time increased to nearly 6 days for PCL3K prepolymers and 9 days for PCLcoPLA prepolymers when a stoichiometric ration of 2:1 (epoxy groups to NH_2 groups) was used. When thin glass plates were used as the molds or thinner sample mixtures used, the

curing time could be improved up to 48 h for the PCLcoPLA prepolymers and 24 h for the PCL3K prepolymers (See Table 4). Apart from the mold material and sample size, there are other possibilities to reducing this gelation time, including using reaction activators, increasing frequency and efficiency of stirring throughout the reaction, etc. However this was not further explored in this work, as it is not the main focus of this thesis.

Evidence for the crosslinking reaction was obtained using FTIR and the monitoring of the peak corresponding to the primary aliphatic amine peak at around 800 cm^{-1}. Although commonly the peak corresponding to the epoxy group at around 915 cm^{-1} is used for epoxy-amine reaction analysis, this peak overlaps with the peak corresponding to the ether group of PEG in this reaction. For all the polymers, it was observed that the peak at 800 cm^{-1} disappeared at the point where gelation was observed (Figure 20).

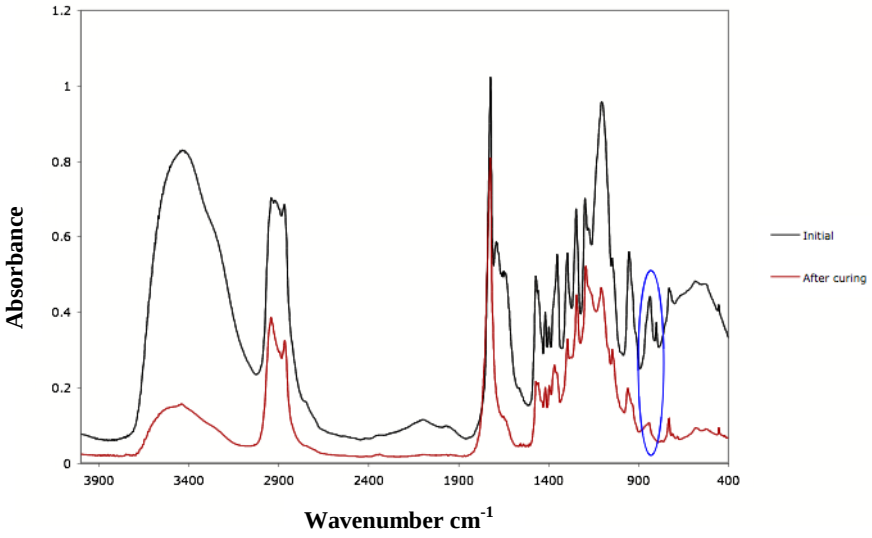

Figure 20. FTIR monitoring of crosslinking reaction

4.2.3. General characteristics of crosslinked polymers

The general characteristics of the obtained crosslinked polymers are outlined in Table 4. First the yields of the crosslinked polymers were measured using soxhlet extraction in methylene chloride over 24 h and calculated using Equation (7). It was found that all the polymers had ~40-50 % gel content by mass when they reached their gelation state. It should be noted that this value does not correspond to the crosslink density. Although all the polymers had similar amounts of gel content, the crosslink densities of those based on the lower molecular weight prepolymer, PCL3K, are expected to be higher due to tighter networks formed (lower molecular weight between crosslink points) as compared to those based on the longer PCLcoPLA18K.

Crosslinked Polymers	**Gelation temperature and time**	**%Gel content by mass, measured via Soxhlet extraction**	**%Swelling**	**T_g /°C**
PCL3K-PEG500	140°C, 24h for films <0.5mm on glass surface, up to 6 days for thicker films on Teflon surface.	41 ± 5	35 ± 3	19.8
PCL3K-PEG1K	140°C, 24h for films <0.5mm on glass surface, up to 6 days for thicker films on Teflon surface.	52 ± 6	58 ± 2	11.7
PCLcoPLA18K-PEG500	160°C, 48h for films <0.5mm on glass surface, up to 9 days for thicker films on Teflon surface.	51 ± 5	7 ± 3	18.5
PCLcoPLA18K-PEG1K	160°C, 48h for films <0.5mm on glass surface, up to 9 days for thicker films on Teflon surface.	39 ± 3	9 ± 4	14.4

Table 4. General properties of crosslinked polymers

A swelling study was then carried out on all the crosslinked polymers to obtain their water uptake by mass at equilibrium. The percentage swelling for the polymers were calculated according to Equation (8). Due to the highly hydrophilic nature of PEG, the polymers crosslinked with PEG1K had expectedly higher amounts of swelling compared to those crosslinked using PEG500. Compared to the polymers based on PCL3K, the PCLcoPLA crosslinked polymers did not show significant swelling in water, possibly due to the hydrophobicity of the PCL and PLA segments, which make up most of the crosslinked polymer due to the relatively high molecular weight of the prepolymers. PCL3K-PEG1K exhibited the highest amount of swelling, gaining up to 60 % of its mass in water.

Thermal characterization on these polymers showed that the crosslinking reaction fully disrupted the crystallinity of the PCL3K prepolymers (Figure 21). All the crosslinked polymers had final T_g values below room temperature, hence were in their rubbery state. This is the most important criterion for elastomeric behaviour.

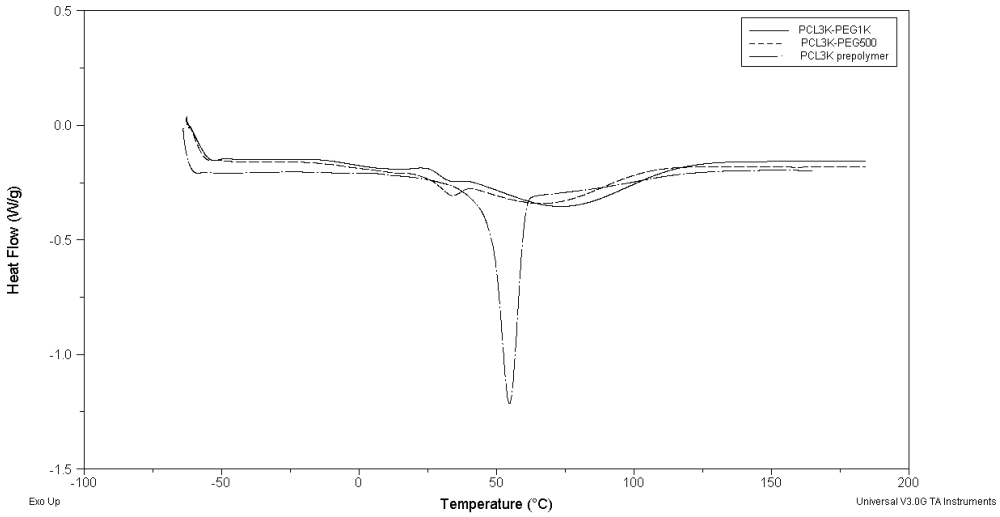

Figure 21. Monitoring loss in crystallinity of PCL using MDSC

4.2.4. Mechanical properties of crosslinked polymers

The crosslinked polymers in their dry state were first subjected to a tensile test at a low loading rate. Figure 22 shows the general curves obtained for all 4 crosslinked polymers. The curves follow the general trend for most elastomers, where a gradual slope is seen from the start with no distinct elastic and plastic regions as seen for thermoplastics. The polymers crosslinked with PEG1K naturally showed higher elongations compared to the ones with PEG500 ($p<0.05$) as the longer crosslinker allowed for more space and flexibility between chains. It was also shown that there was no significant difference between the range of moduli values obtained for the prepolymers crosslinked with PEG500 and those crosslinked with PEG1K ($p>0.05$). This is in accordance with what has been previously found with respect to the effect of varying the lengths of crosslinker on the final mechanical properties of crosslinked polymers [156].

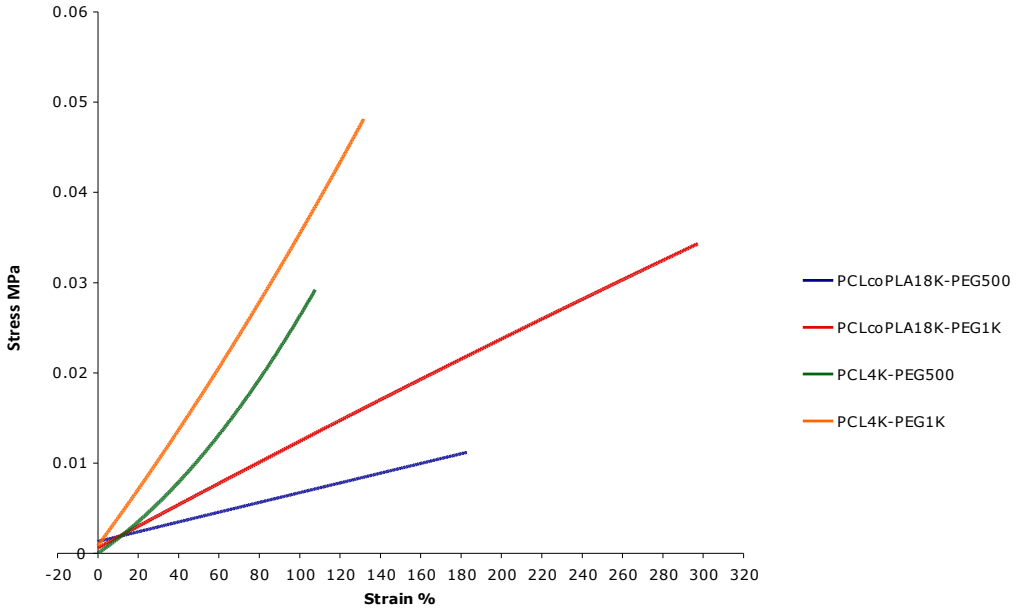

Figure 22. Stress-strain curves of crosslinked polymers

The polymers based on the PCL3K homopolymer also had higher moduli values and lower elongations as compared to those based on the copolymer (See Table 5). This is due to the different molecular weights of the two, the longer prepolymer giving rise to softer and more elastic properties due to the resulting lower crosslink density (longer molecular weight between crosslinks) in the crosslinked polymers.

Crosslinked Polymers	Young's Modulus of dry polymers, kPa (loading rate of 1mm/min)	%Elongation at Break (dry state)	Young's Modulus of swollen polymers, kPa (loading rate of 1mm/min)	%Elongation at Break (swollen state)	Young's Modulus, kPa (loading rate of 10mm/min)	%Strain at which full recovery is observed for at least 3 cycles (loading rate of 10mm/min)
PCL3K-PEG500	28 ± 3	82 ± 8	17 ± 4	68 ± 12	-	-
PCL3K-PEG1K	33 ± 4	126 ± 17	22 ± 2	95 ± 9	67 ± 10	80
PCLcoPLA18K-PEG500	9 ± 3	200 ± 30	-	-	-	-
PCLcoPLA18K-PEG1K	12 ± 5	283 ± 42	-	-	40 ± 16	200

Table 5. Mechanical properties of crosslinked polymers

As the polymers based on PCL3K exhibited a high water uptake in PBS at equilibrium, it was necessary to evaluate their mechanical properties in their swollen state. It was observed that although there was a significant decrease in their modulus values ($p<0.05$), there was no significant change in their ultimate elongations ($p>0.05$) (Table 5). The decrease in rigidity with the uptake of water, as shown by the decrease in the modulus, is due to the softening effect of water within the polymer. As elongation is affected only by the length of the polymer chains, swelling had no effect on this property.

The most attractive property of crosslinked polymers is their ability to recover their strains after more than one cycle of loading. The 2 polymers based on PEG1K were tested on this property as they exhibited higher maximum elongations compared to the

same prepolymer crosslinked using PEG500. It was observed that when the polymer based on PCL3K was elongated to 50 % strain at 10 mm/min and then released at the same rate, the strain was fully recoverable and this 100 % recovery was maintained over 3 cycles of similar loading. The polymer based on PCLcoPLA18K had fully recoverable strains at 200 % strain, also repeatable for 3 cycles of loading. For both polymers, the recovery occurred with zero hysteresis (Figure 23). This recovery with no hysteresis is a remarkable characteristic of chemically crosslinked polymers, one that could not be achieved using physically crosslinked polymers so far.

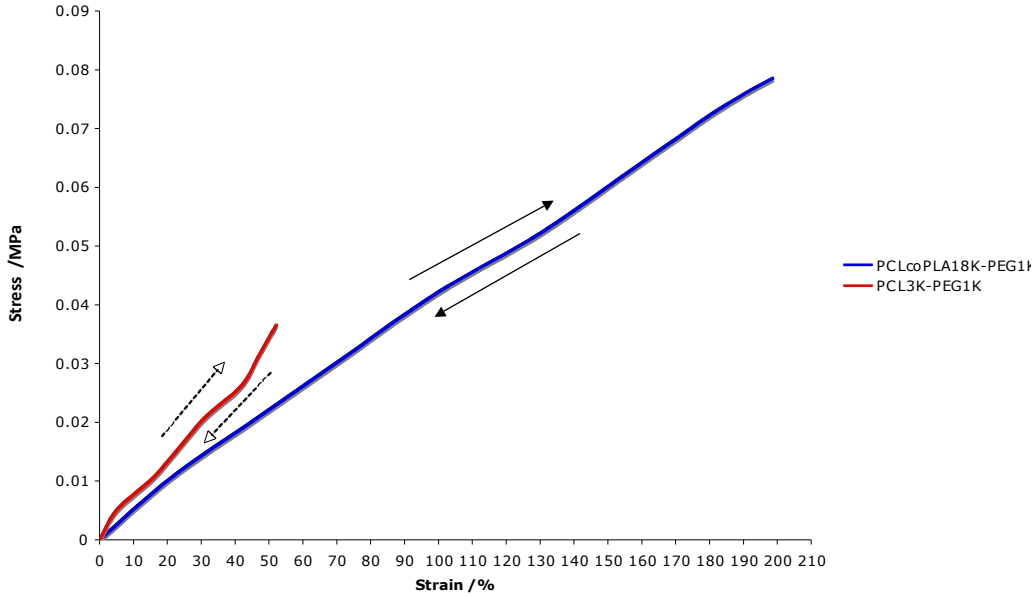

Figure 23. Cyclic testing of crosslinked polymers

4.2.5. Biodegradation of crosslinked polymers

The crosslinked polymers were first washed with PBS in order to remove any leachable, low molecular weight amine-functionalized oligomers. They were then immersed for a maximum degradation period of 28 days. It was observed that with the weekly change of media, the pH of the media remained constant throughout this period (Figure 24). The mass loss of the polymers over this period was calculated according to Equation (5) and the results shown in Figure 25.

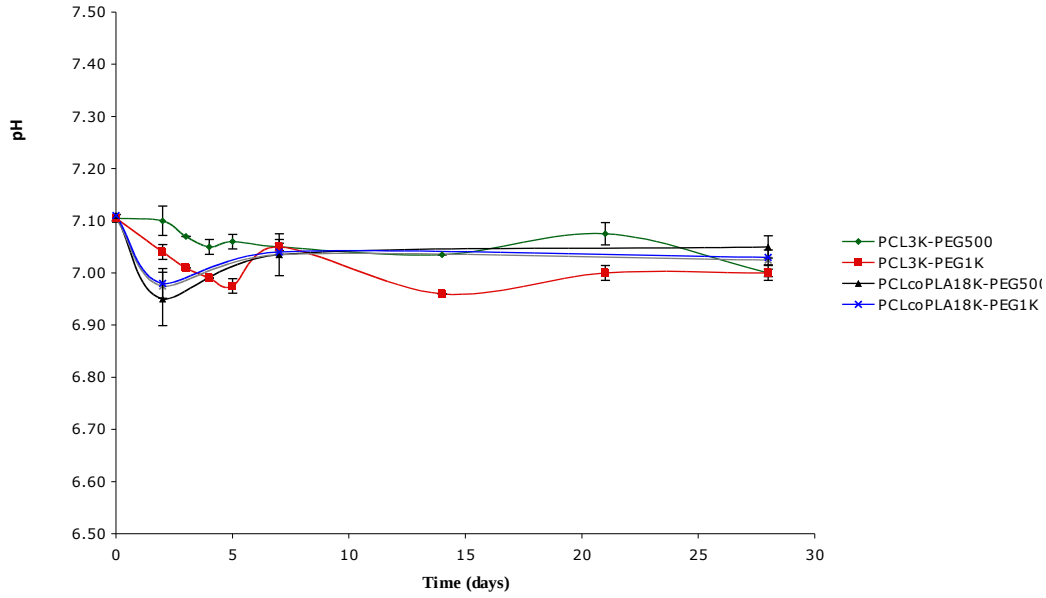

Figure 24. Variation of pH over the degradation period

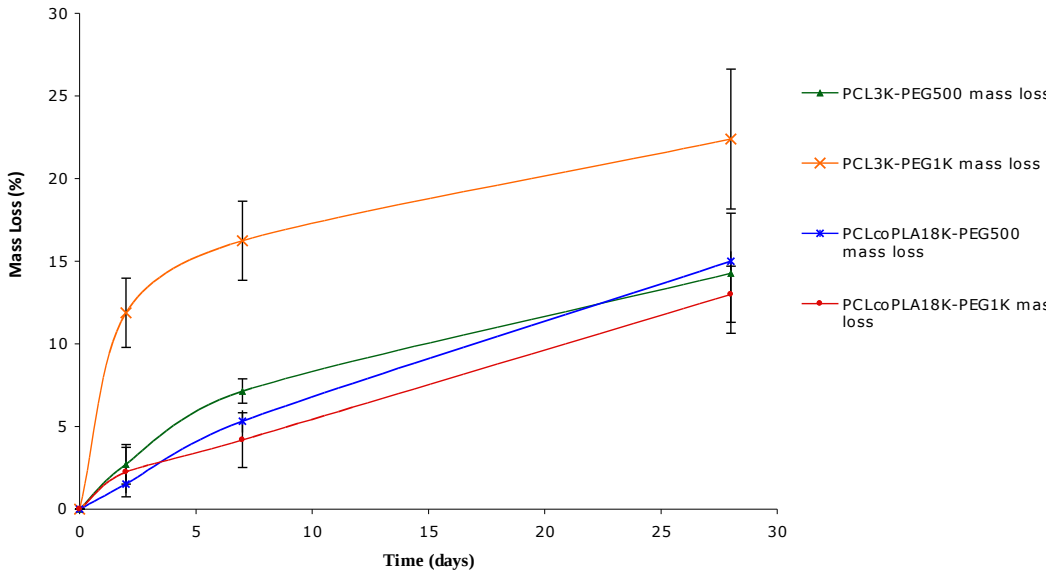

Figure 25. Mass loss profiles of crosslinked polymers

There are several factors that affect the degradation behaviour of a crosslinked polymer. The first is its crosslink density. Generally, the higher the crosslink density, the slower the degradation rate due to the slow diffusion of water molecules through the tight network. However, the hydrophilicity of the overall polymer is also an important factor. Yeganeh et al [123,124,157] found that the higher the content of PEG in their polyurethane networks, the faster the degradation rate observed. This effect is seen here as well for the crosslinked polymers based on PCL3K. PCL3K-PEG1K has a significantly higher rate of mass loss as compared to PCL3K-PEG500, due to its higher hydrophilicity. This effect is not as pronounced in the polymers based on PCLcoPLA18K as the amount of the PEG crosslinkers per unit volume in their networks is not as significant due to the high molecular weight of the prepolymer used.

Comparing just the two prepolymers however, it should be noted from Figure 25 that although the two networks based on PCL3K had an initial high rate of mass loss, this

decreased over time to a more gradual loss while the two based on the PCLcoPLA polymer showed an increase in the rate of mass loss over time. It is well known that PCL is more hydrophobic than PLA, hence the presence of the PLA units in the polymers based on PCLcoPLA18K may have resulted in a higher rate of hydrolysis over time as compared to those based on the homopolymer PCL3K. Another reason could be the lower crosslink density of the polymers based on the longer prepolymer, which results in an overall faster diffusion of water into the network and hence a higher rate of hydrolytic degradation.

4.2.6. Cytotoxicity of crosslinked polymers

The crosslinked polymer samples were first washed with PBS and then immersed in culture medium to prepare the extracts for the cytotoxicity tests. The morphology of cells cultured over 24 h using each sample extract was observed and the toxicities of the extracts were scored following the guidelines in Table 1. The scores obtained are shown in Table 6.

Sample	Grade	Toxicity
PCL3K-PEG500	0	None
PCL3K-PEG1K	0	None
PCLcoPLA18K-PEG500	0	None
PCLcoPLA18K-PEG1K	0	None

Table 6. Toxicity scores of crosslinked polymers based on cell morphology

From these scores, it can be concluded that the extracts from all the crosslinked samples showed no cytotoxicity by observing the cell morphology. The microscope images used for these scores are shown in Figure 26.

Sample	Day 0	Day 1
PCL3K-PEG500	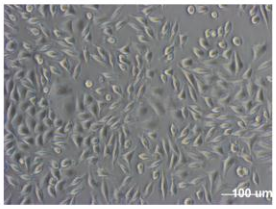	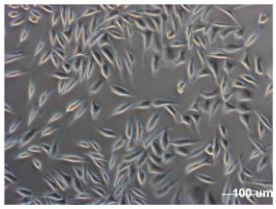
PCL3K-PEG1K	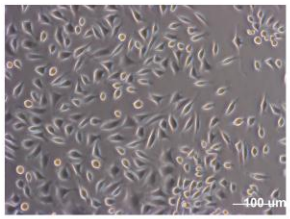	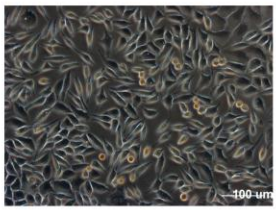
PCLcoPLA 18K-PEG500	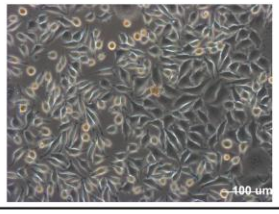	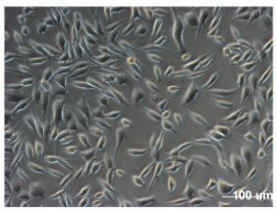
PCLcoPLA 18K-PEG1K	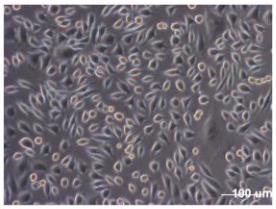	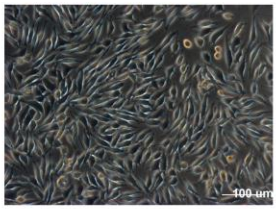
Negative Control	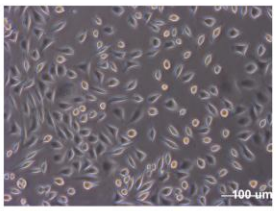	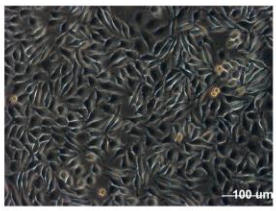
Positive Control	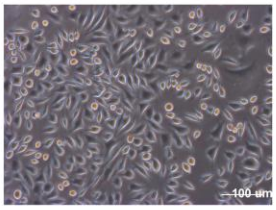	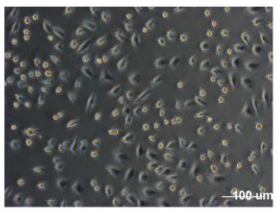

Figure 26. Cell images before and after exposure to sample extracts

The cytotoxicity of the extracts were also measured using the percentage reduction of alamarBlue®, an indicator dye that changes its color in response to the chemical reduction of growth medium, due to cell growth. The percentage reduction values for each sample, together with those for the controls, have been calculated using Equation (8) and the cell viabilities were calculated according to Equation (6).

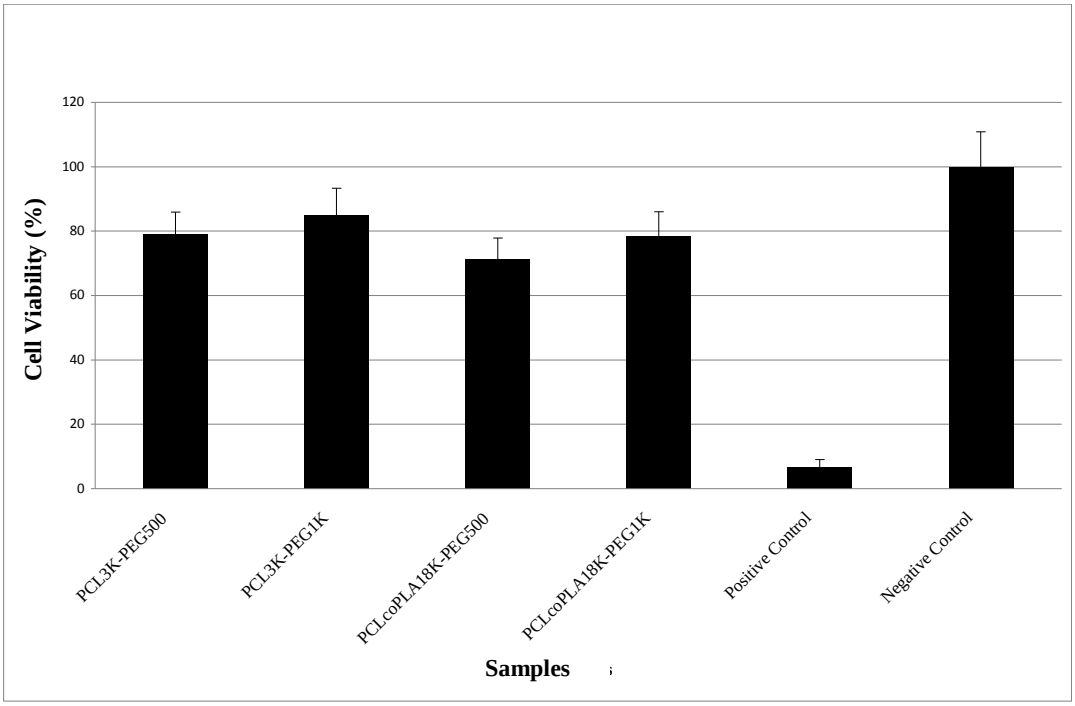

Figure 27. Effect of all sample extracts on cell viability

It can be seen that all the samples displayed 78 ±6 % cell viability. This result, together with the cell morphology observations, supports the conclusion that these crosslinked polymers are non-toxic in the short term.

5 Conclusions

5.1. Photocrosslinked system

It was hypothesized that by incorporating polymeric oligomers into a photopolymerizable monomer, a softer, and more flexible polymer could be achieved. The end objective was to develop a biodegradable, crosslinked polymer with suitable properties for soft tissue engineering.

Three conclusions can be derived from the results of the photopolymerization of diallyl tartrate. (1) Diallyl tartrate was shown to photopolymerize relatively easily via UV irradiation with DMPA as an added photoinitiator, as compared to thermal initiation of the allyl group. (2) The final polymer obtained is non-toxic to cells in the short-term. (3) The as-polymerized diallyl tartrate obtained was very rigid, with a high storage modulus.

The attempts at incorporating biodegradable polymers in order to obtain a soft elastomer could not be taken further due to restrictions on the usage of the extremely reactive catalyst for ring-opening polymerization, triethylaluminum. However this preliminary study on diallyl tartrate opens up a novel and possible route to synthesizing biodegradable and biocompatible polymers with tailorable properties. It is expected that this objective be met if this system were pursued to the fullest.

As-polymerized diallyl tartrate was, however, shown to have great potential as a biomaterial, as demonstrated from its short-term cytotoxicity, which was comparable to the commonly used biopolymer, PLGA. As the photopolymerization rates achieved are too low for in-situ curing applications, the material is ideal for tissue engineering scaffold applications where the scaffold is prepared and seeded with cells *in vitro* before implantation. The use of teflon molds in the desired shapes in this study shows how the

process of photopolymerization allows for the fabrication of complex-shaped polymeric matrices as it allows for good spatial and temporal control. There is also great versatility in terms of formulation and application as a wide range of substances and cells can be entrapped within the polymerizable mixture, and then stored appropriately until use [158]. As the polymer is prepared from a low-viscosity liquid monomer, any scaffold modifications required for improved cell adhesion, such as the introduction of pores using leachable water-soluble salts, can also be carried out with relative ease. The moderate rate of biodegradation shown by photopolymerized diallyl tartrate in this work is further useful, if used as a scaffold material, in order to facilitate the re-growth of tissue around the scaffold as it is gradually resorbed.

This work has hence initiated a new class of monomers to the biopolymer synthesis field. The procedures described could however be used to tailor the biodegradation behaviour or slightly modify the mechanical properties of the final thermoset via the copolymerization of two or more such monomers. This was not explored in this work, as the main objective of achieving soft, elastomeric polymers could not be met via this method. Such polymers based on the photopolymerization of diallyl compounds, however, have great potential for hard tissue engineering instead. Hence the results obtained on the synthesis and characterization of photopolymerized diallyl tartrate have been published [159] for its potential future use in bio-applications.

5.2. Epoxy-amine system

A series of novel crosslinked polymers was synthesized using epoxy-amine chemistry. The two amine-functionalized prepolymers used were of different molecular weights: 3000 g/moL and 18 000 g/mol; and different polymer types: PCL homopolymer

with high crystallinity and a random 50/50 copolymer of PCL and P(dl)LA, which was amorphous. The epoxy reactants were PEG diglycidyl ether of two different molecular weights: 500 g/moL and 1000 g/moL. Four different crosslinked polymers were successfully obtained from the crosslinking reactions among these four components with gel contents of ~40-50 % by mass.

It was found that the length of prepolymer played a part in the ultimate amount of the PEG crosslinker per unit volume of crosslinked polymer, which in turn affected certain properties. For example, the lower the molecular weight of the prepolymer, the higher the amount of PEG there is per unit volume. Hence this leads to the higher amount of swelling observed in aqueous medium due to the high hydrophilicity of PEG. The length of the prepolymer also affects the mechanical properties of the final polymer significantly. The higher the molecular weight of the prepolymer, the larger the maximum elongations obtained and the lower the Young's modulus of the final crosslinked polymer. A longer prepolymer also results in higher recoverable strains under cyclic loading. With respect to the biodegradation behaviour, a prepolymer with a higher molecular weight, which has less PEG per unit volume, degrades at a slower rate as compared to a shorter prepolymer.

The type of prepolymer also affects the final properties of the crosslinked polymer. It is easier to achieve higher gel contents with an amorphous prepolymer, even if it has a high molecular weight. Hence the polymers based on PCLcoPLA18K had gel contents similar to those based on PCL3K. The type of monomers used in the preparation of the prepolymer also affects properties such as degradation. Adding units of a relatively more hydrophilic polymer such as PLA increases the rate of mass loss as compared to using just units of hydrophobic PCL.

Varying the crosslinker length was also found to affect some properties. Using PEG1K instead of PEG500 results in a higher degree of swelling, and larger maximum elongations.

Hence this work has introduced a novel system of crosslinked polymers with tailorable properties in the low young's moduli range. Several factors can be tweaked to obtain the desired final properties. More importantly, the crosslinked polymers exhibited fully reversible strains with zero hysteresis and have shown to be non-toxic in the short-term. These properties make this system of polymers an ideal candidate for the engineering of soft elastic tissue.

6 Future Work and Recommendations

6.1. Photocrosslinked system

The ring-opening polymerization of common cyclic esters using the secondary hydroxyl groups on diallyl tartrate has great potential to be explored further with triethylaluminum as the catalyst. This is expected to result in a series of polymers with tailorable properties. This is because not only can the molecular weight of the polymers incorporated be controlled (by varying the co-initiator : monomer ratio, using diallyl tartrate as the co-initiator); the type of polymer (by varying the type of monomer used) can also be varied for different end properties.

In order to evaluate this material fully for hard tissue engineering applications, it is worth carrying out a cell proliferation and/or differentiation study on the material surface in future. The biodegradation study should also be extended until the material exhibits 100% mass loss, including not only mass loss but also the loss of a mechanical property over time, for a clearer understanding of its degradation behaviour. A specific type of tissue to be engineered using this material could be spongy bone or tendon, which have Young's moduli in the range of 0.1-1 GPa [38].

6.2. Epoxy-amine system

In this work, only two prepolymers were explored, but several more prepolymers may also be synthesized and characterized according to these procedures for a wider

spectrum of properties. Some of the factors of this system that could be varied, and their possible effects on the final crosslinked polymer, are outlined in Table 7 below.

Taking the mechanical properties of the crosslinked polymers synthesized in this work as a reference, the Young's modulus values obtained ranged from 9-12 kPa for those synthesized from the higher molecular weight prepolymer, to 28-33 kPa for those from the lower molecular weight prepolymer. These values further decreased upon hydration and swelling of the polymers. Although these properties may be suitable for tissue such as lung, stiffer materials are required for tissue such as skeletal or cardiac muscle, hence using Table 7, suitable factors can be varied to achieve this. For example, including PGA as a homopolymer or component of a copolymer in the synthesis of the amine-prepolymer can help to increase the stiffness of the final polymer. Based on the specific application in future, many of these factors could be explored in achieving the mechanical properties required.

Looking at the biodegradation behaviour of these polymers, it can be seen that up to 20% mass loss was observed within a month. For future work, the rate of degradation required depends on the specific application as well, as different types of tissue have different regenerative rates. Hence the required rate may be achieved by varying the right factors for this polymer system.

	Factor	Variation	Effect on mechanical properties	Effect on Degradation	Other effects
Prepolymer	**Type**	Homo-polymer of various bio-resorbable monomers (caprolactone, lactide, glycolide, trimethylene carbonate, etc.)	The different polymer types exhibit different properties. For e.g., PGA has a higher modulus than that of PLA or PCL of the same molecular weight.	The different types of polymers degrade at different rates in aqueous media. For e.g., PGA completely degrades within 6-12 months while PCL takes more than 2 years.	The different polymers (or copolymers) can also give rise to varying degrees of surface hydrophilicity, which can affect cell attachment. For e.g., PCL is more hydrophobic compared to PLA.
		Copolymer of various bio-resorbable monomers	Co-polymerization of two or more of different monomers can give rise to intermediate or completely different properties. For e.g., poly(TMC-co-CL) is almost 40 times softer (modulus) than the PCL homopolymer.	Degradation properties can also be very different from that of the individual components in a copolymer. For e.g., PLGA degrades more rapidly compared to PLA or PGA.	
	Length	Increase	A longer prepolymer leads to lower crosslink densities, which results in larger elongations and lower moduli.	A lower crosslink density results in a higher degradation rate as water molecules are able to diffuse into the loose network faster.	-
		Decrease	A shorter prepolymer leads to higher crosslink densities, which results in higher moduli and lower elongations.	A higher crosslink density results in slower degradation as water is not able to penetrate the tight network quickly.	-

	End-group (amino acid)	Type	Besides lysine, there are various other amino acids that can be used. The use of bulky amino acids such as tyrosine would result in a stiffer polymer. However the effect of these end groups on the mechanical properties of the final polymer depends on the prepolymer length. The longer the prepolymer, the less this effect is seen due to fewer end groups per unit volume.	The type of amino acid may also affect the degradation rate of the final polymer due to their different polarities. The use of more polar amino acids (those with side groups such as amines, alcohols, acids and amides) would result in a more hydrophilic polymer than the use of less polar (those with side groups such as alkyls or benzene rings) ones.	Amino acids with functional side groups can be used for the attachment of growth factors, etc. For example, the hydroxyl group on serine.
PEG-Crosslinker	**Length**	Increase	The longer the crosslinker chain length, the higher the maximum elongations achievable.	The longer the PEG chain length, the higher the extent of swelling of the crosslinked polymer. This leads to a faster initial rate of hydrolytic degradation.	The amount of PEG in the final polymer can be used to control cell attachment. The more PEG there is, the more hydrophilic the polymers, hence reducing the attachment of antibodies, proteins, hence reducing any immune response. [26]
		Decrease	The shorter the crosslinker chain length, the lower the maximum elongations obtained.	The shorter the PEG component, the lower the degree of swelling, leading to a more gradual rate of hydrolytic degradation from the start.	

Table 7 Possible future variations applicable to the epoxy-amine system

References

1. Laaksovirta, S. (2003). Biodegradable, Self-reinforced, Self-expandable Lactic and Glycolic Acid (SR-PLGA 80/20) Copolymer Spiral Prostatic Stent. Ph.D. Dissertation University of Tampere Medical School.
2. Williams, D. F. (1999). *The Williams Dictionary of Biomaterials*. Liverpool, UK: Liverpool University Press.
3. Yoshito, I., & Hideto, T. (2000). Biodegradable polyesters for medical and ecological applications. *Macromolecular Rapid Communications, 21*, 117-132.
4. Ashammakhi, N., & Rokkanen, P. (1997). Absorbable polyglycolide devices in trauma and bone surgery. *Biomaterials, 18*, 3-9.
5. Hayashi, T. (1994). Biodegradable Polymers for biomedical applications. *Progress in Polymer Science, 19*, 663-702.
6. Holland, S. J., & Tighe, B. J. (1992). Biodegradable Polymers. In *Advances in Pharamaceutical Science* (pp. 101-164). London: Academic Press.
7. Kohn, J., & Langer, R. (1997). Bioresorbable and bioerodible materials. In B. D. Ratner, A. S. Hoffman, F. J. Schoen & J. E. Lemon (Eds.), *An Introduction to Materials in Medicine* (pp. 65-73). San Diego: Academic Press.
8. Shalaby, S. W. (1988). Bioabsorbable Polymers. In J. Swarbrick & J. C. Boylan (Eds.), *Encyclopedia of Pharmaceutical Technology* (Vol. 1, pp. 465-476): M Dekker.
9. Behravesh, E., Yasko, A. W., Engel, P. S., & Mikos, A. G. (1999). Synthetic Biodegradable Polymers for Orthopaedic Applications. *Clinical Orthopaedics and Related Research, 367*, S118-S129.

10. Middleton, J. C., & Tipton, A. J. (2000). Synthetic biodegradable polymers as orthopedic devices. *Biomaterials, 21*, 2335-2346.

11. Wiggins, J. S., Hassan, M. K., Mauritz, K. A., & Storey, R. F. (2006). Hydrolytic degradation of poly(D,L-lactide) as a function of end group: Carboxylic acid vs. hydroxyl. *Polymer, 47*, 1960-1969.

12. Gunatillake, P. A., & Adhikari, R. (2003). BIODEGRADABLE SYNTHETIC POLYMERS FOR TISSUE ENGINEERING *European Cells and Materials, 5* 1-16.

13. Schakenraad, J. M., Nieuwenhuis, P., Molenaar, I., Helder, J., Dijkstra, P. J., & Feijen, J. (1989). In vivo and in vitro degradation of glycine/DL-lactic acid copolymers. *Journal of Biomedical Materials Research, 23*, 1271-1288.

14. Sliedregt, A., Groot, K., & Blitterswijk, C. A. (1993). In-vitro biocompatibility testing of polylactides. *Journal of Materials Science: Materials in Medicine, 4*, 213-218.

15. Verheyen, C. C. P. M., De Wijn, J. R., van Blitterswijk, C. A., Rozing, P. M., & de Groot, K. (1993). Examination of efferent lymph nodes after 2 years of transcortical implantation of poly(L-lactide) containing plugs: A case report. *Journal of Biomedical Materials Research, 27*, 1115-1118.

16. Gibbons, D. F. (1992). Tissue response to resorbable synthetic polymers. In H. Plank, M. Dauner & M. Renardy (Eds.), *Degradation phenomena on polymeric biomaterials* (pp. 97-104). New York: Springer Verlag.

17. Kronenthal, R. L. (1975). Biodegradable polymers in medicine and surgery. *Polymer Science Technology, 8*, 119-137.

18. Blitterswijk, C. v., Thomsen, P., Lindahl, A., Hubbell, J., Williams, D. F., Cancedda, R., Bruijn, J. D. d., & Sohier, J. (2008). *Tissue Engineering*: Academic Press.

19. Kowalski, A., Duda, A., & Penczek, S. (2000). Kinetics and Mechanism of Cyclic Esters Polymerization Initiated with Tin(II) Octoate. 3.,Ä† Polymerization of l,l-Dilactide. *Macromolecules, 33*, 7359-7370.

20. Kricheldorf, H. R., Kreiser-Saunders, I., & Stricker, A. (2000). Polylactones 48. SnOct2-Initiated Polymerizations of Lactide: A Mechanistic Study. *Macromolecules, 33*, 702-709.

21. O'Driscoll, S. W. (1998). Current Concepts Review - The Healing and Regeneration of Articular Cartilage. *J Bone Joint Surg Am, 80*, 1795-1812.

22. Belgacem, B. Y., Zygourakis, K., & Markenscoff, P. (October 1999). Modeling the growth of three-dimensional tissues. In *BMES/EMBS Conference, 1999. Proceedings of the First Joint* (Vol. 2, pp. 1180). Atlanta, GA , USA

23. Griffith, L. G., & Naughton, G. (2002). Tissue Engineering,ÄîCurrent Challenges and Expanding Opportunities. *Science, 295*, 1009.

24. Di Martino, A., Sittinger, M., & Risbud, M. V. (2005). Chitosan: A versatile biopolymer for orthopaedic tissue-engineering. *Biomaterials, 26*, 5983-5990.

25. Liu, X., & Ma, P. X. (2004). Polymeric Scaffolds for Bone Tissue Engineering. *Annals of Biomedical Engineering, 32*, 477-486.

26. Cheung, H.-Y., Lau, K.-T., Lu, T.-P., & Hui, D. (2007). A critical review on polymer-based bio-engineered materials for scaffold development. *Composites Part B: Engineering, 38*, 291-300.

27. Lee, S.-H., Kim, B.-S., Kim, S. H., Choi, S. W., Jeong, S. I., Kwon, I. K., Kang, S. W., Nikolovski, J., Mooney, D. J., Han, Y.-K., & Kim, Y. H. (2003). Elastic

biodegradable poly(glycolide-co-caprolactone) scaffold for tissue engineering. *Journal of Biomedical Materials Research Part A, 66A*, 29-37.

28. Grijpma, D. W., Hou, Q., & Feijen, J. (2005). Preparation of biodegradable networks by photo-crosslinking lactide, [epsilon]-caprolactone and trimethylene carbonate-based oligomers functionalized with fumaric acid monoethyl ester. *Biomaterials, 26*, 2795-2802.

29. Pêgo, A. P., Siebum, B., Van Luyn, M. J. A., Gallego y Van Seijen, X. J., Poot, A. A., Grijpma, D. W., & Feijen, J. (2003). Preparation of Degradable Porous Structures Based on 1,3-Trimethylene Carbonate and D,L-Lactide (Co)polymers for Heart Tissue Engineering. *Tissue Engineering, 9*, 981-994.

30. Pêgo, A. P., Van Luyn, M. J. A., Brouwer, L. A., van Wachem, P. B., Poot, A. A., Grijpma, D. W., & Feijen, J. (2003). In vivo behavior of poly(1,3-trimethylene carbonate) and copolymers of 1,3-trimethylene carbonate with D,L-lactide or ∈-caprolactone: Degradation and tissue response. *Journal of Biomedical Materials Research Part A, 67A*, 1044-1054.

31. Barrera, D. A., Zylstra, E., Lansbury, P. T., & Langer, R. (1995). Copolymerization and Degradation of Poly(lactic acid-co-lysine). *Macromolecules, 28*, 425-432.

32. Tessmar, J. K., Mikos, A. G., & Gopferich, A. (2001). Amine-Reactive Biodegradable Diblock Copolymers. *Biomacromolecules, 3*, 194-200.

33. Kim, B.-S., Nikolovski, J., Bonadio, J., & Mooney, D. J. (1999). Cyclic mechanical strain regulates the development of engineered smooth muscle tissue. *Nature Biotechnology, 17*, 979-983.

34. Brunelle, D. J. (1993). *Ring-opening Polymerization: Mechanisms, Catalysis, Structure, Utility*: Hanser Publishers.

35. Sautereau, J. P. H. (2002). *Thermosetting Polymers*: Marcel Dekker Inc.

36. Helminen, A. (2003). Branched And Crosslinked Resorbable Polymers Based on Lactic Acid, Lactide and e-Caprolactone. Helsinki University of Technology.

37. Decker, C. (1996). Photoinitiated crosslinking polymerisation. *Progress in Polymer Science, 21,* 593-650.

38. Park, J. B., & Lakes, R. S. (1992). *Biomaterials, An Introduction* (2nd ed.): Plenum Press.

39. Levental, I., Georges, P. C., & Janmey, P. A. (2007). Soft biological materials and their impact on cell function. *Soft Matter, 3,* 299-306.

40. Zdrahala, R. J., & Zdrahala, I. J. (1999). Biomedical Applications of Polyurethanes: A Review of Past Promises, Present Realities, and a Vibrant Future. *Journal of Biomaterials Applications, 14,* 67-90.

41. Gogolewski, S., & Pennings, A. J. (1982). Biodegradable materials of polylactides, 4. Porous biomedical materials based on mixtures of polylactides and polyurethanes. *Die Makromolekulare Chemie, Rapid Communications, 3,* 839-845.

42. McGill, D. B., & Motto, J. D. (1974). An industrial outbreak of toxic hepatitis due to methylenedianiline. *New England Journal of Medicine, 291,* 278-282.

43. Storey, R. F., Wiggins, J. S., & Puckett, A. D. (1994). Hydrolyzable poly(ester-urethane) networks from L-lysine diisocyanate and D,L-lactide/∈-caprolactone homo- and copolyester triols. *Journal of Polymer Science Part A: Polymer Chemistry, 32,* 2345-2363.

44. Zhang, J.-Y., Beckman, E. J., Hu, J., Yang, G.-G., Agarwal, S., & Hollinger, J. O. (2002). Synthesis, Biodegradability, and Biocompatibility of Lysine Diisocyanate,ÄìGlucose Polymers. *Tissue Engineering, 8,* 771-785.

45. Zhang, J.-Y., Doll, B. A., Beckman, E. J., & Hollinger, J. O. (2003). Three-Dimensional Biocompatible Ascorbic Acid-Containing Scaffold for Bone Tissue Engineering. *Tissue Engineering, 9*, 1143-1157.

46. Guan, J., Fujimoto, K. L., Sacks, M. S., & Wagner, W. R. (2005). Preparation and characterization of highly porous, biodegradable polyurethane scaffolds for soft tissue applications. *Biomaterials, 26*, 3961-3971.

47. Guan, J., Sacks, M. S., Beckman, E. J., & Wagner, W. R. (2002). Synthesis, characterization, and cytocompatibility of elastomeric, biodegradable poly(ester-urethane)ureas based on poly(caprolactone) and putrescine. *Journal of Biomedical Materials Research, 61*, 493-503.

48. Guan, J., Sacks, M. S., Beckman, E. J., & Wagner, W. R. (2004). Biodegradable poly(ether ester urethane)urea elastomers based on poly(ether ester) triblock copolymers and putrescine: synthesis, characterization and cytocompatibility. *Biomaterials, 25*, 85-96.

49. Bruin, P., Veenstra, G. J., Nijenhuis, A. J., & Pennings, A. J. (1988). Design and synthesis of biodegradable poly(ester-urethane) elastomer networks composed of non-toxic building blocks. *Die Makromolekulare Chemie, Rapid Communications, 9*, 589-594.

50. Bruin, P., Smedinga, J., Pennings, A. J., & Jonkman, M. F. (1990). Biodegradable lysine diisocyanate-based poly(glycolide-co-[epsilon]-caprolactone)-urethane network in artificial skin. *Biomaterials, 11*, 291-295.

51. De Groot, J. H., Nijenhuis, A. J., Bruin, P., Pennings, A. J., Veth, R. P. H., Klompmaker, J., & Jansen, H. W. B. (1990). Use of porous biodegradable polymer implants in meniscus reconstruction. 1) Preparation of porous

biodegradable polyurethanes for the reconstruction of meniscus lesions. *Colloid & Polymer Science, 268*, 1073-1081.

52. Hirt, T. D., Neuenschwander, P., & Suter, U. W. (1996). Synthesis of degradable, biocompatible, and tough block-copolyesterurethanes. *Macromolecular Chemistry and Physics, 197*, 4253-4268.

53. Saad, B., Hirt, T. D., Welti, M., Uhlschmid, G. K., Neuenschwander, P., & Suter, U. W. (1997). Development of degradable polyesterurethanes for medical applications: In vitro and in vivo evaluations. *Journal of Biomedical Materials Research, 36*, 65-74.

54. Zhang, J. Y., Beckman, E. J., Piesco, N. P., & Agarwal, S. (2000). A new peptide-based urethane polymer: synthesis, biodegradation, and potential to support cell growth in vitro. *Biomaterials, 21*, 1247-1258.

55. Spaans, C. J., Belgraver, V. W., Rienstra, O., De Groot, J. H., Veth, R. P. H., & Pennings, A. J. (2000). Solvent-free fabrication of micro-porous polyurethane amide and polyurethane-urea scaffolds for repair and replacement of the knee-joint meniscus. *Biomaterials, 21*, 2453-2460.

56. Li, S., Molina, I., Martinez, M. B., & Vert, M. (2002). Hydrolytic and enzymatic degradations of physically crosslinked hydrogels prepared from PLA/PEO/PLA triblock copolymers. *Journal of Materials Science: Materials in Medicine, 13*, 81-86.

57. Cohn, D., Stern, T., Gonzalez, M. F., & Epstein, J. (2002). Biodegradable poly(ethylene oxide)/poly(epsilon-caprolactone) multiblock copolymers. *Journal of Biomedical Materials Research Part A, 59*, 273-281.

58. Odian, G. (2004). *Principles of Polymerization*. Hoboken, New Jersey: John Wiley & Sons, Inc.

59. Anseth, K. S., Wang, C. M., & Bowman, C. N. (1994). Reaction behaviour and kinetic constants for photopolymerizations of multi(meth)acrylate monomers. *Polymer, 35*, 3243-3250.

60. Cook, W. D. (1992). Thermal aspects of the kinetics of dimethacrylate photopolymerization. *Polymer, 33*, 2152-2161.

61. Cruise, G. M., Scharp, D. S., & Hubbell, J. A. (1998). Characterization of permeability and network structure of interfacially photopolymerized poly(ethylene glycol) diacrylate hydrogels. *Biomaterials, 19*, 1287-1294.

62. West, J. L., & Hubbell, J. A. (1995). Photopolymerized hydrogel materials for drug delivery applications. *Reactive Polymers, 25*, 139-147.

63. Burdick, J. A., Mason, M. N., Hinman, A. D., Thorne, K., & Anseth, K. S. (2002). Delivery of osteoinductive growth factors from degradable PEG hydrogels influences osteoblast differentiation and mineralization. *Journal of Controlled Release, 83*, 53-63.

64. Piantino, J., Burdick, J. A., Goldberg, D., Langer, R., & Benowitz, L. I. (2006). An injectable, biodegradable hydrogel for trophic factor delivery enhances axonal rewiring and improves performance after spinal cord injury. *Experimental Neurology, 201*, 359-367.

65. Quick, D. J., & Anseth, K. S. (2003). Gene Delivery in Tissue Engineering: A Photopolymer Platform to Coencapsulate Cells and Plasmid DNA. *Pharmaceutical Research, 20*, 1730-1737.

66. Quick, D. J., & Anseth, K. S. (2004). DNA delivery from photocrosslinked PEG hydrogels: encapsulation efficiency, release profiles, and DNA quality. *Journal of Controlled Release, 96*, 341-351.

67. Sawhney, A. S., Pathak, C. P., & Hubbell, J. A. (1993). Bioerodible Hydrogels Based on Photopolymerized Poly(ethylene gylcol)-co-poly(α-hydroxy acid) Diacrylate Macromers. *Macromolecules, 26*, 581-587.

68. Metters, A. T., Anseth, K. S., & Bowman, C. N. (2000). Fundamental studies of a novel, biodegradable PEG-b-PLA hydrogel. *Polymer, 41*, 3993-4004.

69. Metters, A. T., Anseth, K. S., & Bowman, C. N. (2001). A Statistical Kinetic Model for the Bulk Degradation of PLA-b-PEG-b-PLA Hydrogel Networks:¸Äâ Incorporating Network Non-Idealities. *The Journal of Physical Chemistry B, 105*, 8069-8076.

70. Metters, A. T., Bowman, C. N., & Anseth, K. S. (2001). Verification of scaling laws for degrading PLA-b-PEG-b-PLA hydrogels. *AIChE Journal, 47*, 1432-1437.

71. Bryant, S. J., & Anseth, K. S. (2003). Controlling the spatial distribution of ECM components in degradable PEG hydrogels for tissue engineering cartilage. *Journal of Biomedical Materials Research Part A, 64A*, 70-79.

72. Kim, B. S., Hrkach, J. S., & Langer, R. (2000). Biodegradable photo-crosslinked poly(ether-ester) networks for lubricious coatings. *Biomaterials, 21*, 259-265.

73. Storey, R. F., Warren, S. C., Allison, C. J., Wiggins, J. S., & Puckett, A. D. (1993). Synthesis of bioabsorbable networks from methacrylate-endcapped polyesters. *Polymer, 34*, 4365-4372.

74. Takao, A., Fusae, M., & Yu, N. (1994). Preparation of cross-linked aliphatic polyester and application to thermo-responsive material. *Journal of Controlled Release, 32*, 87-96.

75. Amsden, B. G., Misra, G., Gu, F., & Younes, H. M. (2004). Synthesis and Characterization of A Photo-Cross-Linked Biodegradable Elastomer. *Biomacromolecules, 5*, 2479-2486.

76. Coullerez, G., Lowe, C., Pechy, P., Kausch, H. H., & Hilborn, J. (2000). Synthesis of acrylate functional telechelic poly(lactic acid) oligomer by transesterification. *Journal of Materials Science: Materials in Medicine, 11*, 505-510.

77. John, G., & Morita, M. (1999). Synthesis and Characterization of Photo-Cross-Linked Networks Based on l-Lactide/Serine Copolymers,Ä†. *Macromolecules, 32*, 1853-1858.

78. Elisseeff, J. H., Anseth, K. S., Langer, R., & Hrkach, J. S. (1997). Synthesis and Characterization of Photo-Cross-Linked Polymers Based on Poly(L-lactic acid-co-L-aspartic acid). *Macromolecules, 30*, 2182-2184.

79. Horch, R. A., Shahid, N., Mistry, A. S., Timmer, M. D., Mikos, A. G., & Barron, A. R. (2004). Nanoreinforcement of Poly(propylene fumarate)-Based Networks with Surface Modified Alumoxane Nanoparticles for Bone Tissue Engineering. *Biomacromolecules, 5*, 1990-1998.

80. Payne, R. G., McGonigle, J. S., Yaszemski, M. J., Yasko, A. W., & Mikos, A. G. (2002). Development of an injectable, in situ crosslinkable, degradable polymeric carrier for osteogenic cell populations. Part 3. Proliferation and differentiation of encapsulated marrow stromal osteoblasts cultured on crosslinking poly(propylene fumarate). *Biomaterials, 23*, 4381-4387.

81. Porter, B. D., Oldham, J. B., He, S. L., Zobitz, M. E., Payne, R. G., An, K. N., Currier, B. L., Mikos, A. G., & Yaszemski, M. J. (2000). Mechanical Properties of a Biodegradable Bone Regeneration Scaffold. *Journal of Biomechanical Engineering, 122*, 286-288.

82. Shin, H., Quinten, R. P., Mikos, A. G., & Jansen, J. A. (2003). In vivo bone and soft tissue response to injectable, biodegradable oligo(poly(ethylene glycol) fumarate) hydrogels. *Biomaterials, 24*, 3201-3211.

83. Kharas, G. B., Kamenetsky, M., Simantirakis, J., Beinlich, K. C., Rizzo, A.-M. T., Caywood, G. A., & Watson, K. (1997). Synthesis and characterization of fumarate-based polyesters for use in bioresorbable bone cement composites. *Journal of Applied Polymer Science, 66*, 1123-1137.

84. Peter, S. J., Miller, S. T., Zhu, G., Yasko, A. W., & Mikos, A. G. (1998). In vivo degradation of a poly(propylene fumarate)/β-tricalcium phosphate injectable composite scaffold. *Journal of Biomedical Materials Research, 41*, 1-7.

85. Temenoff, J. S., & Mikos, A. G. (2000). Injectable biodegradable materials for orthopedic tissue engineering. *Biomaterials, 21*, 2405-2412.

86. Anseth, K. S., Metters, A. T., Bryant, S. J., Martens, P. J., Elisseeff, J. H., & Bowman, C. N. (2002). In situ forming degradable networks and their application in tissue engineering and drug delivery. *Journal of Controlled Release, 78*, 199-209.

87. Martens, P., & Anseth, K. S. (2000). Characterization of hydrogels formed from acrylate modified poly(vinyl alcohol) macromers. *Polymer, 41*, 7715-7722.

88. Mühlebach, A., Müller, B., Pharisa, C., Hofmann, M., Seiferling, B., & Guerry, D. (1997). New water-soluble photo crosslinkable polymers based on modified poly(vinyl alcohol). *Journal of Polymer Science Part A: Polymer Chemistry, 35*, 3603-3611.

89. Nuttelman, C. R., Henry, S. M., & Anseth, K. S. (2002). Synthesis and characterization of photocrosslinkable, degradable poly(vinyl alcohol)-based tissue engineering scaffolds. *Biomaterials, 23*, 3617-3626.

90. Schmedlen, R. H., Masters, K. S., & West, J. L. (2002). Photocrosslinkable polyvinyl alcohol hydrogels that can be modified with cell adhesion peptides for use in tissue engineering. *Biomaterials, 23*, 4325-4332.

91. Martens, P. J., Bowman, C. N., & Anseth, K. S. (2004). Degradable networks formed from multi-functional poly(vinyl alcohol) macromers: comparison of results from a generalized bulk-degradation model for polymer networks and experimental data. *Polymer, 45*, 3377-3387.

92. Anderson, D. G., Tweedie, C. A., Hossain, N., Navarro, S. M., Brey, D. M., Van Vliet, K. J., Langer, R., & Burdick, J. A. (2006). A Combinatorial Library of Photocrosslinkable and Degradable Materials. *Advanced Materials, 18*, 2614-2618.

93. Brey, D. M., Erickson, I., & Burdick, J. A. (2008). Influence of macromer molecular weight and chemistry on poly(β-amino ester) network properties and initial cell interactions. *Journal of Biomedical Materials Research Part A, 85A*, 731-741.

94. Anseth, K. S., & Quick, D. J. (2001). Polymerizations of Multifunctional Anhydride Monomers to Form Highly Crosslinked Degradable Networks. *Macromolecular Rapid Communication, 22*, 564-572.

95. Burkoth, A. K., & Anseth, K. S. (2000). A review of photocrosslinked polyanhydrides:: in situ forming degradable networks. *Biomaterials, 21*, 2395-2404.

96. Muggli, D. S., Burkoth, A. K., Keyser, S. A., Lee, H. R., & Anseth, K. S. (1998). Reaction Behavior of Biodegradable, Photo-Cross-Linkable Polyanhydrides. *Macromolecules, 31*, 4120-4125.

97. Anseth, K. S., Shastri, V. R., & Langer, R. (1999). Photopolymerizable degradable polyanhydrides with osteocompatibility. *Nature Biotechnology, 17*, 156.

98. Poshusta, A. K., Burdick, J. A., Mortisen, D. J., Padera, R. F., Ruehlman, D., Yaszemski, M. J., & Anseth, K. S. (2003). Histocompatibility of photocrosslinked polyanhydrides: A novel in situ forming orthopaedic biomaterial. *Journal of Biomedical Materials Research Part A, 64A*, 62-69.

99. Bruining, M. J., G.T. Blaauwgeers, H., Kuijer, R., Elisabeth, P., Nuijts, R. M. M. A., & Koole, L. H. (2000). Biodegradable three-dimensional networks of poly(dimethylamino ethyl methacrylate). Synthesis, characterization and in vitro studies of structural degradation and cytotoxicity. *Biomaterials, 21*, 595-604.

100. Timmer, M. D., Ambrose, C. G., & Mikos, A. G. (2003). In vitro degradation of polymeric networks of poly(propylene fumarate) and the crosslinking macromer poly(propylene fumarate)-diacrylate. *Biomaterials, 24*, 571-577.

101. Lang, M., Wong, R. P., & Chu, C.-C. (2002). Synthesis and structural analysis of functionalized poly (ε-caprolactone)-based three-arm star polymers. *Journal of Polymer Science Part A: Polymer Chemistry, 40*, 1127-1141.

102. Turunen, M. P., Korhonen, H., Tuominen, J., & Seppala, J. V. (2002). Synthesis, characterization and crosslinking of functional star-shaped poly(<I>ϵ</I>-caprolactone). *Polymer International, 51*, 92-100.

103. Nagata, M., & Sato, Y. (2004). Biodegradable elastic photocured polyesters based on adipic acid, 4-hydroxycinnamic acid and poly([var epsilon]-caprolactone) diols. *Polymer, 45*, 87-93.

104. Matsumoto, A. (2001). Polymerization of multiallyl monomers. *Progress in Polymer Science, 26*, 189-257.

105. Ohata, T., & Matsumoto, A. (1980). Studies of the polymerization of diallyl compounds. XXVI. Enhanced polymerizability by the hydroxyl group in the polymerization of diallyl hydroxydicarboxylates. *Journal of Polymer Science Part A: Polymer Chemistry, 18*, 465-475.

106. Ohata, T., Matsumoto, A., & Oiwa, M. (1975). Studies on the polymerization of diallyl compounds. XXIII. Thermal polymerization of diallyl tartrate. *Polymer Letter Edition, 13*, 645-649.

107. Wang, Y., Ameer, G. A., Sheppard, B., & Langer, R. (2002). A tough biodegradable elastomer. *Nature Biotechnology, 20*, 602-606.

108. Wang, Y., Kim, Y. M., & Langer, R. (2003). In vivo degradation characteristics of poly(glycerol sebacate). *Journal of Biomedical Materials Research Part A, 66A*, 192-197.

109. Fu, J., Fiegel, J., Krauland, E., & Hanes, J. (2002). New polymeric carriers for controlled drug delivery following inhalation or injection. *Biomaterials, 23*, 4425-4433.

110. Sundback, C. A., Shyu, J. Y., Wang, Y., Faquin, W. C., Langer, R. S., Vacanti, J. P., & Hadlock, T. A. (2005). Biocompatibility analysis of poly(glycerol sebacate) as a nerve guide material. *Biomaterials, 26*, 5454-5464.

111. Bruggeman, J. P., de Bruin, B.-J., Bettinger, C. J., & Langer, R. (2008). Biodegradable poly(polyol sebacate) polymers. *Biomaterials, 29*, 4726-4735.

112. Yang, J., Webb, A. R., & Ameer, G. A. (2004). Novel Citric Acid-Based Biodegradable Elastomers for Tissue Engineering. *Advanced Materials, 16*, 511-516.

113. Yang, J., Webb, A. R., Pickerill, S. J., Hageman, G., & Ameer, G. A. (2006). Synthesis and evaluation of poly(diol citrate) biodegradable elastomers. *Biomaterials, 27*, 1889-1898.

114. Kang, Y., Yang, J., Khan, S., Anissian, L., & Ameer, G. A. (2006). A new biodegradable polyester elastomer for cartilage tissue engineering. *Journal of Biomedical Materials Research Part A, 77A*, 331-339.

115. Qiu, H., Yang, J., Kodali, P., Koh, J., & Ameer, G. A. (2006). A citric acid-based hydroxyapatite composite for orthopedic implants. *Biomaterials, 27*, 5845-5854.

116. Ameer, G. A., & Webb, A. R. (2006). Biodegradabel nanocomposites with enhanced mechanical properties for soft tissue. In U. P. Office (Ed.). U.S.A.

117. Minoru, N., Tetsuya, M., Wataru, S., & Naoto, T. (1999). Synthesis, characterization, and enzymatic degradation of network aliphatic copolyesters. *Journal of Polymer Science Part A: Polymer Chemistry*, *37*, 2005-2011.

118. Minoru, N., Masao, K., Wataru, S., & Naoto, T. (2002). Biodegradable network elastomeric polyesters from multifunctional aromatic carboxylic acids and poly(ε-caprolactone) diols. *Journal of Polymer Science Part A: Polymer Chemistry, 40*, 4523-4529.

119. Lee, L. Y., Wu, S. C., Fu, S. S., Zeng, S. Y., Leong, W. S., & Tan, L. P. Biodegradable elastomer for soft tissue engineering. *European Polymer Journal, In Press, Corrected Proof*.

120. Bettinger, C. J., Bruggeman, J. P., Borenstein, J. T., & Langer, R. S. (2008). Amino alcohol-based degradable poly(ester amide) elastomers. *Biomaterials, 29*, 2315-2325.

121. Chen, Q.-Z., Bismarck, A., Hansen, U., Junaid, S., Tran, M. Q., Harding, S. n. E., Ali, N. N., & Boccaccini, A. R. (2008). Characterisation of a soft elastomer

poly(glycerol sebacate) designed to match the mechanical properties of myocardial tissue. *Biomaterials, 29*, 47-57.

122. Shechter, L., Wynstra, J., & Kurkjy, R. P. (1956). Glycidyl Ether Reactions with Amines. *Industrial & Engineering Chemistry, 48*, 94-97.

123. Yeganeh, H., & Hojati-Talemi, P. (2007). Preparation and properties of novel biodegradable polyurethane networks based on castor oil and poly(ethylene glycol). *Polymer Degradation and Stability, 92*, 480-489.

124. Yeganeh, H., Lakouraj, M. M., & Jamshidi, S. (2005). Synthesis and properties of biodegradable elastomeric epoxy modified polyurethanes based on poly([epsilon]-caprolactone) and poly(ethylene glycol). *European Polymer Journal, 41*, 2370-2379.

125. Guthikonda, R. N., Cama, L. D., Quesada, M., Woods, M. F., Salzmann, T. N., & Christensen, B. G. (1987). Structure-activity relationships in the 2-arylcarbapenem series. Synthesis of 1-methyl-2-arylcarbapenems. *Journal of Medicinal Chemistry, 30*, 871-880.

126. Korhonen, H., Helminen, A., & Seppala, J. V. (2001). Synthesis of polylactides in the presence of co-initiators with different numbers of hydroxyl groups. *Polymer, 42*, 7541-7549.

127. Mecerreyes, D., Dubois, Jerome, R., Hedrick, J. L., & Hawker, C. J. (1999). Synthesis of Dendritic–Linear Block Copolymers by Living Ring-Opening Polymerization of Lactones and Lactides Using Dendritic Initiators. *Journal of Polymer Science Part A: Polymer Chemistry, 37*, 1923-1930.

128. Guerra, R. M., DurÁN, I., & Ortiz, P. (1996). FTIR monomer conversion analysis of UDMA-based dental resins. *Journal of Oral Rehabilitation, 23*, 632-637.

129. Pamedytyte, V., Abadie, M. J. M., & Makuska, R. (2002). Photopolymerization of N,N-dimethylaminoethylmethacrylate studied by photocalorimetry. *Journal of Applied Polymer Science, 86,* 579-588.

130. Kerr, J. A. (1996). Bond dissociation energies by kinetic methods. *Chemical Reviews, 66,* 465-500.

131. Abadie, J. M. J. (1991). *European Coatings Journal, 11,* 788.

132. Sestak, J., & Berggren, G. (1971). Study of the kinetics of the mechanism of solid-state reactions at increasing temperatures. *Thermochimica Acta, 3,* 1-12.

133. Abadie, M. J. M., Novikova, O. O., Voytekunas, V. Y., Syromyatnikov, V. G., & Kolendo, A. Y. (2003). Differential scanning photocalorimetry studies of 1,6-hexanedioldiacrylate photopolymerization initiated by some organic azides. *Journal of Applied Polymer Science, 90,* 1096-1101.

134. Boey, F. Y. C., & Qiang, W. (2000). Experimental modeling of the cure kinetics of an epoxy-hexaanhydro-4-methylphthalicanhydride (MHHPA) system. *Polymer, 41,* 2081-2094.

135. Furniss, B. S., Hannaford, A. J., Smith, P. W. G., & Tatchell, A. R. (1989). *Vogel's Textbook of Practical Organic Chemistry* (5th ed.). England: Pearson Education Limited.

136. Wang, D., Carrera, L., & Abadie, M. J. M. (1993). Photopolymerization of glycidyl acrylate and glycidyl methacrylate investigated by differential photocalorimetry and FT-I.R. *European Polymer Journal, 29,* 1379-1386.

137. Scherzer, T., & Decker, U. (1999). Real-time FTIR-ATR spectroscopy to study the kinetics of ultrafast photopolymerization reactions induced by monochromatic UV light. *Vibrational Spectroscopy, 19,* 385-398.

138. Belfield, K. D., & Crivello, J. V. (2003). Photoinitiated Polymerization. In *ACS Symposium Series 847-Advances in Photoinitiated Polymerizations* USA: American Chemical Society.

139. Naghash, H. J., & Okay, O. (1997). Gel formation by chain-crosslinking photopolymerization of methyl methacrylate and ethylene glycol dimethacrylate. *Polymer, 38*, 1187-1196.

140. Nguyen, K. T., & West, J. L. (2002). Photopolymerizable hydrogels for tissue engineering applications. *Biomaterials 23*, 4307–4314.

141. Abadie, M. J. M., Xiong, Y., & Boey, F. Y. C. (2003). UV photo curing of N,N'-bismaleimido-4, 4'-diphenylmethane. *European Polymer Journal, 39*, 1243-1247.

142. Sun, F., Jiang, S. L., & Liu, J. (2007). Study on cationic photopolymerization reaction of epoxy polysiloxane. *Nuclear Instruments and Methods in Physics Research Section B: Beam Interactions with Materials and Atoms, 264*, 318-322.

143. Cho, J.-D., Ju, H.-T., & Hong, J.-W. (2005). Photocuring kinetics of UV-initiated free-radical photopolymerizations with and without silica nanoparticles. *Journal of Polymer Science Part A: Polymer Chemistry, 43*, 658-670.

144. Cho, J.-D., & Hong, J.-W. (2005). Photo-curing kinetics for the UV-initiated cationic polymerization of a cycloaliphatic diepoxide system photosensitized by thioxanthone. *European Polymer Journal, 41*, 367–374.

145. Chen, S., Wayne, D., & Chen, C. F. (2007). Thermal and photopolymerization of divinyl ethers using an iodonium initiator: the effect of temperature. *Polymer International, 56*, 1423-1431.

146. Li, F., Hanson, M. V., & Larock, R. C. (2001). Soybean oil-divinylbenzene thermosetting polymers: synthesis, structure, properties and their relationships. *Polymer, 42*, 1567-1579.

147. Menard, K. P. (2008). *Dynamic Mechanical Analysis : A Practical Introduction* (2nd ed.): CRC Press, Taylor and Francis Group.

148. Young, J. S., Kannurpatti, A. R., & Bowman, C. N. (1998). Effect of comonomer concentration and functionality on photopolymerization rates, mechanical properties and heterogeneity of the polymer. *Macromolecular Chemistry and Physics, 199*, 1043-1049.

149. Kannurpatti, A. R., Anseth, J. W., & Bowman, C. N. (1998). A study of the evolution of mechanical properties and structural heterogeneity of polymer networks formed by photopolymerizations of multifunctional (meth)acrylates. *Polymer, 39*, 2507-2513.

150. Hong, K., Nakayama, K., & Park, S. (2002). Effects of protective colloids on the preparation of poly(l-lactide)/poly(butylene succinate) microcapsules. *European Polymer Journal, 38*, 305-311.

151. Lu, L., Garcia, C. A., & Mikos, A. G. (1999). In vitro degradation of thin poly(DL-lactic-co-glycolic acid) films. *Journal of Biomedical Materials Research, 46*, 236-244.

152. Ba, C., Yang, J., Hao, Q., Liu, X., & Cao, A. (2003). Syntheses and Physical Characterization of New Aliphatic Triblock Poly(l-lactide-b-butylene succinate-b-l-lactide)s Bearing Soft and Hard Biodegradable Building Blocks. *Biomacromolecules, 4*, 1827-1834.

153. Lu, F.-Z., Xiong, X.-Y., Li, Z.-C., Du, F.-S., Zhang, B.-Y., & Li, F.-M. (2002). A Convenient Method for the Synthesis of Amine-Terminated Poly(ethylene oxide) and Poly(e-caprolactone). *Bioconjugate Chemistry, 13*, 1159-1162.

154. Chen, R., & Benicewicz, B. C. (2003). Preparation and properties of poly(methacrylamide)s containing oligoaniline side chains. *Macromolecules, 36*, 6333-6339.

155. Nishi, C., Nakajima, N., & Ikada, Y. (1995). In vitro evaluation of cytotoxicity of diepoxy compounds used for biomaterial modification. *Journal of Biomedical Materials Research, 29*, 829-834.

156. Deb, S., Braden, M., & Bonfield, W. (1997). Effect of crosslinking agents on poly(ethylmethacrylate) bone cements. *Journal of Materials Science: Materials in Medicine, 8*, 829-833.

157. Yeganeh, H., Jamshidi, H., & Jamshidi, S. (2007). Synthesis and properties of novel biodegradable poly(ε-caprolactone)/ poly(ethylene glycol)-based polyurethane elastomers. *Polymer International, 56*, 41-49.

158. Baroli, B. (2006). Review: Photopolymerization of biomaterials: issues and potentialities in drug delivery, tissue engineering, and cell encapsulation applications. *J Chem Technol Biotechnol, 81*, 491–499

159. Herath, K. I. K., Tan, L. P., Chai, C. L. L., & Abadie, M. J. M. Diallyl Tartrate as a Multifunctional Monomer for Bio-polymer Synthesis. *Journal of Biomaterials Science -- Polymer Edition, 21*, 1459-1481.

APPENDIX I

Coupling of CBZ-lysine to PCL

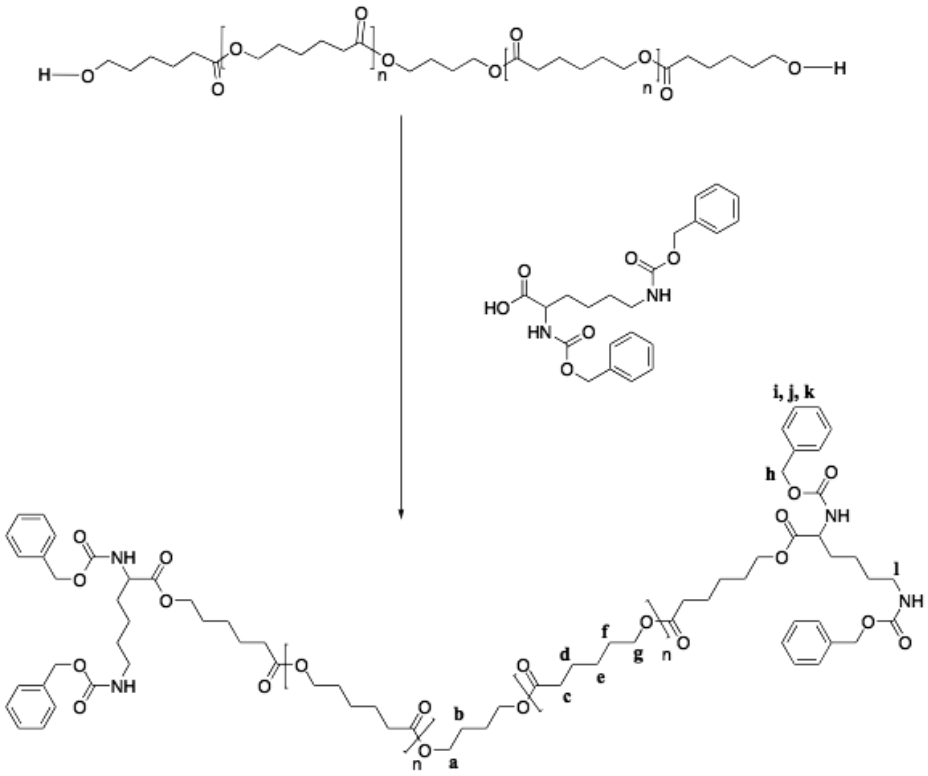

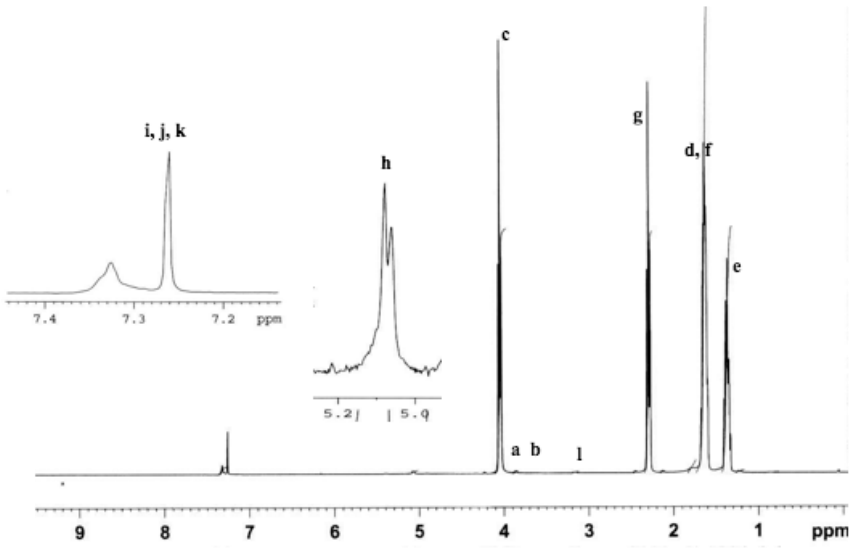

APPENDIX II

Calculation method using ^{1}HNMR for obtaining molecular weights of polymers synthesized via ring-opening polymerization

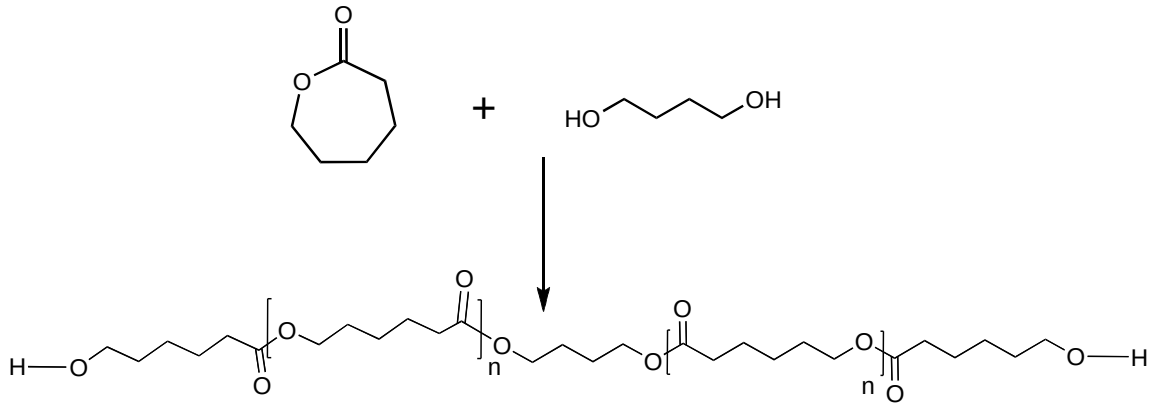

Procedure used:

1. Calibrate peak integral of any CH_2 group of butanediol to 1.
2. Peak integral of CH_2 group of butanediol : Peak integral of any repeating CH_2 group of poly(caprolactone) **= 1: χ**
3. Total number of caprolactone units in polymer = 2 χ

Molecular weight of polymer = 2 χ x Molecular weight of single caprolactone unit

= χ x 114 g/mol